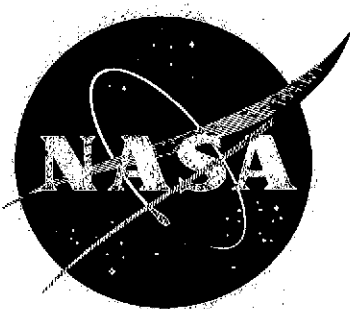


NASA CR-134535
MDC E0913



OUTER SKIN PROTECTION OF COLUMBIUM THERMAL PROTECTION SYSTEM (TPS) PANELS

(NASA-CR-134535) OUTER SKIN PROTECTION
OF COLUMBIUM THERMAL PROTECTION SYSTEM
(TPS) PANELS Final Technical Report
(McDonnell-Douglas Astronautics Co.)

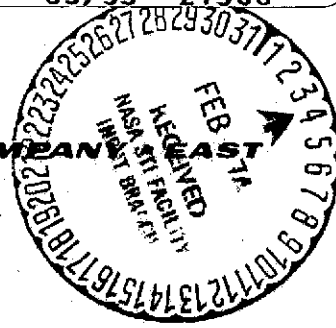
N74-16614

CSCL 20M G3/33 27368 Unclassified

by
John D. Culp

MCDONNELL DOUGLAS ASTRONAUTICS COMPANY EAST

Saint Louis, Missouri



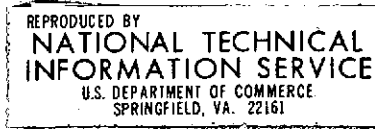
prepared for

NATIONAL AERONAUTICS AND SPACE ADMINISTRATION

NASA Lewis Research Center

Contract NAS3-15546

John P. Merutka, Project Manager



1. Report No. CR-134535	2. Government Accession No.	3. Recipient's Catalog No.
4. Title and Subtitle Outer Skin Protection of Columbium Thermal Protection System (TPS) Panels		5. Report Date September, 1973
7. Author(s) John D. Culp		6. Performing Organization Code
9. Performing Organization Name and Address McDonnell Douglas Astronautics Company - East St. Louis, Missouri 63166		8. Performing Organization Report No. MDC E0913
12. Sponsoring Agency Name and Address National Aeronautics and Space Administration Washington, D.C. 20546		10. Work Unit No.
		11. Contract or Grant No. NAS3-15546
		13. Type of Report and Period Covered Final Technical
		14. Sponsoring Agency Code
15. Supplementary Notes Project Manager, John P. Merutka, NASA Lewis Research Center, Cleveland, Ohio		
16. Abstract A coated columbium alloy material system 0.04 centimeter (0.016 inch) thick was developed which provides for increased reliability to the load bearing character of the system in the event of physical damage to and loss of the exterior protective coating. The increased reliability to the load bearing columbium alloy (FS-85) was achieved by interposing an oxidation resistant columbium alloy (B-1) between the FS-85 alloy and a fused slurry silicide coating. The B-1 alloy was applied as a cladding to the FS-85 and the composite was fused slurry silicide coated. Results of material evaluation testing included cyclic oxidation testing of specimens with intentional coating defects, tensile testing of several material combinations exposed to reentry profile conditions and emittance testing after cycling of up to 100 simulated reentries. The clad material, which was shown to provide greater reliability than unclad materials, holds significant promise for use in the thermal protection system of hypersonic reentry vehicles.		
17. Key Words (Suggested by Author(s)) Columbium Alloys Claddings Silicide Coatings Mechanical Properties Oxidation Testing Emittance		18. Distribution Statement Unclassified - unlimited
19. Security Classif. (of this report) Unclassified	20. Security Classif. (of this page) Unclassified	?

FOREWORD

This is the final report for the Outer Skin Protection of Columbium Thermal Protection (TPS) Panels Program conducted under Contract NAS3-15546. The program technical effort was conducted between May 1971 and August 1973, under the cognizance of NASA-Lewis Research Center, with John P. Merutka as Project Manager.

The program was conducted at McDonnell Douglas Astronautics Company - East, with John Culp study leader. Initial technical direction of the program was furnished by R. J. Kotfila. The laboratory evaluations at MDAC-E were conducted by M. B. Munsell and D. N. Drennan. Major subcontractor contributions were made by R. L. Ammon of Westinghouse Astronuclear Laboratory in producing the clad sheet material, and by B. D. Reznik formerly of HiTemCo and L. Sama of HiTemCo in selecting and applying the fused slurry silicide coatings.

ABSTRACT

A coated columbium alloy material system 0.04 centimeter (0.016 inch) thick was developed which provides for increased reliability to the load bearing character of the system in the event of physical damage to and loss of the exterior protective coating. The increased reliability to the load bearing columbium alloy (FS-85) was achieved by interposing an oxidation resistant columbium alloy (B-1) between the FS-85 alloy and a fused slurry silicide coating. The B-1 alloy was applied as a cladding to the FS-85 and the composite was fused slurry silicide coated. Results of material evaluation testing included cyclic oxidation testing of specimens with intentional coating defects, tensile testing of several material combinations exposed to reentry profile conditions and emittance testing after cycling of up to 100 simulated reentries. The clad material, which was shown to provide greater reliability than unclad materials, holds significant promise for use in the thermal protection system of hypersonic reentry vehicles.

SUMMARY

The object of the program was to determine the feasibility of improving the reliability of coated columbium thermal protection system panels by interposing an oxidation resistant columbium alloy between a load bearing columbium substrate and a conventional silicide protective coating. In the event of local damage to the protective coating, the oxidation resistant cladding would provide a secondary zone of protection for the load bearing core.

Manufacture of the outer skin clad system was accomplished by melting the B-1 cladding alloy (Cb-15Ti-10Ta-10W-2Hf-2.5Al), fabricating it into sheet, hot roll bonding it to an FS-85 alloy (Cb-27Ta-10W-1Zr) load bearing core, and rolling to the desired thickness. During the program, the clad sheet product improved to a uniform consistent material of good quality. The process, with a moderate scale-up effort, could produce large quantities of clad sheet material at a nominal cost over unclad sheet.

Fused slurry silicide coatings were used as the primary protection system; the R-512E composition (20Cr-20Fe-Si) was the best of several coatings checked. Edge beading was employed to provide reliable edge protection in spite of the fact that both alloys had to be protected simultaneously on the unclad edges. The inherent life of the coating was well in excess of 100 reentry cycles.

The primary evaluation test determined the oxidation protection offered by the cladding at intentional coating defect sites. Reentry conditions of time, temperature, and pressure were imposed automatically in flight simulation furnaces. The B-1 cladding reduced oxidation consumption of the core by a factor of approximately 20 in 50 cycle exposures, and oxygen contamination of the core was significantly reduced, particularly in the first critically-important 5 to 15 cycles (Figures i and ii). It was concluded that a thermal protection system panel with 50 micrometers of B-1 cladding would have a minimum assured life of 15 reentry cycles, and 100 micrometers of cladding would assure a minimum life of 25 reentry cycles.

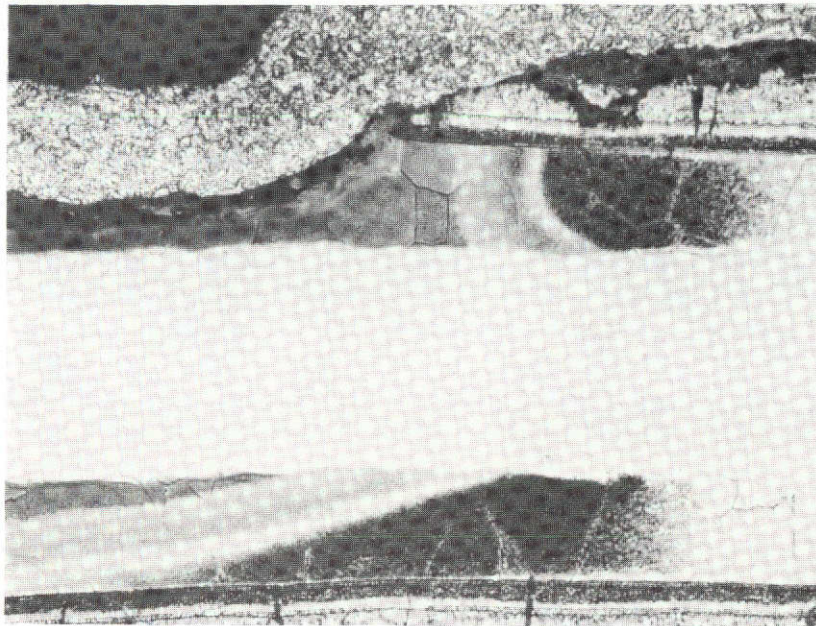
Extensive tensile testing was performed at room and elevated temperatures. It was determined that the strength of the composite was dominated by the strength properties of the load bearing core when the B-1 cladding thickness after coating was up to 50 micrometers. At a 100 micrometer cladding thickness, the cladding had a major influence on the composite tensile properties; strength increased and ductility decreased. Interdiffusion of the cladding and core did not occur within 100 reentry cycles and core strength remained at predicted levels. Strength testing was culminated with stress profile testing under reentry conditions, including loads. The clad systems carried the design loads for 100 cycles without oxidation failures and without any indicated loss of the good creep strength properties of the FS-85 core (Figure iv).

Emittance testing of clad and unclad systems was performed after various profile exposures up to 100 cycles. Emittance values were typical of the R-512E coating, but values for the coated B-1 clad were slightly lower

OUTER PROTECTIVE SKIN

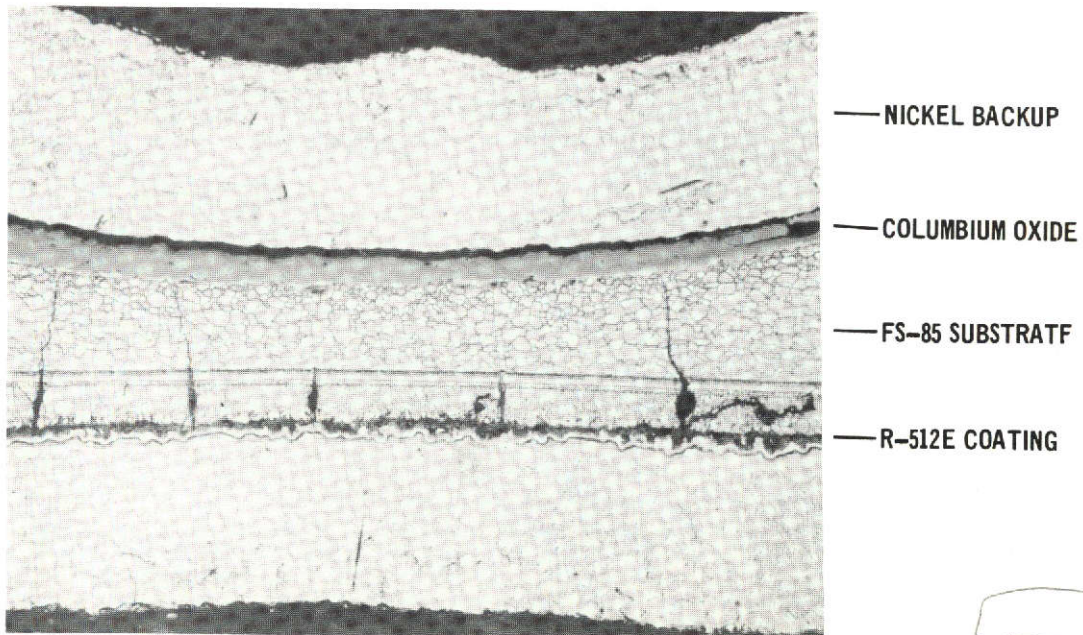
Report MDC E0913
September 1973

150X



NOMINAL 100 μm CLADDING AFTER 15 REENTRY CYCLES

100X



UNCLAD FS-85 AFTER 15 REENTRY CYCLES

This page is reproduced at the back of the report by a different reproduction method to provide better detail.

B-1 CLADDING PROTECTS FS-85 CORE FROM OXIDATION OF LOAD BEARING AREA

FIGURE i

(approximately 3 percent) than the R-512E coated FS-85 baseline. The emittance values measured were acceptable for hypersonic reentry vehicle applications (Figure iii).

A limited trade study was performed to assess the potential of the outer skin clad system to operational hypersonic vehicle applications. It was determined that improved reliability could be achieved with only modest sacrifices of increased weight and installation cost. The material systems were judged to be very promising as a means of providing improved fail-safe reliability and improved hardware life and performance.

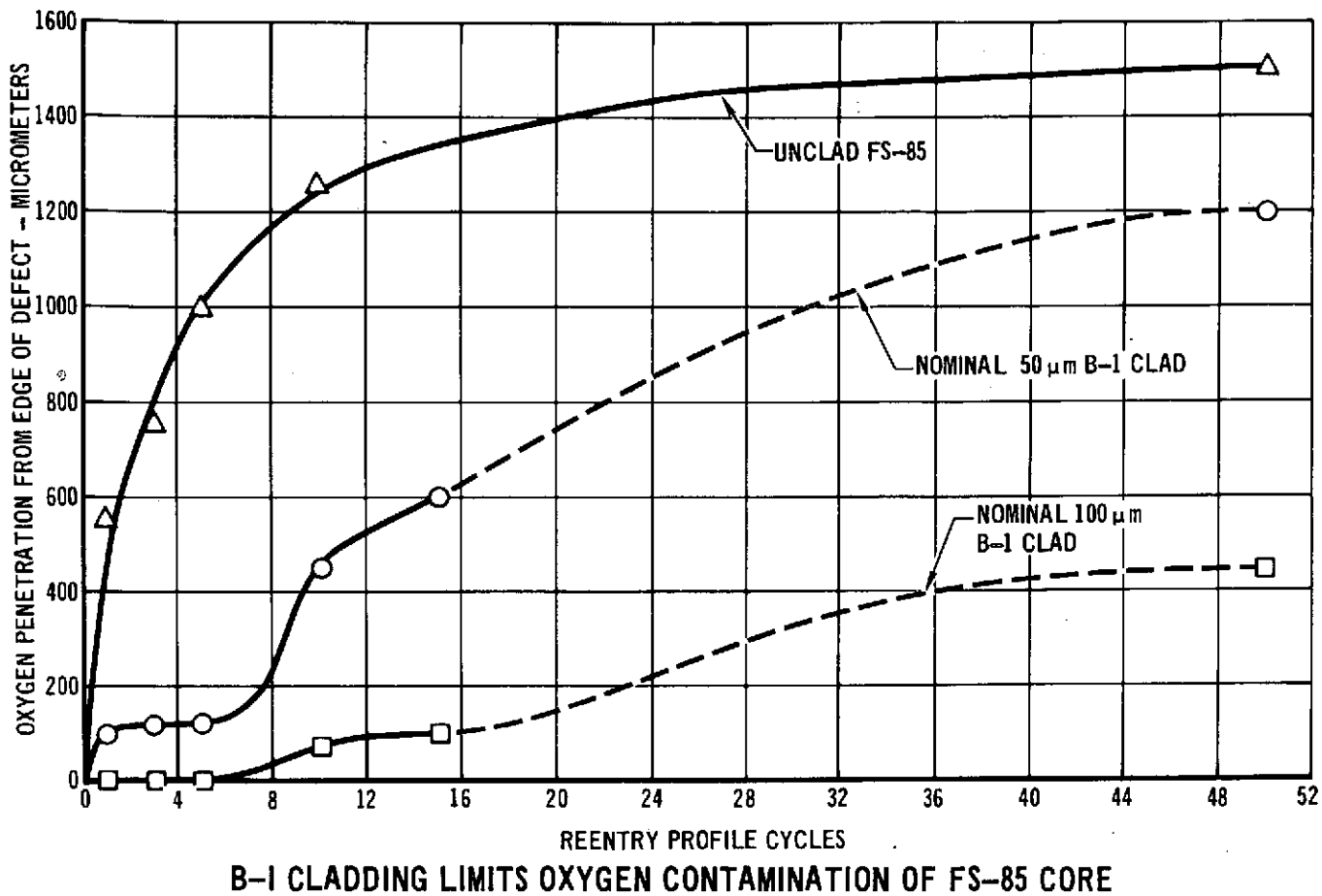
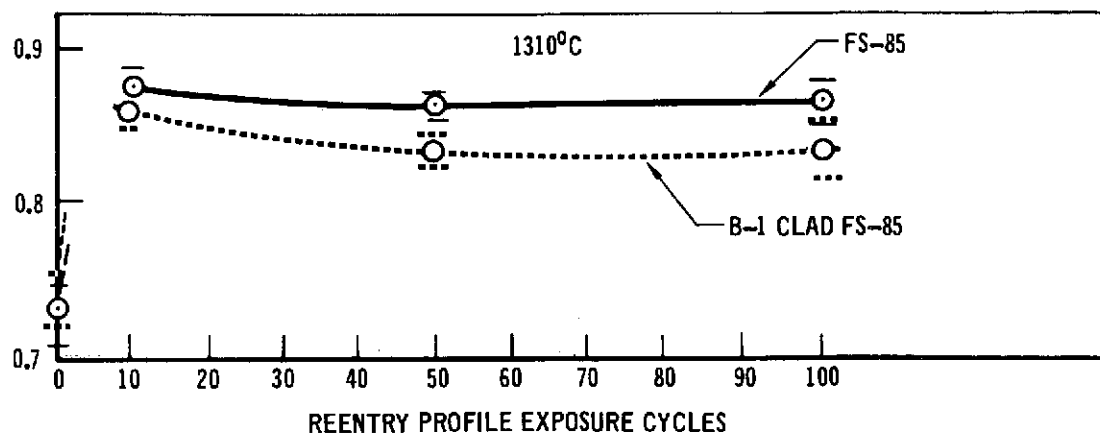


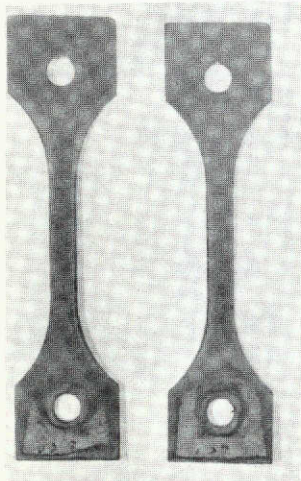
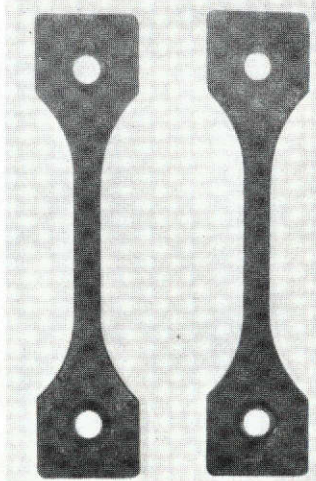
FIGURE ii



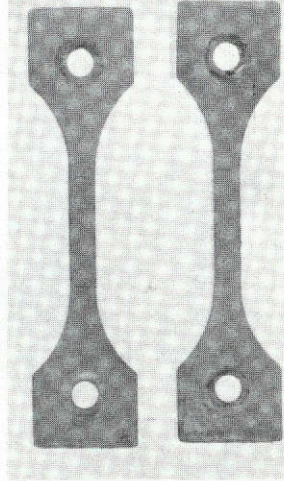
ACCEPTABLE EMITTANCE FOR R-512E COATING ON B-1 CLAD FS-85

FIGURE iii

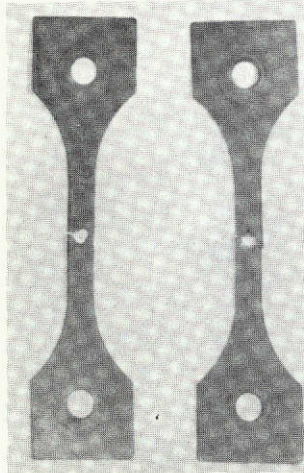
AFTER 100 REENTRY STRESS CYCLES WITHOUT INTENTIONAL DEFECTS

50 μm B-1 CLAD

UNCLAD FS-85

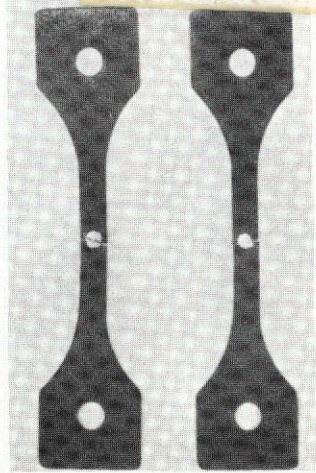
100 μm B-1 CLAD

This page is reproduced at the back of the report by a different reproduction method to provide better detail.



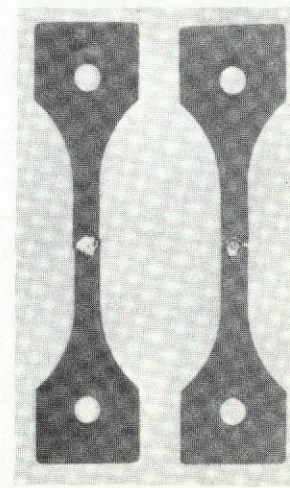
41

44



26

25



58

54

VARIOUS REENTRY STRESS CYCLES TO FAILURE

B-1 CLADDING MAINTAINS STRENGTH OF FS-85 CORE

FIGURE iv

TABLE OF CONTENTS

<u>Section</u>	<u>Page</u>
FOREWORD	ii
ABSTRACT	iii
SUMMARY	iv
1 INTRODUCTION	1
2 OUTER SKIN DEVELOPMENT AND CHARACTERIZATION	3
2.1 Clad System Design and Sheet Fabrication	3
2.1.1 System Design and Materials Selection	3
2.1.1.1 Core Material Selection	3
2.1.1.2 Cladding Material Selection	4
2.1.1.3 Protective Coating Selection	7
2.1.1.4 Selection of Baseline Material	9
2.1.2 Cladding Alloy Preparation	9
2.1.2.1 B-1 Alloy Ingot Melting	9
2.1.2.2 B-1 Alloy Sheet Fabrication	11
2.1.3 Bonding of Cladding to Core	13
2.1.4 Reduction of Clad Sheet	13
2.1.4.1 Rolling of Task One Material	13
2.1.4.2 Rolling of Task Two Material	15
2.1.4.3 Rolling of Task Three Material	18
2.2 Specimen Preparation and Coating Application	23
2.2.1 Specimen Preparation	23
2.2.2 Task One Coating Application and Performance	23
2.2.3 Task Two Coating Application and Performance	25
2.2.4 Task Three Coating Application and Performance	25

TABLE OF CONTENTS (CONT'D)

<u>Section</u>	<u>Page</u>
2.2.5 General Coating Observations	29
2.3 Oxidation Resistance Evaluation	32
2.3.1 Evaluation Test Procedure	32
2.3.2 Defect Exposure Evaluation Results	35
2.3.2.1 Evaluation of Metal Consumption Oxidation	36
2.3.2.2 Bend Test and Metallographic Evaluation	39
2.4 Mechanical Property Determination	57
2.4.1 Tensile Property Determination	57
2.4.1.1 Tensile Properties of Nominal 50 Micrometer Thick B-1 Clad Material	58
2.4.1.2 Tensile Properties of Nominal 100 Micrometer Thick B-1 Clad Material	58
2.4.2 Reentry Profile Cycling Under Load	60
2.4.3 Exposure Cycling of Defected Tensile Specimens	60
2.4.4 Profile Exposure Evaluation of Clad Specimens Without Coating	69
2.4.5 Tensile Properties of B-1 Alloy	70
2.5 Emittance Measurements	75
2.6 Electron Microprobe Analysis	79
3 DISCUSSION OF RESULTS	87
3.1 Comparison With Other Clad Systems	87
3.2 Utilization of the Outer Skin Concept In A Reentry System	88
3.2.1 Cladding Thickness and Reentry System Reliability	88
3.2.2 Evaluation of Material Property Allowables	90
3.2.3 Assessment of Cladding Weight Penalty	91

TABLE OF CONTENTS (CONT'D)

<u>Section</u>	<u>Page</u>
3.2.4 Panel Design and Fabrication	92
3.2.5 Survey of Cost Factors	98
4 CONCLUSIONS AND RECOMMENDATIONS	101
5 REFERENCES	103
APPENDIX A - DETAILED TENSILE TEST DATA	104
APPENDIX B - DEFECT TENSILE TEST DATA	111
APPENDIX C - CONVERSION FACTORS TO INTERNATIONAL SYSTEM OF UNITS (SI)	114

LIST OF PAGES

Title	Page
ii through xvi	
1 through 113	

LIST OF FIGURES

<u>FIGURE</u>	<u>PAGE</u>
i B-1 CLADDING PROTECTS FS-85 CORE FROM OXIDATION OF LOAD BEARING AREA	vi
ii B-1 CLADDING LIMITS OXYGEN CONTAMINATION OF FS-85 CORE	vii
iii ACCEPTABLE EMITTANCE FOR R-512E COATING ON B-1 CLAD FS-85	vii
iv B-1 CLADDING MAINTAINS STRENGTH OF FS-85 CORE	viii
1 COMPARISON OF CONTINUOUS WEIGHT GAIN DATA FOR B1 ALLOY AND PURE COLUMBIUM IN AIR AT 1040°C	5
2 SURFACE RECESSSION BEHAVIOR OF B-1 ALLOY OXIDIZED IN FLOWING AIR (DATA REPRESENTS 1/2 OF THE DIFFERENCE IN THICKNESS BEFORE AND AFTER EXPOSURE)	6
3 FUSED SLURRY SILICIDE COATED B-1-400X	8
4 MICROSTRUCTURE OF ROLL BONDED B-1/FS-85 AFTER ANNEALING AT 1315°C	14
5 ROLLING SCHEDULE OF B-1 CLAD FS-85 PREPARED IN TASK 1	16
6 ROLLING SCHEDULE OF B-1 CLAD FS-85 PREPARED IN TASK 2	17
7 MICROSTRUCTURE OF B-1 CLAD FS-85	19
8 ROLLING SCHEDULE OF B-1 CLAD FS-85 PREPARED IN TASK 3	21
9 B-1 CLAD FS-85 PRODUCED DURING FINAL TASK SHOWING SURFACE DELAMINATIONS	22
10 TENSILE SPECIMEN	24
11 R-512E COATING ON CB-752	26
12 MICROSTRUCTURE OF R-512E COATING ON FS-85 (EDGE) AND B-1 (SURFACE)	27
13 MICROSTRUCTURE OF R-512E COATING AS APPLIED IN TASK NO. 2	28
14 R-512E COATED TENSILE SPECIMENS SHOWING OXIDATION SITES AFTER 100 REENTRY PROFILE EXPOSURE CYCLES	30
15 EDGE MICROSTRUCTURE OF R-512E CLAD TENSILE SPECIMENS ADJACENT TO COATING FAILURES OCCURRING WITHIN 100 REENTRY PROFILE CYCLES	31

LIST OF FIGURES (CONTINUED)

<u>FIGURE</u>	<u>PAGE</u>
16 TEST APPARATUS USED FOR REENTRY PROFILE EXPOSURE CYCLING	33
17 TEST CONDITIONS USED FOR REENTRY PROFILE EXPOSURE TESTING	34
18 R-512E COATED COUPONS WITH INTENTIONAL COATING DEFECTS AFTER VARIOUS PROFILE EXPOSURE CYCLES	37
19 DEPTH OF OXYGEN PENETRATION IN B-1 CLAD AND UNCLAD FS-85 ALLOY	40
20 EFFECT OF ONE PROFILE EXPOSURE ON UNCLAD BASELINE ALLOYS	42
21 EFFECT OF ONE PROFILE EXPOSURE CYCLE ON B-1 CLAD FS-85	43
22 EFFECT OF THREE PROFILE EXPOSURE CYCLES ON CLAD AND UNCLAD FS-85	44
23 NOMINAL 100 MICROMETER THICK B-1 CLAD FS-85 AFTER THREE AND FIVE EXPOSURE CYCLES	45
24 EFFECT OF FIVE REENTRY PROFILE EXPOSURE CYCLES ON UNCLAD FS-85	46
25 B-1 CLAD FS-85 AFTER FIVE REENTRY PROFILE EXPOSURE CYCLES	48
26 EFFECT OF TEN PROFILE EXPOSURE CYCLES ON CLAD AND UNCLAD FS-85	49
27 NOMINAL 100 MICROMETER CLADDING ON FS-85 AFTER 10 AND 15 REENTRY PROFILE CYCLES	50
28 EFFECT OF 15 REENTRY EXPOSURE CYCLES ON B-1 CLAD AND UNCLAD FS-85	51
29 EFFECT OF 50 REENTRY PROFILE CYCLES ON CLAD AND UNCLAD FS-85	52
30 EFFECT OF 50 REENTRY PROFILE EXPOSURE CYCLES ON NOMINAL 100 MICROMETER B-1 CLADDING	53
31 MICROSTRUCTURE OF CLAD AND UNCLAD FS-85 COUPONS AFTER 100 REENTRY PROFILE CYCLES	55
32 MICROSTRUCTURE OF NOMINAL 100 MICROMETER B-1 CLAD FS-85 AFTER 100 PROFILE REENTRY CYCLES	56
33 R-512E COATED CLAD AND UNCLAD FS-85 TENSILE SPECIMENS AFTER STRESS PROFILE CYCLES	62

LIST OF FIGURES (CONTINUED)

<u>FIGURE</u>	<u>PAGE</u>
34 DEFECTED R-512E COATING ON CLAD AND UNCLAD FS-85 TENSILE SPECIMENS AFTER FAILURE DURING STRESS PROFILE CYCLING	63
35 ROOM TEMPERATURE ULTIMATE TENSILE STRENGTH OF DEFECTED SPECIMENS AFTER VARIOUS REENTRY PROFILE EXPOSURES	65
36 CLAD COUPONS WITHOUT R-512E COATED AFTER VARIOUS REENTRY PROFILE EXPOSURE CYCLES	66
37 B-1 CLAD TENSILE SPECIMENS WITHOUT R-512E COATING AFTER VARIOUS REENTRY PROFILE EXPOSURE CYCLES	67
38 MICROSTRUCTURE OF UNCOATED B-1 CLAD ON FS-85 AFTER REENTRY PROFILE EXPOSURE CYCLING	71
39 EDGE OF UNCOATED B-1 CLAD SPECIMEN AFTER 3 REENTRY PROFILE EXPOSURE CYCLES ILLUSTRATING OXYGEN CONTENT GRADIENT	72
40 MICROSTRUCTURE OF B-1 ALLOY SHEET	74
41 DIAGRAM OF ROTATING SAMPLE EMISSOMETER	76
42 ROTATING SAMPLE EMISSOMETER	77
43 CHECK OUT RESULTS FOR ROTATING SAMPLE EMISSOMETER	80
44 EMITTANCE OF R-512E COATED B-1 CLADDING AND FS-85	81
45 ELECTRON MICROPROBE SCANS OF B-1 CLAD FS-85 WITH THE R-512E COATING AFTER 100 REENTRY PROFILE CYCLES (TASK 1 EXPERIMENT)	82
46 ELECTRON MICROPROBE SCANS OF B-1 CLAD FS-85 WITH 30Cr-20Fe-Si COATING AFTER 100 REENTRY PROFILE CYCLES (TASK 1 EXPERIMENT)	83
47 ELECTRON MICROPROBE SCANS OF CB-752 BASELINE MATERIAL WITH THE R-512E COATING AFTER 100 REENTRY PROFILE CYCLES (TASK 1 EXPERIMENT)	84
48 ELECTRON MICROPROBE SCANS OF B-1 CLAD FS-85 WITH THE R-512E COATING AFTER 100 REENTRY PROFILE CYCLES	85
49 ELECTRON MICROPROBE SCANS OF R-512E COATED FS-85 WITHOUT CLADDING AFTER 100 REENTRY PROFILE CYCLES	86
50 EFFECT OF B-1 CLADDING ON MASS OF FS-85 SHEET	94
51 CURRENT COLUMBIUM DESIGN APPROACHES	96
52 FUDJ WELDED COLUMBIUM JOINTS	97
53 OUTER SKIN CLADDING ON BOTH SURFACES OF FUDJ JOINT OUTER SKIN CLADDING ON EXTERIOR OF FUDJ JOINT	99

LIST OF TABLES

<u>TABLE</u>	<u>PAGE</u>
I CHEMICAL COMPOSITION OF FS-85 CORE MATERIAL	4
II VENDOR CERTIFIED PROPERTIES OF BASELINE MATERIALS	10
III CHEMICAL ANALYSIS OF MODIFIED B-1 CLADDING ALLOY INGOTS	12
IV INTENTIONAL COATING DEFECT TESTING SCOPE	36
V OXIDATION OF B-1 CLAD FS-85 AND UNCLAD COLUMBIUM ALLOY AT AN INTENTIONAL COATING DEFECT SITE	38
VI SUMMARY OF CLAD AND UNCLAD FS-85 TENSILE PROPERTIES	59
VII RESULTS OF REENTRY PROFILE CYCLING UNDER STRESS FOR CLAD AND UNCLAD FS-85 COLUMBIUM ALLOY	61
VIII TENSILE PROPERTIES OF UNCOATED CLAD SPECIMENS AFTER VARIOUS PROFILE EXPOSURE CYCLES	68
IX TENSILE PROPERTIES OF COATED AND UNCOATED B-1 ALLOY	73
X MASS OF CLAD AND UNCLAD FS-85 SHEET REQUIRED FOR COATED HEATSHIELD PANELS FOR 100 REENTRY CYCLES	93
A1 TENSILE PROPERTIES OF B-1 CLAD FS-85 AND UNCLAD CB-752 - TASK 1	105
A2 TENSILE PROPERTIES OF B-1 CLAD FS-85 AND UNCLAD FS-85 BASELINE - TASK 2	106
A3 TENSILE PROPERTIES OF B-1 CLAD FS-85 AND UNCLAD FS-85 BASELINE - TASK 3	109
B1 EFFECT OF COATING DEFECTS ON TENSILE PROPERTIES OF CLAD AND UNCLAD FS-85 ALLOY COLUMBIUM - TASK 2	112
B2 ROOM TEMPERATURE TENSILE PROPERTIES OF CLAD AND UNCLAD DEFECTED SPECIMENS AFTER VARIOUS REENTRY PROFILE EXPOSURES - TASK 3	113

1. INTRODUCTION

The concept of employing an intermediate layer of an oxidation resistant columbium alloy between a conventional coating and a high strength alloy to offer a backup protective mechanism in the event of damage to the primary coating had been suggested in the mid-nineteen sixties. At that time, the design of columbium heatshield panels and the development of protective coatings was in a formative stage and the true value of an outer skin protective system could not have been realistically assessed. Consideration of coated columbium as a jet engine turbine component material provided the first opportunity to seriously consider the fail-safe backup system, since engines are required to operate many hours between routine inspections. Westinghouse Astronuclear Laboratory performed an alloy development effort toward the application of claddings to turbine components. This cladding alloy was required to have the best possible oxidation resistance while maintaining a functional level of ductility. The product of this effort was the B-1 alloy, reported in reference 1. The potential use of coated columbium in the thermal protection system of hypersonic reentry vehicles designed for extensive multiple reuse made possible a system that could use the clad outer skin concept to advantage. Heatshield panels, as turbine components, are subject to a small but statistically significant probability of early coating failures. The additional possibility of local physical damage to the coatings made the study of a backup protection system a viable approach to improving panel reliability. This program was designed to determine the feasibility of employing the outer skin protective system to heatshield panels for multiple reuse in hypersonic reentry vehicles. The testing was broad in scope to ensure that all relevant factors regarding the material applicability to an operational vehicle system were considered. Final compositional judgements, scale-up, and the establishment of design allowables could be accomplished in a subsequent effort, should merits of the material system warrant it.

The purpose of the program was to produce an outer skin clad protective system 0.040 centimeter (0.016 inch) thick, to determine the functional properties of the system, and to assess its applicability to the improvement of the reliability of a coated columbium thermal protection system. The study was conducted both within the context of the current understanding of panel design and performance criteria and established future trends and requirements.

The technical approach selected was to employ a development, improvement and optimization series of tasks in which the material system was progressively refined and characterized. The material system components, consisting of a load bearing core, protective cladding and oxidation resistant coating, were selected to provide the best combination of proven materials to emphasize evaluation of the concept, as opposed to a materials optimization study. A team was formed in which Westinghouse Astronuclear Laboratory provided the clad composite fabrication technology; coating selection and application were furnished by HiTemCo; and the material evaluation for hypersonic reentry conditions was accomplished by MDAC-E. During the initial task, two B-1 cladding thicknesses were produced and two coating compositions were applied. Evaluation showed that the cladding thickness was not sufficiently uniform and one coating

composition (R-512E) had a life in excess of requirements. The clad systems proved to be superior to the Cb-752 baseline material in oxidation resistance and strength. The second task employed two cladding thicknesses, one coating composition, and FS-85 as the baseline material. The cladding was of uniform thickness, but the two thicknesses were not sufficiently separated to warrant testing both. Strength evaluation included elevated temperature tensile testing and room temperature testing of defected tensile specimens after various profile exposure cycles. During the third task two cladding thicknesses were evaluated. In addition to repeating the oxidation and tensile tests, stress profile cycles of defected and undefected tensile specimens were performed. Emittance tests were also performed on clad and unclad specimens with the fused slurry silicide coating after various reentry exposures up to 100 cycles.

OUTER PROTECTIVE SKIN

2. OUTER SKIN DEVELOPMENT AND CHARACTERIZATION

The development and characterization of a clad material was required to assess the potential of the outer skin protective system for improving the reliability of coated columbium heatshield panels on operational reentry vehicles. After appropriate materials for the composite system had been selected, clad sheet fabrication and coating were alternated with evaluation testing to progressively refine and characterize the outer skin material.

2.1 CLAD SYSTEM DESIGN AND SHEET FABRICATION

The outer skin concept of interposing an oxidation resistant cladding between a columbium alloy substrate and a standard silicide coating to improve the reliability of the material, should in-service coating damage occur, was defined as the main subject of the program. The initial effort was to review materials which in combination would produce the best composite system for use in hypersonic reentry heatshield applications. After the material system was defined, it was necessary to produce the cladding alloy sheet, bond it to the load bearing core, and reduce the clad composite to the thin gauges typical of current heatshield requirements.

2.1.1 System Design and Materials Selection

The outer skin material system, intended for the exterior surface of hypersonic reentry vehicles, was a composite of a load bearing core, an oxidation resistant cladding and a fused slurry silicide protective coating. The core was assumed to carry the total load for the system, and the cladding and silicide coating were used to protect and maintain the load bearing characteristics of the core.

2.1.1.1 Core Material Selection

The criteria for the selection of the core material were the same as those for a columbium alloy reentry vehicle heatshield panel. The alloy had to have good strength-to-weight characteristics up to 1600°C, good creep strength, metallurgical stability and manufacturing qualities sufficient to ensure economical fabrication of heatshield hardware. After a survey was made of available columbium alloys, FS-85 (Cb-27Ta-10W-1Zr) was selected because it represented the best overall agreement with the established criteria. The FS-85 was purchased as a sheet 0.635 centimeter thick, fully recrystallized, and of the chemical composition presented in table I.

Note: Conversion factors between English and S.I. Units are presented in Appendix C.

TABLE I
CHEMICAL COMPOSITION OF FS-85 CORE MATERIAL

<u>Elements</u>	<u>Percent</u>
Carbon	0.0047
Oxygen	0.0075
Nitrogen	0.0054
Hydrogen	0.0005
Zirconium	0.70
Tungsten	10.5
Tantalum	26.8
Columbium	Balance

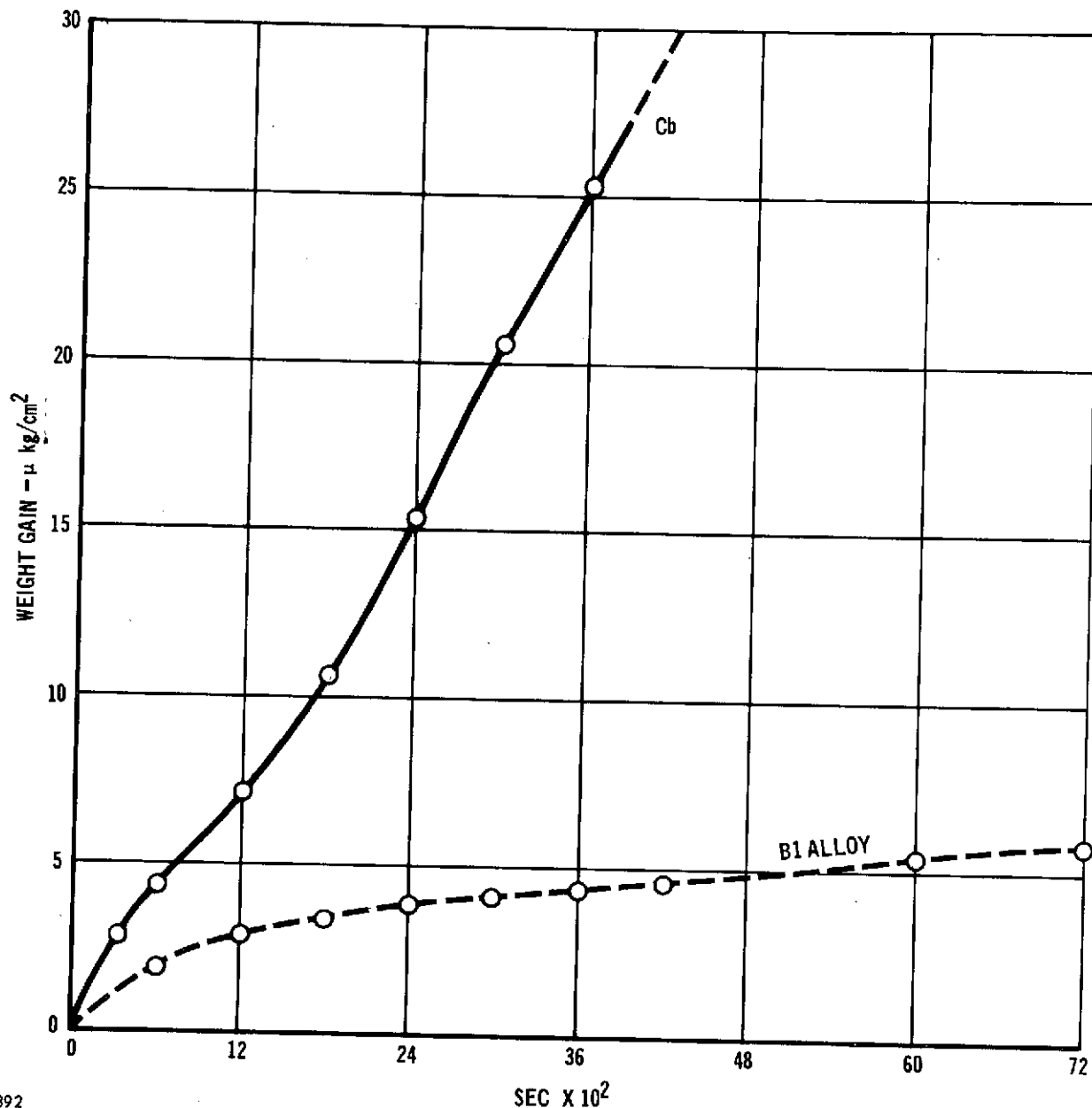
2.1.1.2 Cladding Material Selection

The second element of the outer skin protective system was the oxidation resistant columbium alloy cladding. The primary function of the cladding was to provide a secondary defense against oxidation of the load bearing core in the event of local damage to the protective silicide coating. Oxidation resistance, therefore, was considered the most important criterion of the cladding. Secondary considerations, such as manufacturability and composite strength retention in service, were required if the system was to be of practical value to a hypersonic reentry vehicle system.

The following two cladding compositions were selected initially as cladding alloys for evaluation: (references 1, 2, 3, 4 and 5)

- (a) Cb-15Ti-10Ta-10W-2Hf-2.5Al (Modified B-1)
- (b) Cb-30Hf-10W-5Ti-1.5Zr (Modified WC-3015)

The modified B-1 alloy was thought to be better in terms of oxidation resistance. (Figures 1 and 2 show oxidation test data for the B-1 available at the time of material selection.) The modified WC-3015 was considered to provide the program with information regarding strength of the composite system. While the minimum strength criterion was to maintain the core strength for 100 reuse cycles, it was believed that the WC-3015 might make a positive contribution to the composite strength. Prior to initiating manufacture of the WC-3015 cladding sheet, additional oxidation resistance data for the WC-3015 was published (reference 6). Reassessment of the oxidation resistance of the



457-1392

FIGURE 1 COMPARISON OF CONTINUOUS WEIGHT GAIN DATA FOR B1 ALLOY
AND PURE COLUMBIUM IN AIR AT 1040°C

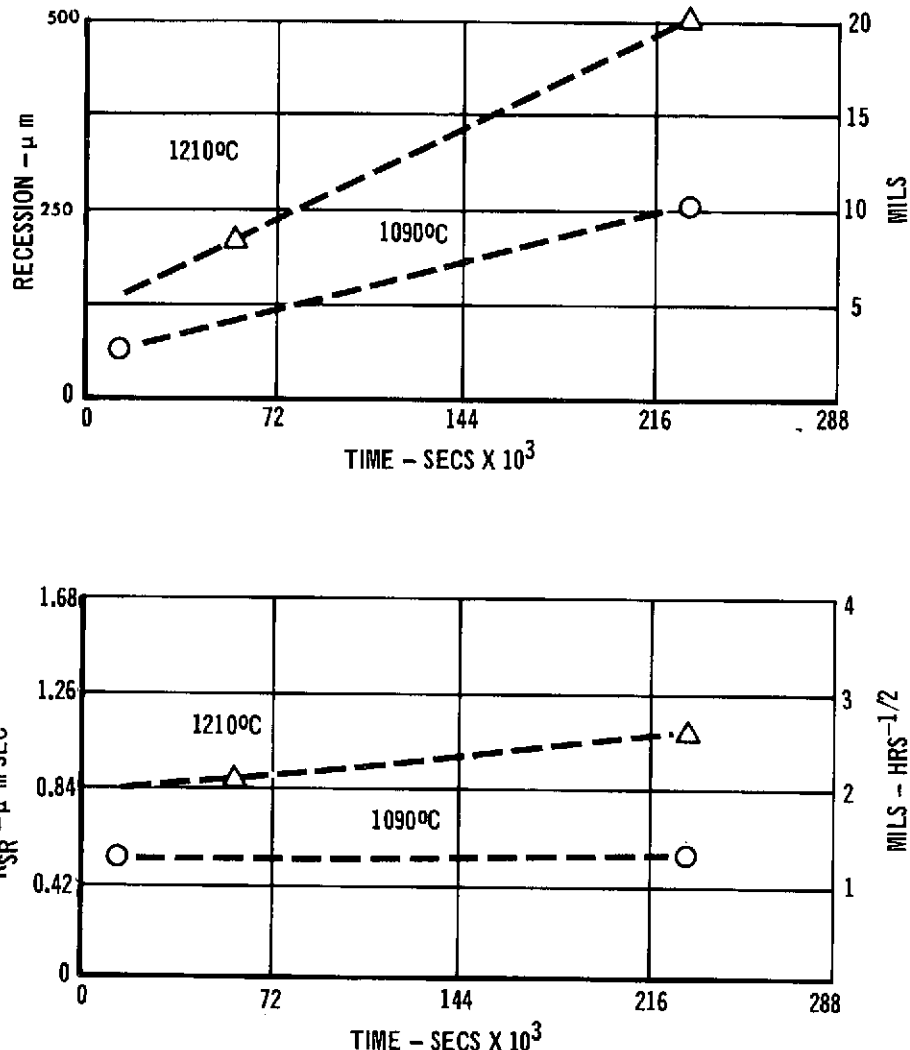


FIGURE 2 SURFACE RECESSION BEHAVIOR OF B-1 ALLOY OXIDIZED IN FLOWING AIR (DATA REPRESENTS 1/2 OF THE DIFFERENCE IN THICKNESS BEFORE AND AFTER EXPOSURE)

WC-3015 showed that the oxidation resistance was not sufficient to meet the primary oxidation objective of the cladding system.

Cladding thickness was recognized from the beginning to be of major importance since the trade between gaining increased system reliability through thicker cladding had to be contrasted with the associated increased weight of the material system. Indeed, cladding thickness proved to be the most important system variable studied in the three distinct program tasks. Initial cladding thicknesses selected for manufacture were 50 and 75 micrometers. After a portion of the cladding was consumed during protective coating formation, the nominal cladding thicknesses remaining for service were calculated to be 25 and 50 micrometers. The cladding was applied to both surfaces of the FS-85 core sheet.

Since Westinghouse Astronuclear Laboratory was the developer of the B-1 alloy and had significant experience in the fabrication of columbium alloy products, they were selected to do all the metallurgical processing required to produce the B-1 clad FS-85 sheet material.

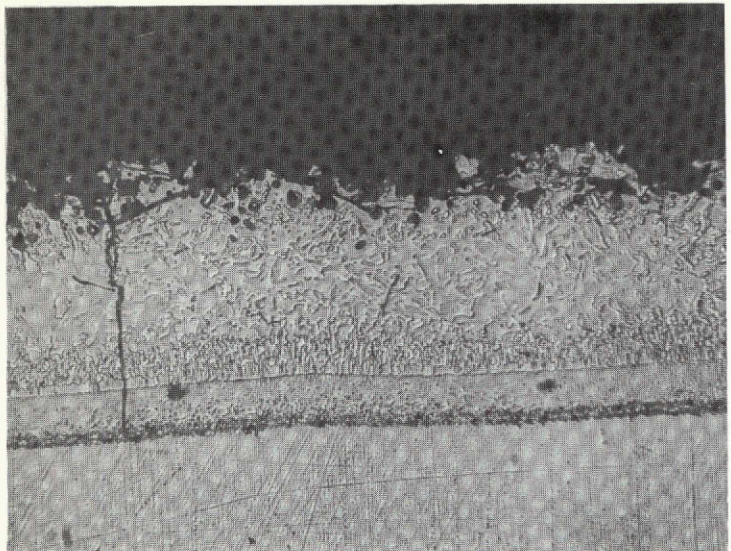
2.1.1.3 Protective Coating Selection

Criteria for the protective coating were the same as for any columbium alloy being used in a reentry application, with protection of the substrate from oxidation and oxygen contamination for a minimum of 100 reentry cycles of primary importance. The fused slurry silicide coating process was selected because of its superiority in protecting reentry type hardware and the great latitude it provided in potential coating compositions. Since there had been very little coating work with the B-1 alloy, the most appropriate fused slurry silicide coating composition was not known. An additional complication in selecting a coating composition was that the coating had to provide adequate protection to both the B-1 cladding and FS-85 core alloys simultaneously (B-1 on the surfaces and FS-85 on the unclad edges).

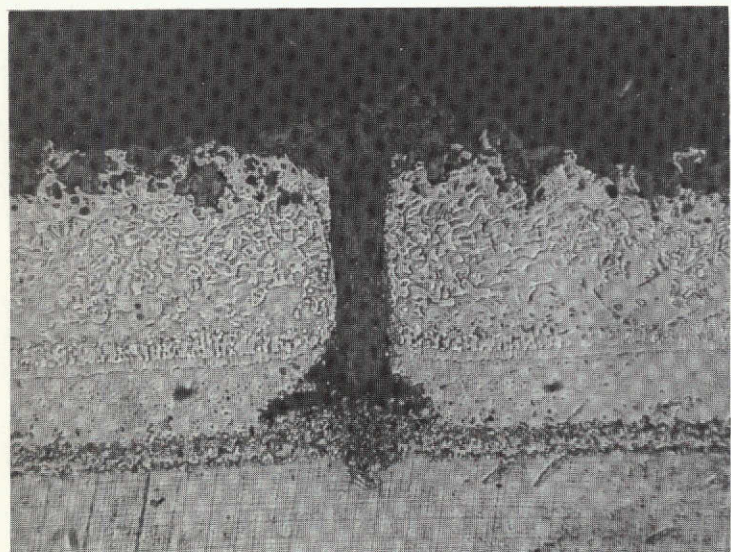
Before the clad sheet was coated, an experiment was conducted to insure that an adequate fused slurry silicide coating could be achieved on the B-1 cladding alloy. Two compositions, Si-20Cr-5Ti (R-512A) and Si-20Cr-20Fe (R-512E), were applied to B-1 alloy coupons. Oxidation testing was accomplished by slow thermal cycling to 1350°C at one atmosphere pressure. This form of oxidation testing has been established to be more severe than typical hypersonic reentry conditions. Oxidation failures occurred on both coating systems after 81 cycles. Metallographic examination revealed that the R-512E coating sustained very little internal oxidation for the extent of the oxidation exposure (see figure 3). Conversely, the R-512A showed extensive oxidation in the tension cracks, as shown in figure 3. It was decided to use the R-512E and that the R-512A was not an appropriate composition for the B-1 alloy. Concurrent experimentation was being conducted on several structural columbium alloys (reference 7). After the results achieved on the B-1 alloy were compared with this broader compositional study, it was concluded that the slurry composition Si-30Cr-20Fe would produce satisfactory results on the B-1 clad FS-85 sheet material. The two fused slurry silicide compositions selected for application to the initial group of clad specimens were the

OUTER PROTECTIVE SKIN

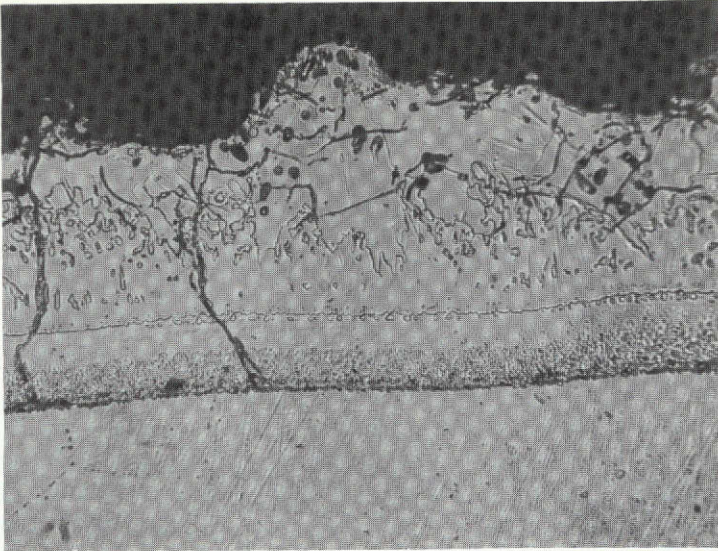
Report MDC E0913
September 1973



As Coated



R-512A



R-512E

After 81 Oxidation Cycles

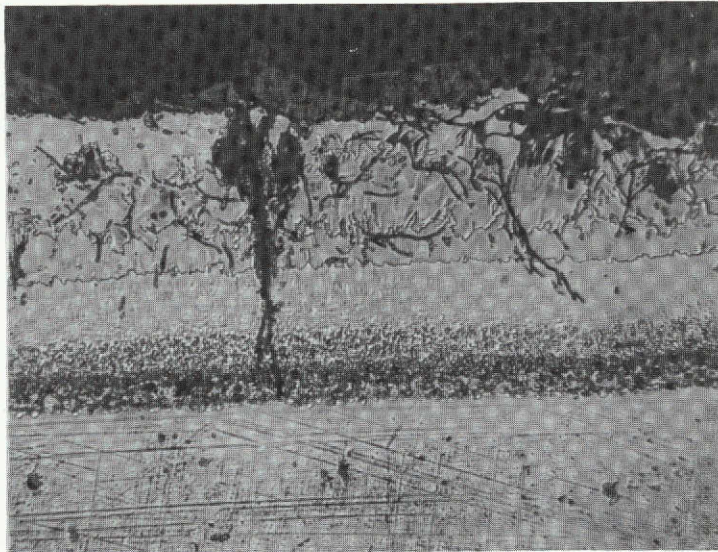


FIGURE 3 FUSED SLURRY SILICIDE COATED B-1-400X

OUTER PROTECTIVE SKIN

Si-20Cr-20Fe (R-512E) and the Si-30Cr-20Fe. HiTemCo (formerly Sylvania High Temperature Composites Laboratory) was selected to apply the fused slurry silicide coating because of their recognized superiority in this field.

2.1.1.4 Selection of Baseline Material

It was predetermined that each oxidation or strength experiment would include baseline specimens for a comparison with the results achieved on the clad materials. The initial program task employed Cb-752 columbium alloy with an R-512E fused slurry silicide protective coating. This baseline material system was selected because of the vast amount of data and experience available. The results achieved during the initial evaluation showed that the B-1 clad FS-85 was superior to the Cb-752 in oxidation resistance and strength. Since the performance of the B-1 clad FS-85 was quite encouraging, the question of the specific contribution of the cladding to the total system performance became more important. Therefore, FS-85 was chosen as the baseline for the second and third tasks in order to provide a direct comparison of clad and unclad FS-85. The FS-85 sheet material available for use on the second task was below nominal tensile properties. Although this did not appreciably affect the ability to compare the oxidation resistance or defect sensitivity of the clad and unclad FS-85 in task two, nominal strength FS-85 baseline material was obtained and used for the final task. Table II presents the vendor certified properties of the three baseline sheets (one Cb-752 and two different FS-85) used on the program.

2.1.2 Cladding Alloy Preparation

The initial phase of the effort was to prepare the modified B-1 alloy for bonding to the FS-85 core. The aluminum, which is essential to the oxidation resistance, tends to complicate the metallurgical processing of the alloy. In order to improve the fabrication characteristics and lower the ductile to brittle transition temperature the aluminum content was reduced from the original 3.0 percent (reference 1) to 2.5 percent. The object of this phase of the effort was to produce the modified B-1 alloy in a sheet approximately 0.2 centimeter thick for bonding to the FS-85 core.

2.1.2.1 B-1 Alloy Ingot Melting

The difficulty in melting the modified B-1 (Cb-15Ti-10Ta-10W-2Hf-2.5Al) alloy arises from the significant disparity in melting points between the elements. Ingots 7.1 centimeters in diameter were made by consumable electrode vacuum arc melting employing various combinations of master alloying and methods of electrode fabrication. The following procedures for making B-1 ingots were employed:

- (a) The initial B-1 ingot was cast from an electrode composed of elemental strips of the alloy constituents. The stack of strips was tack welded to form an electrode which was alternating current arc melted into a water-cooled copper mold 7.1 centimeters in diameter. The resulting ingot was quartered by cutting parallel to the billet axis, and small areas of tungsten segregation were noted in the

TABLE II
VENDOR CERTIFIED PROPERTIES OF BASELINE MATERIALS

ITEM	PROGRAM TASK AND ALLOY		
	I/Cb-752	II/FS-85	III/FS-85
NOMINAL CHEMISTRY	Cb-10W-2.5Zr	Cb-27Ta-10W-1Zr	Cb-27Ta-10W-1Zr
HEAT NUMBER	86 D 1185	85 D -2934	85 D -3009
R.T. TENSILE ULTIMATE	558 MN/m ² 81x10 ³ LB/IN ²	489 MN/m ² 71x10 ³ LB/IN ²	606 MN/m ² 88x10 ³ LB/IN ²
R.T. TENSILE YIELD	400 MN/m ² 58x10 ³ LB/IN ²	379 MN/m ² 55x10 ³ LB/IN ²	483 MN/m ² 70x10 ³ LB/IN ²
% ELONGATION IN 2.5 CM	23	21	20
ASTM GRAIN SIZE	8	8	8
DP HARDNESS	206	182	215
SHEET CHEMICAL CONSTITUENTS -- %			
Ta	-	27.5	26.90
W	10.45	10.4	10.50
Zr	2.62	0.85	1.0
C	0.0070	0.0016	0.0053
O	0.0170	0.0235	0.0153
N	0.0063	0.0040	0.0032
H	0.0005	0.0005	0.0005

center of the ingot. It was set aside, but later salvaged by dissolving the tungsten in the trough melter and reconsumable arc melting the ingot.

- (b) One ingot was prepared by nonconsumably melting four 2.5 centimeters wide by 58 centimeters long by 0.95 centimeter thick bars in a trough melter. Each charge was made to conform to the B-1 composition of Cb-15Ti-10Ta-10W-2Hf-25Al. Each bar was melted, inverted and remelted a second time in the trough melter. The resulting four bars were bundled together and tack welded to form a consumable electrode for vacuum arc melting. The second melt electrode was melted into a 7.1 centimeter diameter water-cooled copper mold using alternating current.
- (c) The next ingot was prepared in a similar manner except that the number and the compositions of the charges to the nonconsumable arc melts were modified. Two bars containing all the high melting point constituents, Cb-Ta-W were melted. The remaining four bars contained the low melting constituents, Ti-Hf-Al. Two bars of the Ti-Hf-Al composition were combined with two bars of the high melting constituents, Cb-W-Ta. This was done by melting one of each bar in the trough melter to produce a total four bars which when combined and consumably arc melted to produce the desired composition. The objective of this procedure was to reduce the disparity between melting points at each consolidation step, thus reducing the possible loss of aluminum and minimizing the possibility of unmelted tungsten in the final ingot. The four trough melted bars were bundled together and vacuum arc melted. The resulting 7.1 centimeter diameter ingot was cut into quarters parallel to the axis of the ingot, the quarter sections were butted end to end and welded to form an electrode and remelted.

The chemical analysis of the B-1 ingots is presented in table III. The small elemental differences between ingots, even in the cases where segregation was noted, indicated that the segregation was of minor significance.

2.1.2.2 B-1 Alloy Sheet Fabrication

Processing the B-1 ingots into sheet material for bonding to the FS-85 core was accomplished without difficulty and all ingots were processed in essentially the same manner. After the ingots were cleaned by machining, samples from the top and bottom were removed for chemical analysis. The ingots were then given a homogenization anneal at 1700°C for 3600 seconds. After the ingots were canned in mild steel, they were extruded at 1100°C with a 4 to 1 reduction ratio. The extruded bar was annealed at 1200°C, trimmed and cut into 12.7 centimeter lengths for forging. Forging, performed at 1100°C, reduced the B-1 plate to 0.95 centimeter thickness. In the case of one ingot (number 3 of table III), the forging was successfully accomplished without prior extrusion. After forging, the steel can was removed and the material was annealed at 1300°C for 3600 seconds. At this stage the material was

TABLE III
CHEMICAL ANALYSIS OF MODIFIED B-1 CLADDING ALLOY INGOTS

INGOT NO. AND LOCATION	MELTED PER PARAGRAPH	CONSTITUTENT WEIGHT PERCENT									
		W	Ta	Ti	Hf	Al	C	O	N	H	Cb
1 TOP	2.1.2.1a	9.92	10.22	14.75	1.97	2.15	0.0082	0.0320	0.0032	0.0004	B
1 BOTTOM		9.88	10.08	14.68	1.82	2.31	0.0089	0.0270	0.0048	0.0001	A
2 TOP (1)	2.1.2.1b	9.86	10.40	14.87	1.91	2.69	0.0090	0.0250	0.0049	0.0011	L
2 BOTTOM		9.94	10.48	14.83	1.95	2.62	-	-	-	-	A
3 TOP	2.1.2.1c	9.98	10.36	14.89	1.90	2.32	0.0100	0.0400	0.0053	0.0004	C
3 BOTTOM		10.10	10.42	14.83	1.96	2.25	-	-	-	-	E

NOTE: (1) THIS INGOT WAS SCRAPPED AND NOT USED.

OUTER PROTECTIVE SKIN

X-rayed to check for tungsten segregation. The final step was to reduce the material thickness to 0.2 centimeter by warm (315°C) rolling.

2.1.3 Bonding of Cladding to Core

Bonding of the B-1 oxidation resistant cladding to the FS-85 load bearing core was anticipated to be the most difficult part of the process. Roll bonding, considered to be the simplest and most straightforward approach, was tried first. It proved to be successful and was employed for all of the material used on the program.

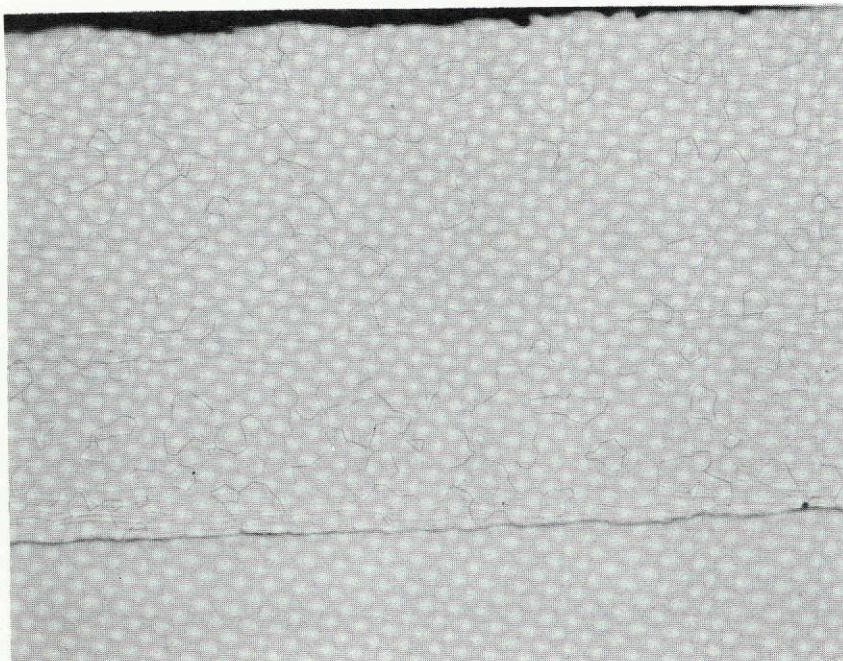
The first step in the roll bonding process was to clean the sheets by pickling. The sheets were assembled in packs of an appropriate combination and the edges were welded closed using the gas tungsten arc technique. A short length was left unsealed for evacuation, which was accomplished in an electron beam weld chamber. The final closure was made by electron beam welding and the packs were annealed at 1315°C for 3600 seconds. Each pack was placed in a stainless steel envelope, evacuated and sealed by electron beam welding. The bonding was then accomplished by hot rolling at 1090°C to obtain a 50 percent reduction, after which the material was removed from the stainless steel and the ends trimmed. The material was inspected by penetrant inspection, bend testing and metallographic examination, and was found to be well bonded by each inspection method. Figure 4 shows a typical joint after bonding. One surface of one pack (from a total of 12 packs) was found to be unbonded. The problem was traced to an incomplete weld in one area. This weld could have been found and repaired with more extensive weld inspection. Except for this minor occurrence, all bonding was 100 percent effective and accomplished with very little difficulty.

2.1.4 Reduction of Clad Sheet

After the B-1 alloy cladding was bonded to the FS-85 core, the material had to be reduced to the appropriate thickness. Several different pieces of equipment and rolling procedures were employed to produce the various batches of material. Since the primary purpose of the program was to evaluate the oxidation resistance and strength characteristics of the clad composite, an optimum fabrication schedule was not developed. A tight program schedule and availability of equipment were both factors in selecting the reduction procedures employed.

2.1.4.1 Rolling of Task I Material

The cladding thickness required for the desired level of redundant protection was recognized as the most significant factor in determining the ultimate potential of the outer skin protective system. Two cladding thicknesses, 51 micrometers and 76 micrometers, were established as the target B-1 thicknesses in the initial evaluation task. For the initial rolling, proportional reduction of the clad and core were assumed and the following three packs were prepared for bonding:



X75

FIGURE 4 MICROSTRUCTURE OF ROLL BONDED B-1/FS-85 AFTER ANNEALING AT 1315°C

This page is reproduced at the back of the report by a different reproduction method to provide better detail.

- (1) 0.4 cm FS-85 with 0.2 cm B-1 on each side,
- (2) 0.3 cm FS-85 with 0.15 cm B-1 on each side,
- (3) 0.2 cm FS-85 with 0.10 cm B-1 on each side.

When the FS-85 core reached the target thickness of 0.02 centimeter the cladding should have been 0.01 centimeter thick with the excess cladding to be removed by pickling. The roll bonding was accomplished at 1090°C, as previously described in Section 2.1.3, employing a 50 percent thickness reduction followed by an anneal at 1320°C to improve the metallurgical bond. Subsequent rolling to achieve final dimensions was accomplished on a 20 by 20 centimeter Stanat Laboratory Rolling Mill per the rolling schedule presented in figure 5. As the material approached the desired thickness, the B-1 quickly became workhardened, making rolling difficult. The mill was not stiff enough for the job and repeated passes were required for the necessary reductions.

Metallurgical examination of the material with the nominal 76 micrometer cladding showed the actual cladding thickness to vary between 65 and 80 micrometers. The interface between the cladding and the core was wavy and the cladding was slightly thicker on one side of the sheet. The material was considered reasonably good for the first attempt and well within the required quality for an effective evaluation for the initial task. The cladding having a nominal thickness of 51 micrometers was not of an acceptable quality for a meaningful evaluation. The cladding substrate interface was quite wavy with the cladding thickness varying between 10 and 32 micrometers on one surface and 18 and 43 micrometers on the opposite surface. Since approximately 25 micrometers of cladding was necessary to form the fused slurry silicide coating, there would have been many areas in which no cladding would have remained after coating. The material with the nominal 51 micrometer cladding was set aside and the nominal 76 micrometer clad material was carried into the coating and evaluation phase.

2.1.4.2 Rolling of Task 2 Material

The results of the evaluation of the material from the initial task were very encouraging, but the amount of cladding to achieve the desired level of redundant oxidation protection was still a major question. It was decided to make cladding thickness the major parameter to be evaluated during the testing, and the improvement of the clad-core interface to remove the waviness the primary objective of the clad material fabrication step. The same two target cladding thicknesses, 51 and 76 micrometers, established for the initial task were selected for the second task.

Roll bonding was accomplished as described in Section 2.1.3 with 3 units of B-1 cladding on either side of 8 units of FS-85 core material and a total pack thickness of 0.89 centimeter. One rolling schedule, presented in figure 6, was initially employed for both material thicknesses, with additional reduction used to obtain the thinner material. The intermediate anneal temperature (1150°C) was selected to match the flow stress of B-1 and FS-85. Tension rolling on a four-high mill was required to minimize cladding thickness

PROCESSING STEP	MATERIAL THICKNESS (cm)					
	PACK 1		PACK 2		PACK 3	
	THICK.	% RED.	THICK.	% RED.	THICK.	% RED.
INITIAL THICKNESS	0.81	-	0.58	-	0.41	-
ROLL BOND AT 1090°C AND ANNEAL 3600 SEC AT 1315°C	0.36	56	0.25	57	0.185	55
ROLL AT 315°C AND ANNEAL 3600 SEC AT 1200°C	0.178	50	0.120	52	0.0915	51
ROLL AT 315°C AND ANNEAL 3600 SEC AT 1200°C	0.071	60	0.071	41	0.056	38
ROLL AT 315°C AND ANNEAL 3600 SEC AT 1200°C	0.050	30	0.050	30	0.043	23
ROLL AT 315°C AND ANNEAL 3600 SEC AT 1200°C	0.037	26	0.043	14	0.036	16
PICKLE	0.036	-	0.030	-	0.030	-

FIGURE 5 ROLLING SCHEDULE OF B-1 CLAD FS-85
PREPARED IN TASK 1

OUTER PROTECTIVE SKIN

Report MDC E0913
September 1973

PROCESSING STEP	MATERIAL THICKNESS (cm)	
	THICKNESS cm	% REDUCTION
INITIAL THICKNESS	0.35	
ROLL BOND AT 1090°C AND ANNEAL 3600 SEC AT 1315°C	0.182	53
ROLL AT 315°C AND ANNEAL 3600 SEC AT 1150°C	0.117	36
TENSION ROLL AT RT AND ANNEAL 3600 SEC AT 1150°C	0.058	50
TENSION ROLL AT RT AND ANNEAL 3600 SEC AT 980°C (FOR NOMINAL 76 MICROMETER CLAD MATERIAL)	0.036	38
TENSION ROLL AT RT AND ANNEAL 3600 SEC AT 980°C (FOR NOMINAL 51 MICROMETER CLAD MATERIAL)	0.029	50

FIGURE 6 ROLLING SCHEDULE OF B-1 CLAD FS-85
PREPARED IN TASK 2

OUTER PROTECTIVE SKIN

variations by removing the waviness of the interface. The stiffer four-high mill proved to be a significant improvement over the mill used in the initial task.

When the clad sheet was inspected for thickness and uniformity by micrometer measurements and metallographic examination, the following values were obtained for cladding and core thicknesses for both groups of material:

	Desired Thickness	Total		Clad		Core	
		Centi-meters	Inches	Micro-meters	Mils	Micro-meters	Mils
First Group	Desired Thickness	0.0356	0.0142	76	3.0	203	8.0
	Actual Thickness	0.0356	0.0142	61	2.4	234	9.2
Second Group	Desired Thickness	0.0305	0.0120	51	2.0	203	8.0
	Actual Thickness	0.0294	0.0113	53	2.1	188	7.4

The interface between the cladding and the core was reasonably smooth and was a significant improvement over the initial material. The two thicknesses were to represent two parameters in the evaluation of the Task 2 material, but with such a subtle difference between the two claddings, it was decided to test only one thickness. The second, thinner group was eliminated because the cladding thickness was almost the same as that evaluated in Task 1 and the core thickness was more variable, averaging below nominal desired thickness. The additional rolling to achieve the thinner material primarily affected the core, with thickness as low as 0.015 centimeter (0.060 inch) observed. The first group had the more even core thickness and the greater cladding thickness, almost midway between the two desired thicknesses. Figure 7 shows a photo-micrograph of the B-1 cladding on the FS-85 core. The material was considered to be of good quality and was the material that was subsequently evaluated.

2.1.4.3 Rolling of Task 3 Material

The evaluation testing of the Task 2 material yielded good performance results and showed that the metallurgical quality of the material was good. An attempt was made to maintain the cladding/core interface smoothness and obtain two cladding thicknesses closer to the selected target values. Again 76 micrometers was one of the target B-1 cladding thicknesses but the actual material was approximately 15 micrometers less than desired. The second target thickness was 125 micrometers. This would provide a material for use in generating the desired oxidation data. This data was needed to select a cladding thickness for a heatshield panel. This thickness also was considered capable of providing valuable data which might be useful in the application of coated columbium to leading edges for hypersonic reentry vehicles.

200X

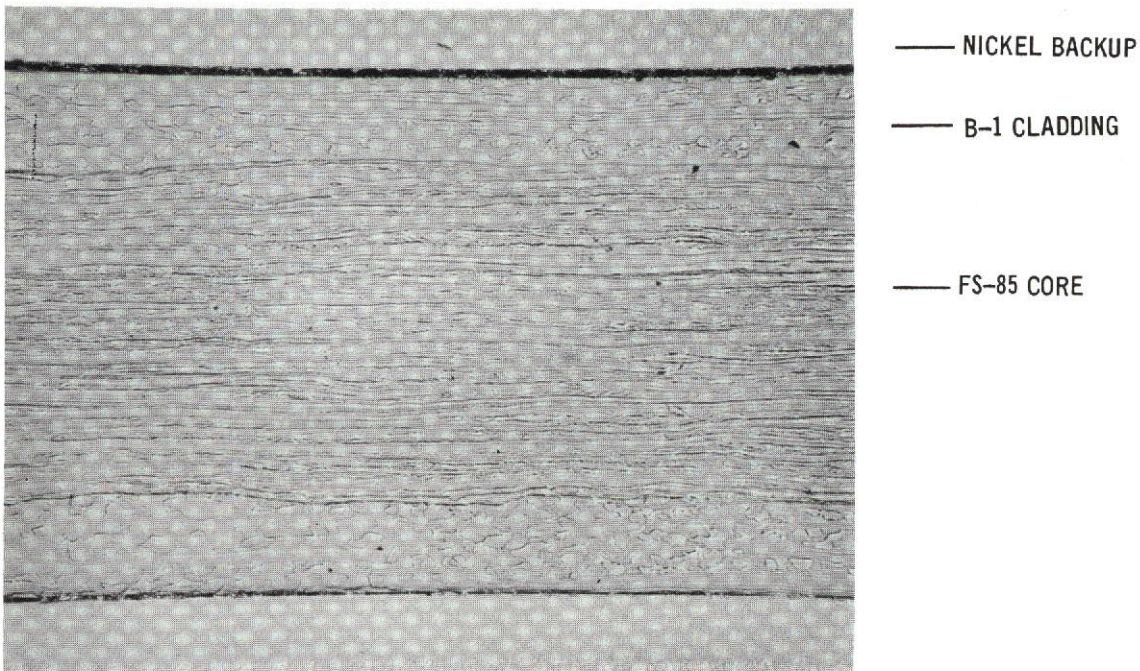


FIGURE 7 MICROSTRUCTURE OF B-1 CLAD FS-85

457-3402

This page is reproduced at the back of the report by a different reproduction method to provide better detail.

OUTER PROTECTIVE SKIN

The roll bonding was carried out as previously described. Two packs with 5 units of B-1 alloy on either side of 8 units of FS-85 core were assembled to produce the nominal 125 micrometer clad material. Similar packs with a 3-8-3 relationship were assembled to produce the nominal 76 micrometer clad material. The material was reduced to the desired thicknesses in accordance with the rolling schedule presented in figure 8. Tension rolling was employed to maintain the smooth interface as has been previously described. A minor amount of surface delamination occurred during the final rolling. The most severe defect area is shown in figure 9. The condition could have been caused by minor segregation within the B-1 or by excessive cold work without annealing. The defective areas were discarded without loss of the minimum required material for evaluation.

The clad sheet was inspected for thickness and uniformity by micrometer measurements and metallographic examination. The following values were obtained for the cladding and core thicknesses for both groups of material:

		Thickness in Centimeters		
		Total	Clad	Core
First Group	Desired Thickness	0.0356	0.0076	0.0203
	Actual Thickness	0.0320	0.0052	0.0216
Second Group	Desired Thickness	0.0457	0.0126	0.0203
	Actual Thickness	0.0440	0.0104	0.0216

The interface between the cladding and the core was reasonably smooth and was essentially the same as the material shown in figure 7. Both materials were considered to be of good quality and were evaluated in the final task of the program.

PROCESSING STEP	MATERIAL THICKNESS (cm)			
	PACKS 1 & 2		PACKS 3 & 4	
	THICK.	% RED.	THICK.	% RED.
INITIAL THICKNESS	0.898	-	0.716	-
ROLL BONDING AT 1090°C AND ANNEAL AT 1315°C	0.457	49	0.363	50
ROLL AT 315°C AND ANNEAL AT 1090°C	0.203	56	0.190	48
TENSION ROLL AT RT AND ANNEAL AT 1090°C	0.407	77	0.037	82

**FIGURE 8 ROLLING SCHEDULE OF B-1 CLAD FS-85
PREPARED IN TASK 3**

OUTER PROTECTIVE SKIN

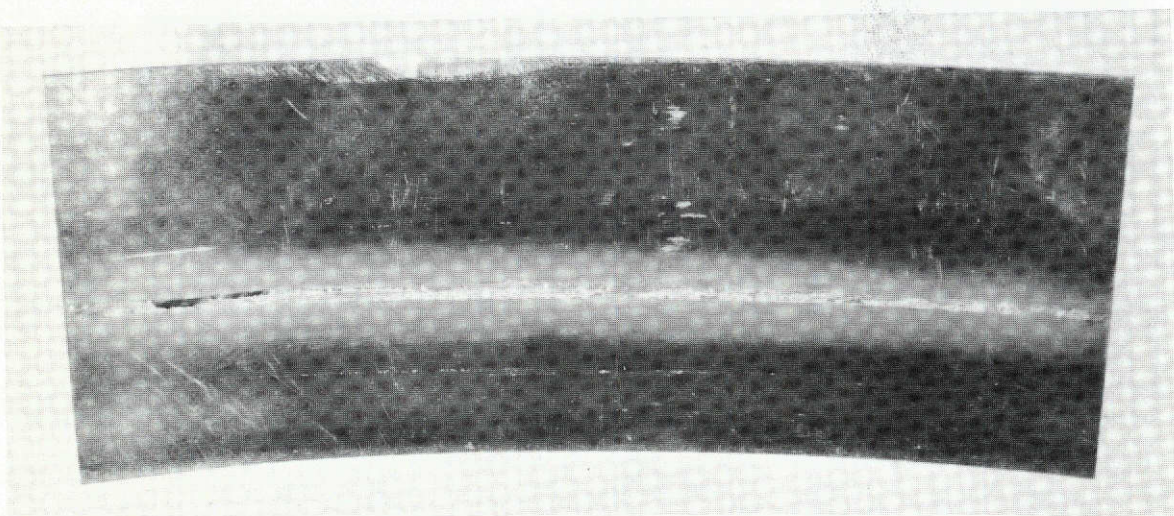


FIGURE 9 B-1 CLAD FS-85 PRODUCED DURING FINAL TASK SHOWING SURFACE DELAMINATIONS

This page is reproduced at the back of the report by a different reproduction method to provide better detail.

2.2 SPECIMEN PREPARATION AND COATING APPLICATION

The fused slurry silicide coating was designed into the system as the primary mode of oxidation protection for both the cladding and the load bearing core. Two coating compositions, 20Cr-20Fe-Si (R-512E) and 30Cr-20Fe-Si were selected during the system design, as described in paragraph 2.1.2. Evaluation of the coated composite required the fabrication of standard tensile and bend test specimens.

2.2.1 Specimen Preparation

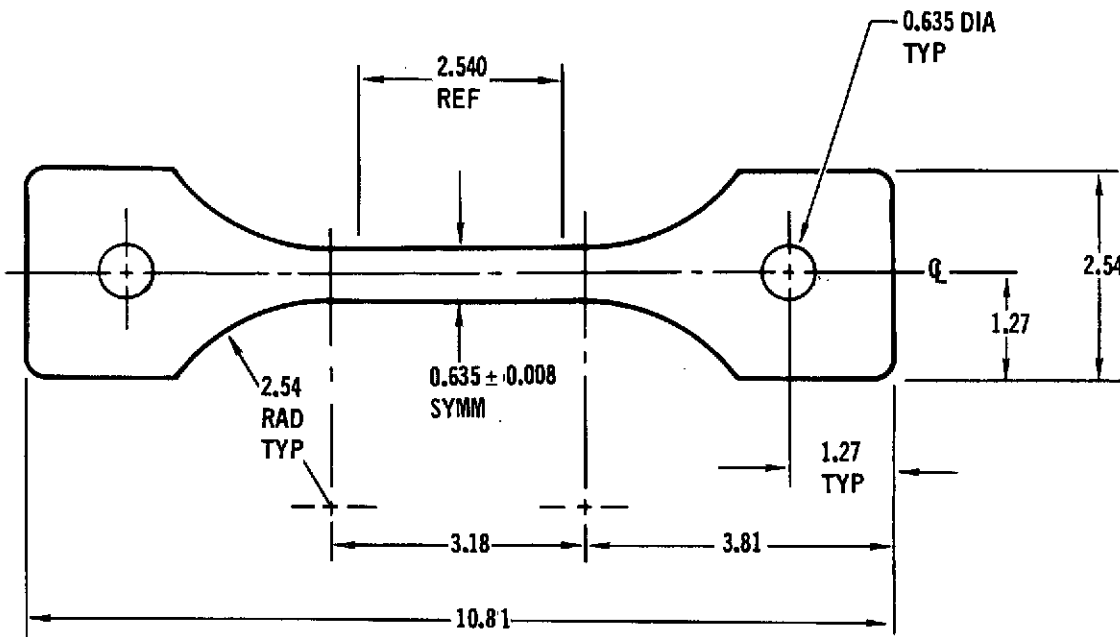
The B-1 clad FS-85 was fabricated into specimens for coating and evaluation. Bend coupons 2.5 by 5 centimeters, emittance specimens 2.5 by 2.5 centimeters and tensile coupons 2.5 by 10 centimeters as shown in figure 10 were fabricated using standard columbium alloy techniques. Shearing, drilling, machining (in the case of the tensile coupons) and edge preparation were accomplished without special handling and without difficulty. In no case did the B-1 cladding give an indication of becoming unbonded. It was found that steel stamping could be accomplished without detrimental effects to the cladding or the bond between the cladding and the core. The manufacturing procedures were acceptable and the results achieved were the same for the B-1 clad FS-85 and the Cb-752 and FS-85 baseline materials. Prior to coating, the thickness of each specimen and the gauge width of the tensile specimens were micrometer measured for coating thickness determination and for strength calculations.

2.2.2 Task One Coating Application and Performance

Two coating compositions, 30Cr-20Fe-Si and 20Cr-20Fe-Si (R-512E), were applied to the B-1 clad specimens and the R-512E was applied to the Cb-752 baseline. A dimensional change thickness of 51 micrometers per coated surface was requested (total coating thickness of 76 micrometers per surface). The following coating thickness results were determined.

TASK 1 AVERAGE COATING THICKNESS

Substrate and Coating	Coating Weight $\mu\text{kg}/\text{cm}^2$	Dimensional Change Thickness $\mu\text{m}/\text{surface}$	Total Coating Thickness $\mu\text{m}/\text{surface}$
R-512E/Cb-752	21.9	78	113
R-512E/B-1	21.2	87	130
30Cr-20Fe-Si/B-1	18.0	96	144



NOTE: ALL MEASUREMENTS ARE EXPRESSED IN CENTIMETERS

457-1393

FIGURE 10 TENSILE SPECIMEN

The R-512E coating on the Cb-752 baseline alloy had a normal coating structure, as shown in figure 11. The R-512E coating on the B-1 cladding alloy was slightly thicker and had a typical fused slurry silicide coating structure. Figure 12 shows the R-512E coating on the edge where a coating structure transition can be noted between the coating on the B-1 clad surface and the FS-85 alloy edge. The 30Cr-20Fe-Si composition on the B-1 clad material was the thickest. Most of the additional thickness was attributed to surface roughness, which has been previously noted with higher chromium content fused slurry silicide coatings (reference 7).

The performance of the coatings was generally good; each of the three alloy-coating composition systems has an intrinsic coating life in excess of 100 reentry profile exposure cycles. (Details of the exposure cycling are presented in Section 2.3.1.) There was, however, a minor problem with small coating failures on the edges of tensile specimens. Edge preparation of tensile specimens normally is held to a minimum so that the load bearing area will be constant and accurately known. It is probable that the major cause of the early edge failures was due to inadequate edge preparation. However, it was noted that more failures occurred on the specimens coated with the 30Cr-20Fe-Si composition than with the R-512E composition. The performance of the R-512E was slightly better than the 30Cr-20Fe-Si composition and the R-512E coating thickness was much more uniform. While both coating compositions were believed to meet the objectives of the program, the R-512E was considered superior and was selected for the remaining two evaluation tasks.

2.2.3 Task Two Coating Application and Performance

The R-512E composition was applied to the B-1 clad sheet and to the FS-85 baseline (the Cb-752 was eliminated as the baseline). The requested nominal dimensional change coating thickness was 51 micrometers per surface, which would produce a total coating thickness of 76 micrometers per surface. The R-512E coatings received were 51 and 53 micrometers thick, respectively for the B-1 clad specimens and FS-85 baseline. The coatings for both alloys were uniform and consistent in thickness and structure, as shown in figure 13. The oxidation performance of both alloy-coating combinations was good. None of the undefected coupons experienced oxidation failures through 100 profile reentry cycles, and only three small edge failures occurred after 100 profile exposure cycles under reentry conditions.

2.2.4 Task Three Coating Application and Performance

The R-512E was applied to the B-1 clad and FS-85 baseline alloy specimens. The requested dimensional change coating thickness was 51 micrometers. The actual thicknesses received for the B-1 and FS-85 specimens were 48 and 41 micrometers, respectively. The coating microstructure was normal in appearance, uniform in thickness and generally the same as the previously received second task specimen shown in figure 13. The coating performance was generally good with one major exception. There were no coating oxidation failures after 100 profile exposure cycles for the coupons, emittance specimens, or profile cycles underload. The coating and clad microstructures after 100 cycles were normal and indicated good coating performance (see paragraph 2.3.2.2). An

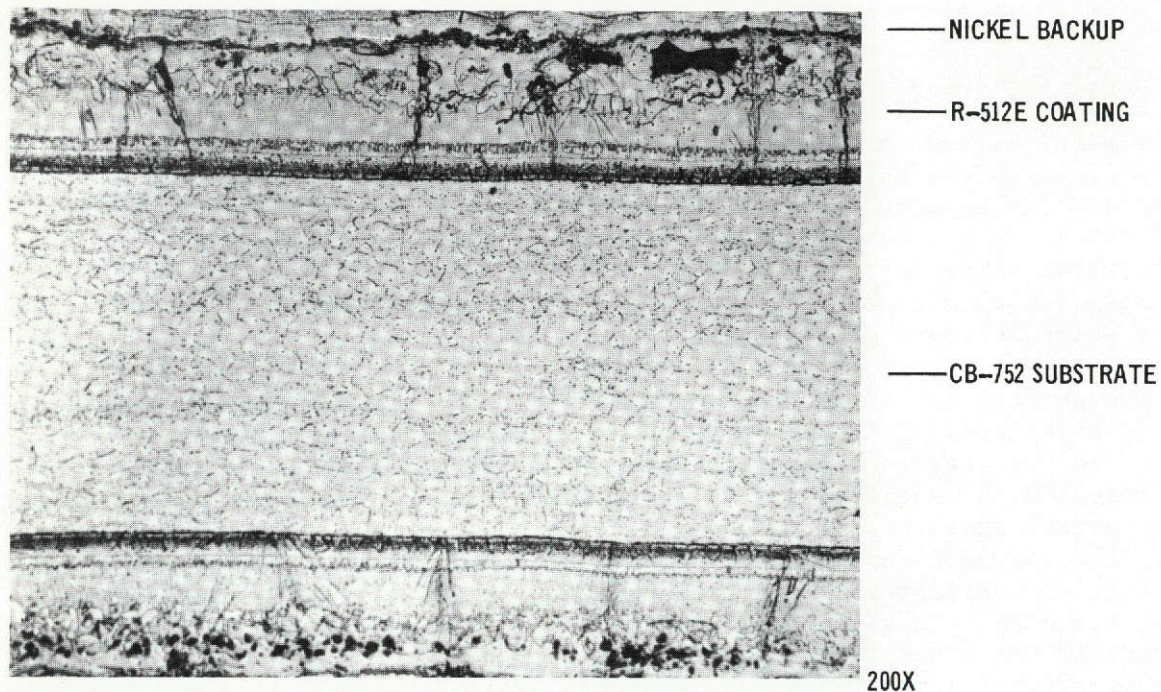


FIGURE 11 R-512E COATING ON CB-752

This page is reproduced at the back of the report by a different reproduction method to provide better detail.

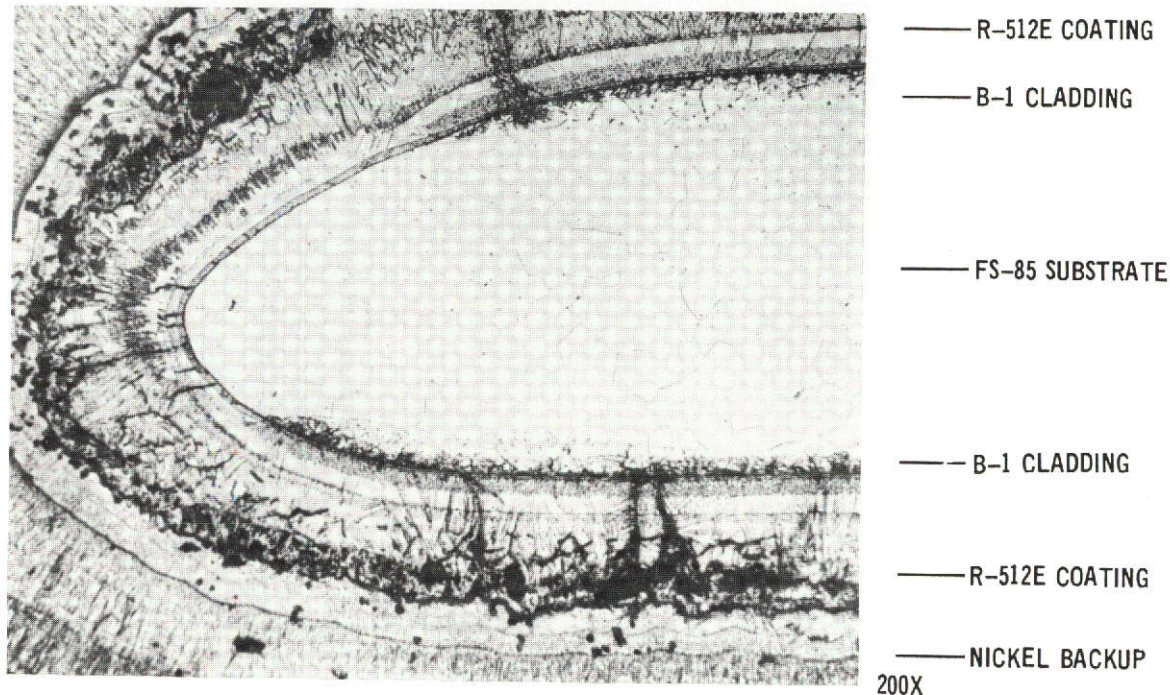


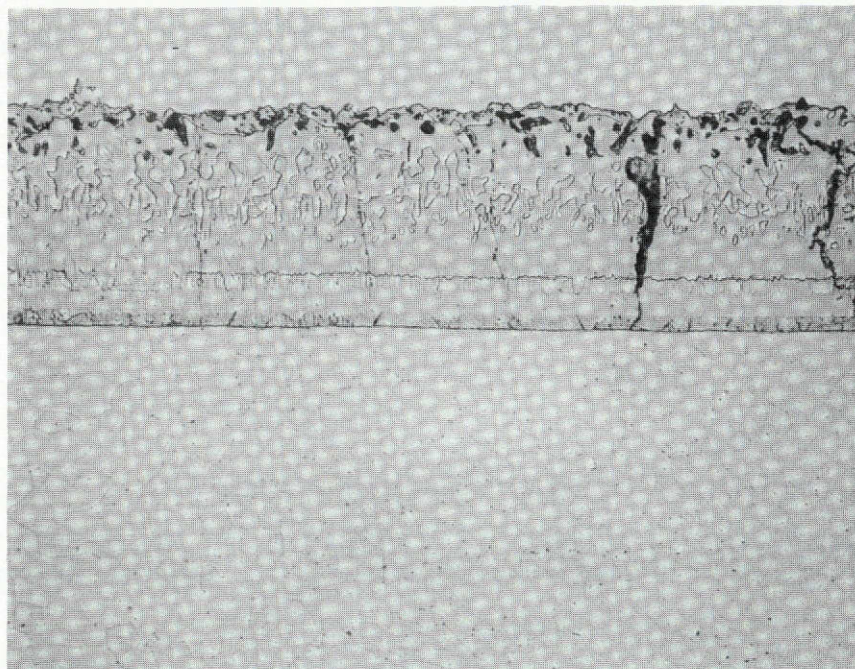
FIGURE 12 MICROSTRUCTURE OF R-512E COATING ON FS-85 (EDGE) AND B-1 (SURFACE)

This page is reproduced at the back of the report by a different reproduction method to provide better detail.

OUTER PROTECTIVE SKIN

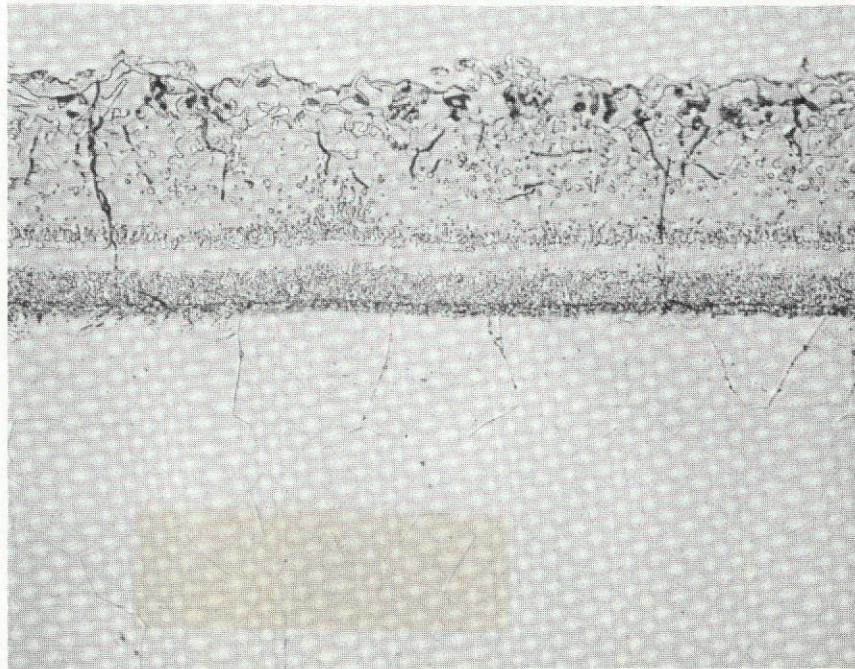
Report MDC E0913
September 1973

400X



FS-85 BASELINE

400X



B-1 CLAD FS-85 COMPOSITE

FIGURE 13 MICROSTRUCTURE OF R-512E COATING AS APPLIED IN TASK NO. 2

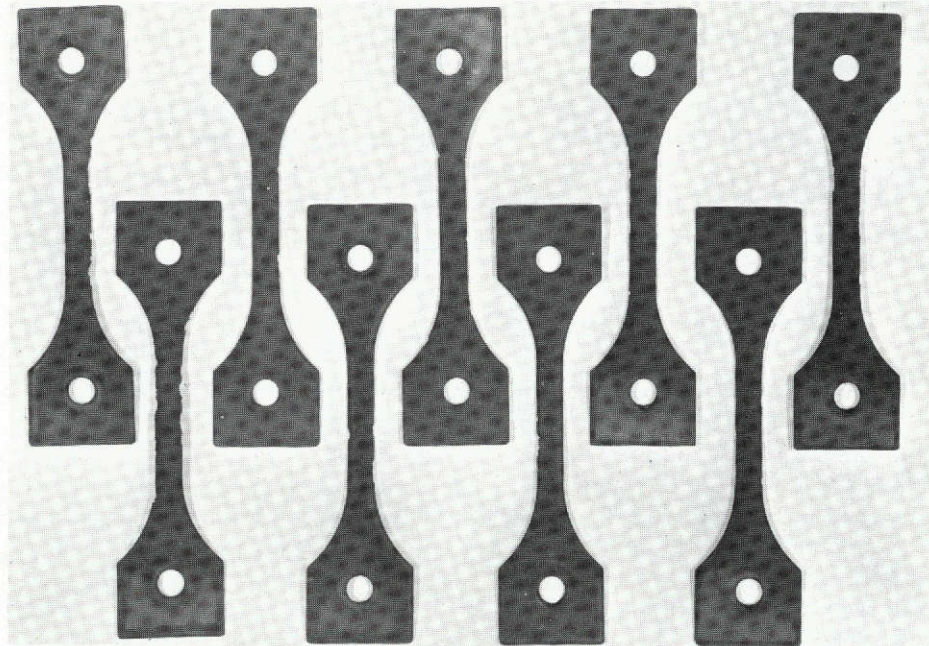
457-3403

This page is reproduced at the back of the report by a different reproduction method to provide better detail.

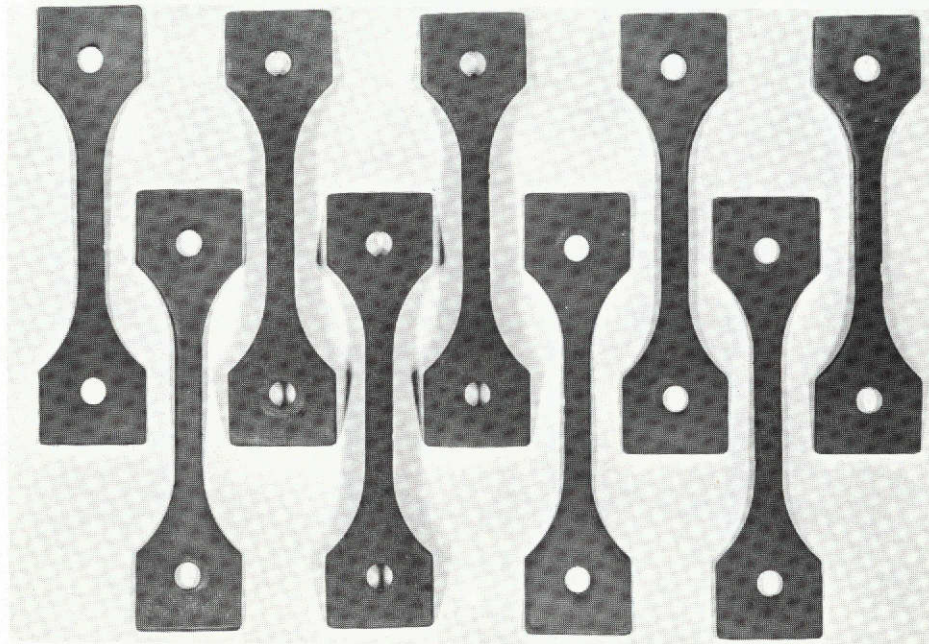
anomaly occurred with the clad tensile specimens during the 100 cycle exposure when numerous oxidation failures (shown in figure 14) occurred between the 88th and 100th cycle. Examination of metallographic sections made from both clad systems adjacent to an oxidation failure site did not reveal an obvious weakness in the protective system or the reason for the unusual premature failures. Figure 15 shows the edge microstructure observed for each of the clad systems. While incipient coating failures were observed in both specimens, the edges did not appear to be excessively sharp and the coating was of adequate thickness.

2.2.5 General Coating Observations

The fused slurry silicide coating performed very well, with few exceptions. The R-512E composition provided acceptable protection to the B-1 alloy for 100 reentry profile exposure cycles. The R-512E was generally in slightly better condition on the FS-85 baseline alloy tends to indicate that some improvements in the coating for B-1 could be achieved through compositional studies. The observations made indicate that the two different coating structures, which are contiguous at cladding termination points, are structurally and chemically compatible. Since coatings fail first on the edges as compared with surfaces, and the cladding terminated at the edges, it is not possible to differentiate between the two possible causes of edge failures. Additional studies of edge failure mechanisms and coating compositional edge effects are required to determine if coating life improvements at the point of cladding termination could be made.



50 μ m B-1 Clad Specimens



100 μ m B-1 Clad Specimens

FIGURE 14 R512E COATED TENSILE SPECIMENS SHOWING OXIDATION SITES AFTER
100 REENTRY PROFILE EXPOSURE CYCLES

This page is reproduced at the back of the report by a different reproduction method to provide better detail.

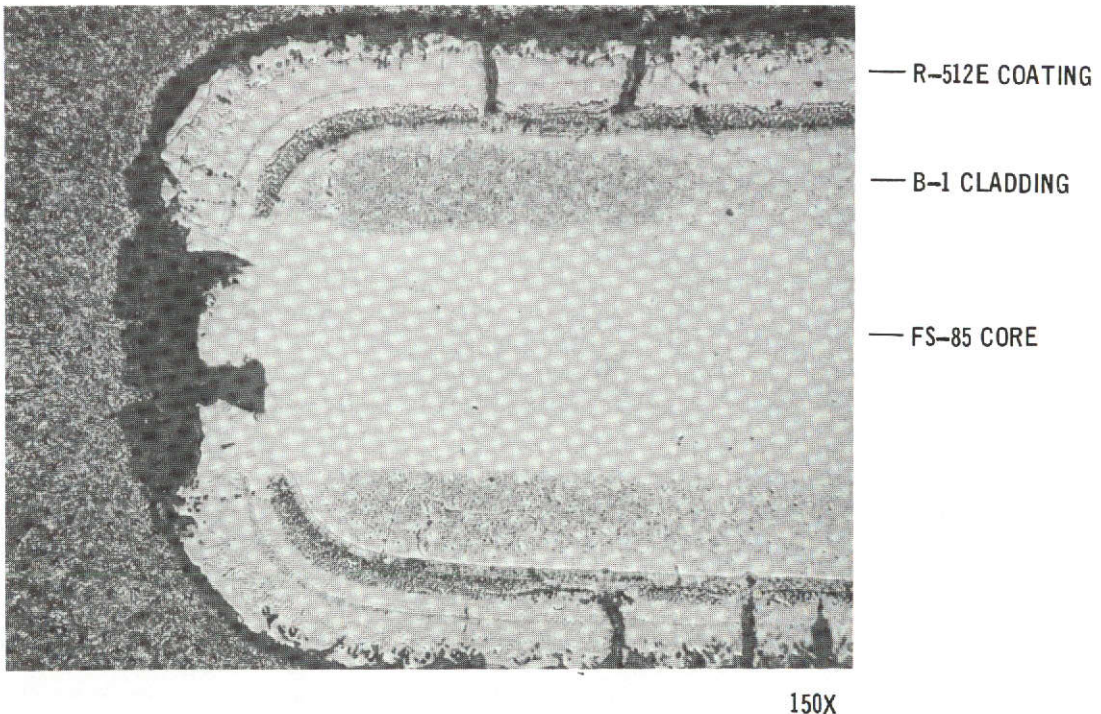
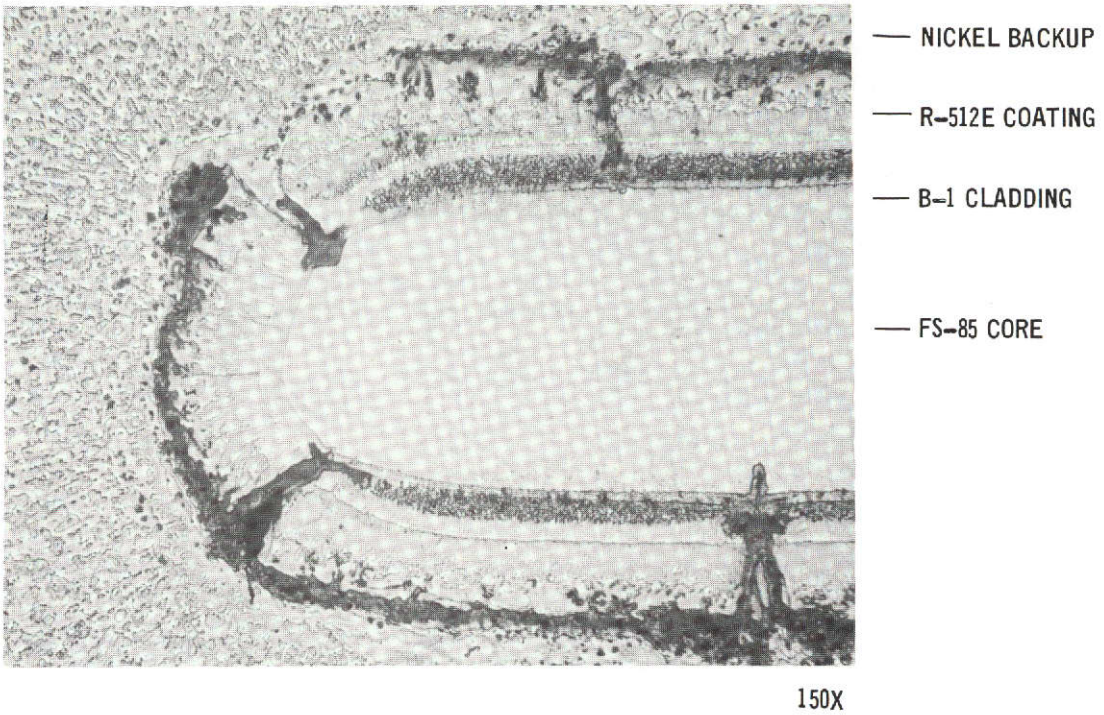


FIGURE 15 EDGE MICROSTRUCTURE OF R-512E COATED CLAD TENSILE SPECIMENS
ADJACENT TO COATING FAILURES OCCURRING WITHIN 100 REENTRY
PROFILE CYCLES

This page is reproduced at the back of the report by a different reproduction method to provide better detail.

2.3 OXIDATION RESISTANCE EVALUATION

The primary purpose of the cladding was to provide a secondary zone of oxidation protection in the event of the damage to the fused slurry silicide coating. Thus a significant portion of the evaluation involved removing the coating in a local area and determining the amount of protection afforded by the oxidation resistant cladding. The test conditions were selected to simulate the important environmental parameters of reentry. A standard highly reproducible defect was employed to obtain a precise comparison between clad systems and also between clad and unclad systems.

2.3.1 Evaluation Test Procedure

Coupons 2.5 by 5 centimeters were fabricated from the B-1 clad and unclad baseline alloy to be evaluated. The edges of the coupons were dressed to remove burrs and sharp edges and fused slurry silicide coated. Although the primary coating was the R-512E (20Cr-20Fe-Si), a 30Cr-20Fe-Si composition was included in the evaluation for the initial task. The defect performance of the cladding was the same for both coating compositions, and the coating performance is presented in paragraph 2.2. In all three tasks a nominal cladding thickness of 50 micrometers was evaluated and produced virtually the same results in each experiment. The final task included a nominal 100 micrometer cladding. In each experiment, an unclad coated columbium alloy was included in the evaluation to provide a baseline for comparison. The initial task employed R-512E coated Cb-752 and the two final tasks employed R-512E coated FS-85 alloy.

Defects were cut through the coating to the underlying cladding or columbium alloy interface by gritblasting with minus 220 mesh aluminum oxide. A mask was secured to the specimen to protect all areas except the 0.15 centimeter defect area. Blasting was done carefully so that the coating was removed without cutting into the columbium. A 10-power stereomicroscope was employed to assure that all of the fused slurry silicide coating was removed. Prior to defecting the specimens, a metallographic examination confirmed that the procedure used did indeed completely remove the coating without cutting into the columbium.

Reentry profile exposure cycling was accomplished in the apparatus shown in figure 16. The specimens to be exposed were positioned in the center of the hot zone of the 4.5 centimeter diameter tube furnace. The temperature, air pressure and stress were varied independently as a function of reentry time by a system of automated programmers, controllers, and recorders. The test conditions used are shown in figure 17. These were selected because they represent a broad range of hypersonic reentry conditions and are the same as those employed on other current columbium evaluation programs (references 7 and 9). Exposure cycles were performed in groups of 22, unless fewer were required to achieve a specific desired number of cycles.



457-3404

FIGURE 16 TEST APPARATUS USED FOR REENTRY PROFILE EXPOSURE CYCLING

This page is reproduced at the back of the report by a different reproduction method to provide better detail.

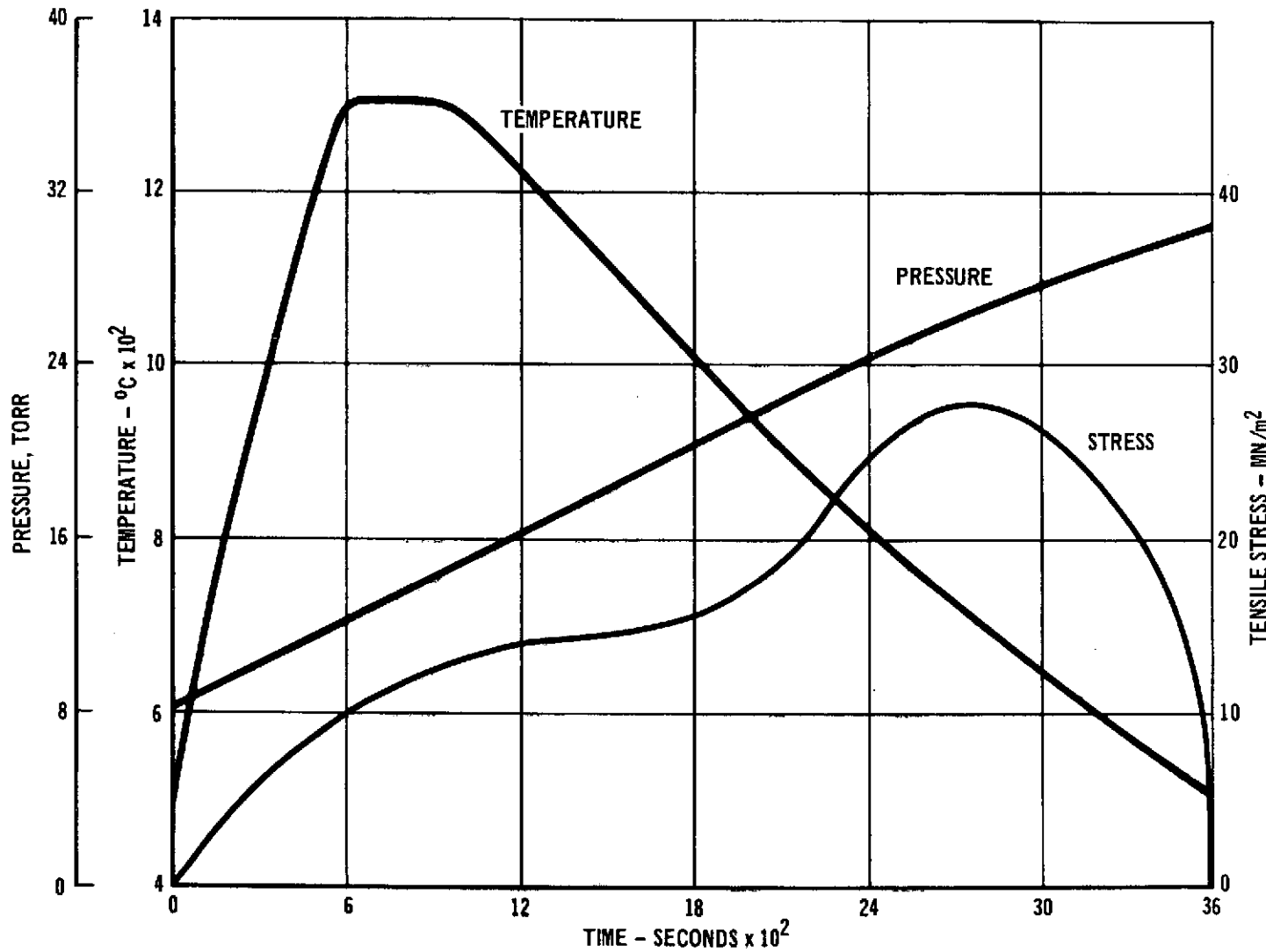


FIGURE 17|TEST CONDITIONS USED FOR REENTRY PROFILE EXPOSURE TESTING

457-3405

Reentry profile exposure cycles were imposed on B-1 clad and equivalent numbers of unclad baseline specimens. Defected coupons were exposed to 1, 3, 5, 10, 15, and 50 cycles while undefected specimens were exposed to 100 profile cycles. Visual inspection was employed to assess the progress of oxidation in defect areas and to determine general coating performance. After exposure cycling, bend testing was accomplished through an area which was not defected. A 4T bend radius was used in the initial task. Since no failures occurred, subsequent tasks employed a 2T bend radius for a more stringent evaluation. Metallographic examination through the center of the defect area was used in conjunction with microhardness testing to assess the internal condition of the columbium alloy cladding and core.

2.3.2 Defect Exposure Evaluation Results

Oxidation of columbium alloys produces two distinct effects to be considered. The first, easily observed by visual examination is the formation of columbium oxide (Cb_2O_5). The primary consideration of the gross oxidation is the loss of load bearing cross section of the columbium alloy, followed within moderate time duration by a hole through the sheet. The second effect is the solution of oxygen within the sheet below the oxidation site, which, in the case of a local coating defect, is larger than the area affected by the gross oxidation. The properties of the columbium are altered in the area contaminated by the oxygen solution. Strength may increase or decrease depending on the alloy and the oxygen content, with embrittlement in such areas to be expected. The ultimate significance of these oxidation effects depends upon the application and the design criteria. Since both effects are considered undesirable for reentry heatshields, the object of the cladding was to eliminate or substantially minimize them. Therefore, the performance of the cladding was evaluated for mitigation of both effects.

Results of exposure testing for the defected coupons and tensile specimens for all tasks were virtually the same and with respect to oxidation and will be reported collectively, with only the significant differences pointed out. Table IV presents the scope of the coating defect exposure testing performed.

OUTER PROTECTIVE SKIN

TABLE IV
INTENTIONAL COATING DEFECT TESTING SCOPE

TASK NO.	NO. OF MATERIAL SYSTEMS EVALUATED	NUMBER OF COUPONS AND TENSILE SPECIMENS PER CYCLIC EXPOSURE CONDITION						
		0	1	3	5	10	15	50
1	3	3	3	3		3		3
2	2	8	8	8		8		8
3	3	6	12	12	10	12	10	6

2.3.2.1 Evaluation of Metal Consumption Oxidation

Metal consumption through oxidation at local coating defect sites was evaluated by loss of load bearing columbium. Figure 18 shows representative samples from the task 3 exposure tests and illustrates the oxidation retarding characteristic of the B-1 cladding exhibited in each experiment. Table V presents the average data on the columbium substrate consumption. The results are considered to be valid for system comparisons. Specimens for each material system were exposed concurrently to insure equivalent conditions. The particular profile (used to evaluate patterns of oxidation behavior) is representative of a broad class of hypersonic reentry vehicles. Should absolute oxidation rate data be desired, one would need to apply the specific parameters of interest.

The baseline materials (Cb-752 and FS-85) began to oxidize immediately, losing approximately 40 micrometers in one cycle, oxidizing through the sheet in approximately 20 cycles and growing to a 1 centimeter diameter hole in 50 cycles. The B-1 clad systems followed a slightly different sequence of events. Initially, the cladding in the defect area absorbed oxygen by solution and oxidized slowly. Cladding recession losses in one cycle were undetectable or up to approximately 12 micrometers, depending upon the volume of cladding present in the defect area. The nominal 50 micrometer cladding required approximately 16 cycles to be consumed. After the cladding was lost in the defect area, the core began to lose load bearing cross section through oxidation, but the rate of consumption was reduced by the presence of adjacent cladding. The number of cycles to oxidize through the core varied considerably due to the effects of cracks in the defect area. The formation of the bulky columbium oxide in a defect site causes stresses in the coating and the columbium sheet around the defect. Typically, radial cracks (longitudinal in cross section) form in the columbium below the coating on the defect side of the sheet. The occurrence and propagation of these cracks have a significant influence upon the volume of columbium lost and the number of cycles required to form a hole through the sheet. Thus, one 50 micrometer clad specimen

Reentry Profile Cycles

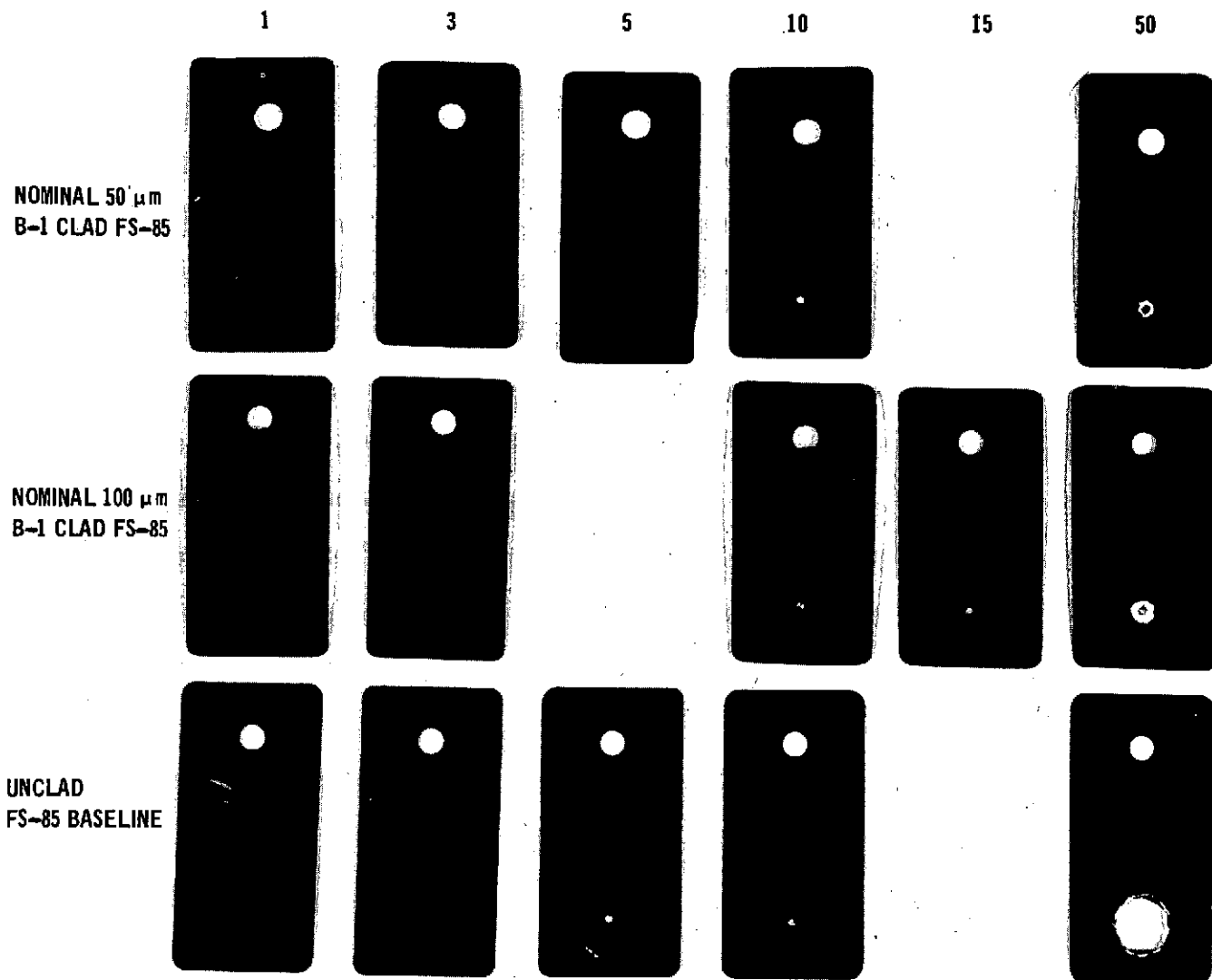


FIGURE 18 R-512E COATED COUPONS WITH INTENTIONAL COATING DEFECTS
AFTER VARIOUS PROFILE EXPOSURE CYCLES

TABLE V
OXIDATION OF B-1 CLAD FS-85 AND UNCLAD COLUMBIUM ALLOY
AT AN INTENTIONAL COATING DEFECT SITE

OXIDATION CHARACTERISTIC IN AREA OF INTENTIONAL COATING DEFECT OF 0.15 CENTIMETERS	AVERAGE OXIDATION VALUE PER MATERIAL SYSTEM			
	100 μ m B-1 CLAD FS-85	50 μ m B-1 CLAD FS-85	FS-85 ALLOY BASELINE	Cb-752 ALLOY BASELINE
PROFILE CYCLES TO OXIDIZE THROUGH CLADDING	16	5	-	-
CLADDING OXIDATION RECESSION RATE (μ m/CYCLE)	6	10	-	-
ESTIMATED CYCLES TO OXIDIZE THROUGH CORE OR BASELINE SUBSTRATE	44	32	21	19
RATE OF CORE OR SUBSTRATE RECESSION (μ m/CYCLE, AV. FOR 50 CYCLES)	0.49	0.63	0.96	1.2
HOLE DIAMETER OCCURRING IN 50 CYCLES (cm)	0.15	0.15	0.96	95
VOLUME OF CORE OR SUBSTRATE OXIDIZED IN 50 CYCLES (mm ³)	1.06	1.28	23.78	17.1

did not oxidize through the total thickness within 50 cycles, while most 50 cycle specimens had a through-hole in an estimated 32 cycles. The shapes of the oxidized holes were very irregular. The holes for the samples that did break through were 0.15 centimeter in diameter, which was the same diameter as the original defect. The loss rate of the FS-85 core was a combination of oxidation and fracturing of small sections of columbium. The beneficial influence of the cladding in retarding oxidation and local cracking was dramatically illustrated by the total volume of columbium consumed in 50 cycles. The unclad FS-85 baseline had an average volume loss of 23.78 cubic millimeters with the 50 and 100 micrometer thick B-1 clad specimens losing an average core volume of 1.28 and 1.06 cubic millimeters, respectively.

The effect of oxidation in a heatshield panel for reentry applications has two distinct considerations. The loss of strength is the most obvious yet not the most significant since the presence of a local oxidation spot, even a hole through a skin, has been shown to have very little influence on the structural performance of a panel (references 7 and 9). The effects of a hole in a skin which would allow leakage of hot boundary layer gases into the interior of a vehicle or cause a local perturbation of the boundary layer could be a very serious problem. The ability of the cladding to retard hole formation and substantially limit the total volume of columbium consumed in a coating defect area is a significant and important advantage of this system.

2.3.2.2 Bend Test and Metallographic Evaluation

After exposure testing, the coupons were mechanically evaluated by bend testing and metallographically examined. Bend testing was accomplished at room temperature using a 4T bend radius during the initial experiment and a 2T bend radius for the subsequent experiments. In each case the coupons were bent through a minimum relaxed angle of 105 degrees and no fractures were experienced.

Metallographic sections were prepared for each material system and cyclic profile condition for each defect coupon or tensile specimen during each task. The purpose was to assess the metallurgical condition of the core, cladding, and coating, and to determine the penetration of oxygen into the load bearing substrate adjacent to the coating defect. The penetration of oxygen was defined as the distance from the edge of the coating defect to the point at which the microhardness values reached a stable nominal sheet level. The average oxygen penetration, determined by microhardness testing, is presented in figure 19. The unclad FS-85 showed the typical diffusion controlled parabolic oxygen penetration depth values expected. The beneficial qualities of the B-1 claddings were significant, both in the short term effects and after 50 cycles. For both cladding thicknesses the oxygen contamination was limited to the immediate area of the defect until the cladding was consumed by oxidation. This phase was followed by the further contamination of the core radially but at a significantly lower rate than was the case for the unclad FS-85 baseline material.

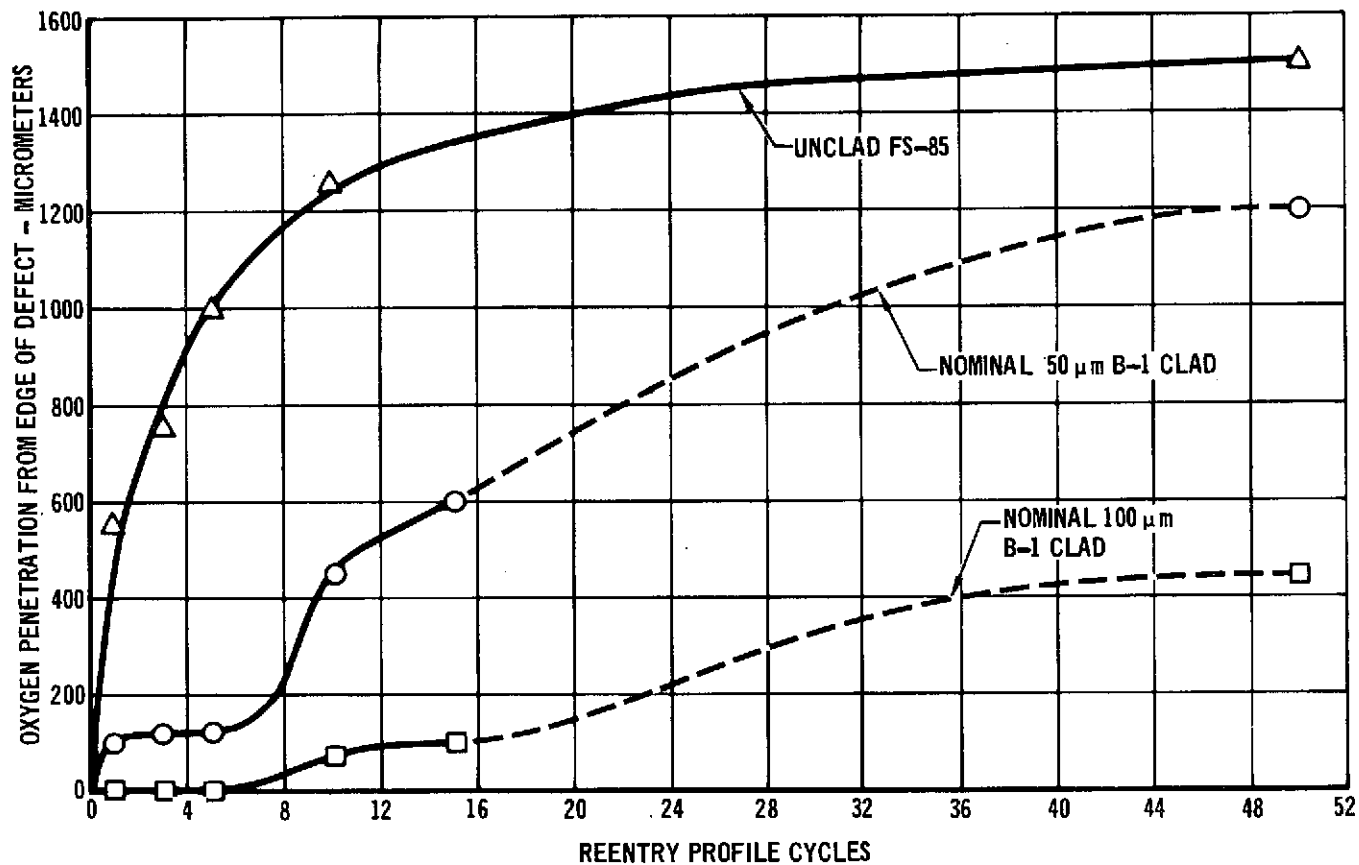


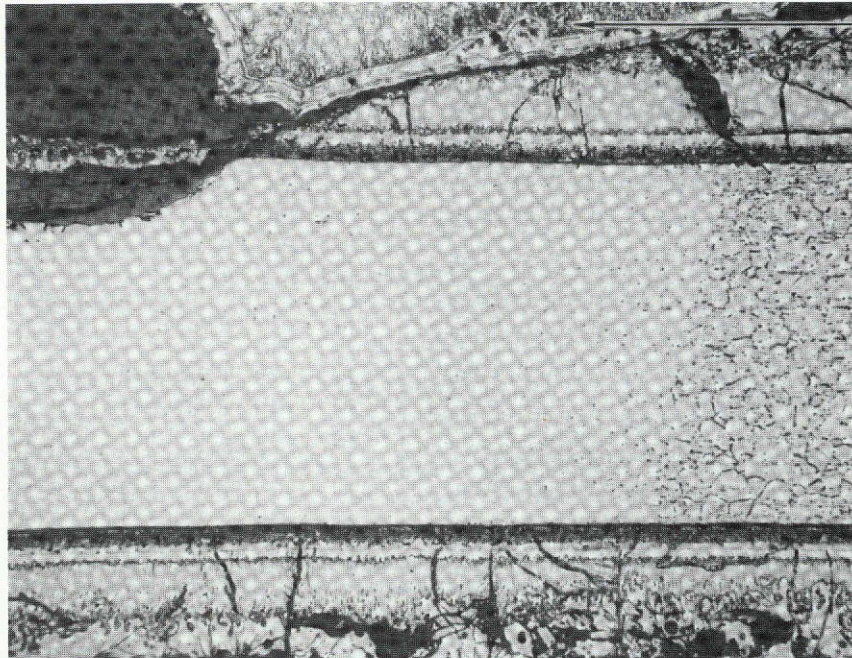
FIGURE 19 DEPTH OF OXYGEN PENETRATION IN B-1 CLAD AND UNCLAD FS-85 ALLOY

Metallographic examinations conducted were extensive and yielded a visual model which was consistent with the other test results achieved. It was found that the metallographic results obtained during the various experiments were consistent for both the clad and the baseline systems. Each exposure cycle is discussed separately and the various material systems are compared.

- (a) Results of One Profile Exposure Cycle - Within one exposure cycle the oxidation of the baseline FS-85 and Cb-752 was well underway as shown in figure 20. In addition to the substrate surface recession, the embrittled oxygen contamination zone had progressed below the coating into the substrate an average of 450 micrometers. The two B-1 clad thicknesses, after one cycle, are shown in figure 21. The nominal 50 micrometer B-1 clad samples showed a slight surface recession of cladding but no loss of FS-85 core material. An oxygen contamination zone occurred within the darker, etched portion of the B-1 clad. The rapid diffusion of oxygen through the FS-85 core was illustrated by the mirror image of oxygen contamination within the cladding on the opposite side of the core from the defect. The hardness increase in the FS-85 core showed the core in the defect area to be contaminated with oxygen and embrittled. The increased hardness was restricted to the defect area and bounded by the visual limits of contamination of the B-1 cladding. The nominal 100 micrometer B-1 cladding had sufficient volume of cladding to absorb the incoming oxygen. No cladding recession was noted and no oxygen contamination of the FS-85 core below the defect or on the opposite surface of cladding occurred. The etching of the contaminated zone shows three distinct areas of oxygen content gradation. This pattern was typical for the B-1 in all exposure conditions and is particularly clear in figure 21 because of the single exposure cycle.
- (b) Results of Three Profile Exposure Cycles - The condition of the two clad systems and the unclad baseline was qualitatively similar to the single condition. The unclad baseline experienced continued surface recession and the hardness increase of oxygen progressed parabolically (see figures 22 and 23). The 50 micrometer thick B-1 cladding appeared virtually the same as the one cycle specimen with the incoming oxygen being absorbed within the cladding and core of the defect area, without increasing the extent of the contamination (see figure 22). The nominal 100 micrometer cladding is shown in figure 23. The incoming oxygen continued to be absorbed in the exterior cladding. A small amount of cladding surface recession was observed, but no increase in the hardness of the core was found.
- (c) Results of Five Profile Exposure Cycles - After five reentry profile cycles significant changes occurred in both cladding systems. The unclad FS-85 continued the previously noted behavioral pattern of surface recession and parabolic oxygen penetration into the substrate beneath the coating. Figure 24 shows the unclad FS-85 after five

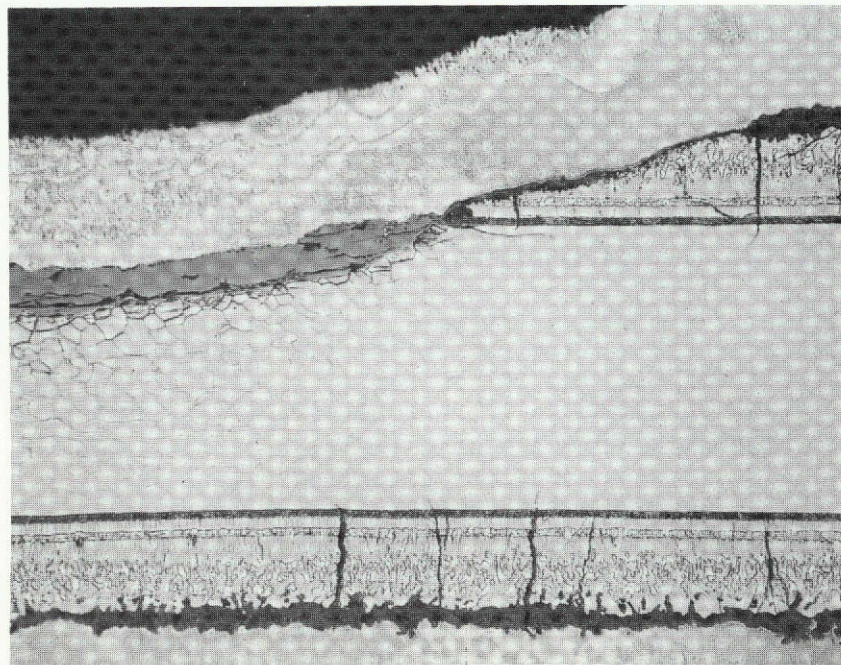
OUTER PROTECTIVE SKIN

200X



UNCLAD Cb-752

200X



UNCLAD FS-85

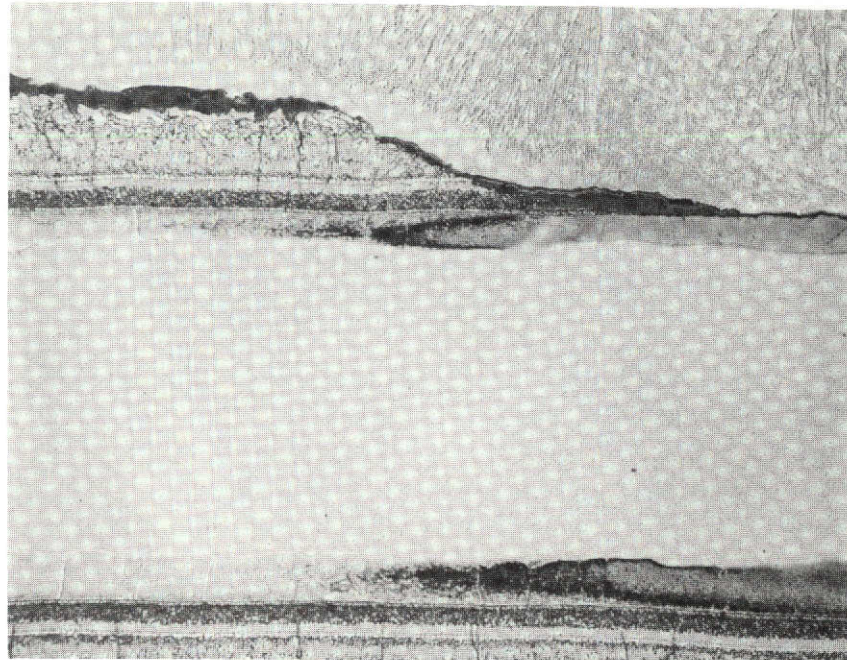
This page is reproduced at the back of the report by a different reproduction method to provide better detail.

FIGURE 26 EFFECT OF ONE PROFILE EXPOSURE ON UNCLAD BASELINE ALLOYS

OUTER PROTECTIVE SKIN

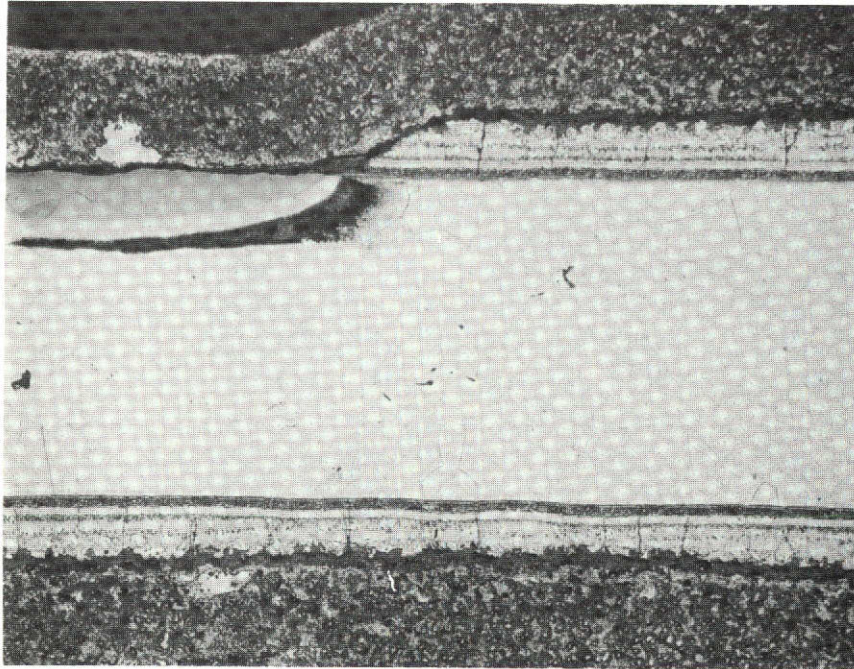
Report MDC E0913
September 1973

NICKEL BACKUP _____
R-512E COATING _____
B-1 CLADDING _____
FS-85 CORE _____



NOMINAL $50 \mu\text{m}$ B-1 CLAD

100X



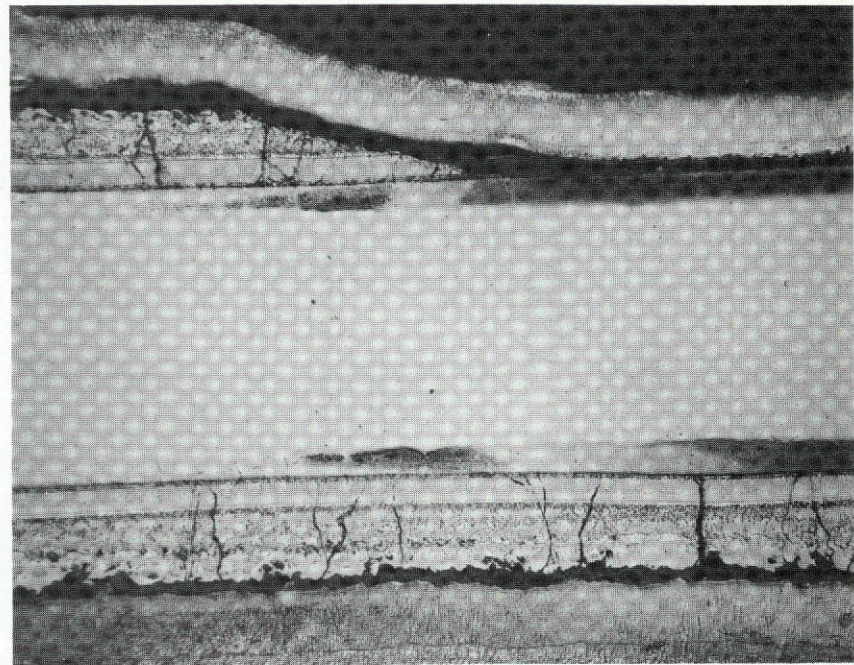
NOMINAL $100 \mu\text{m}$ B-1 CLAD

This page is reproduced at the back of the report by a different reproduction method to provide better detail.

FIGURE 21 EFFECT OF ONE PROFILE EXPOSURE CYCLE ON B-1 CLAD FS-85

OUTER PROTECTIVE SKIN

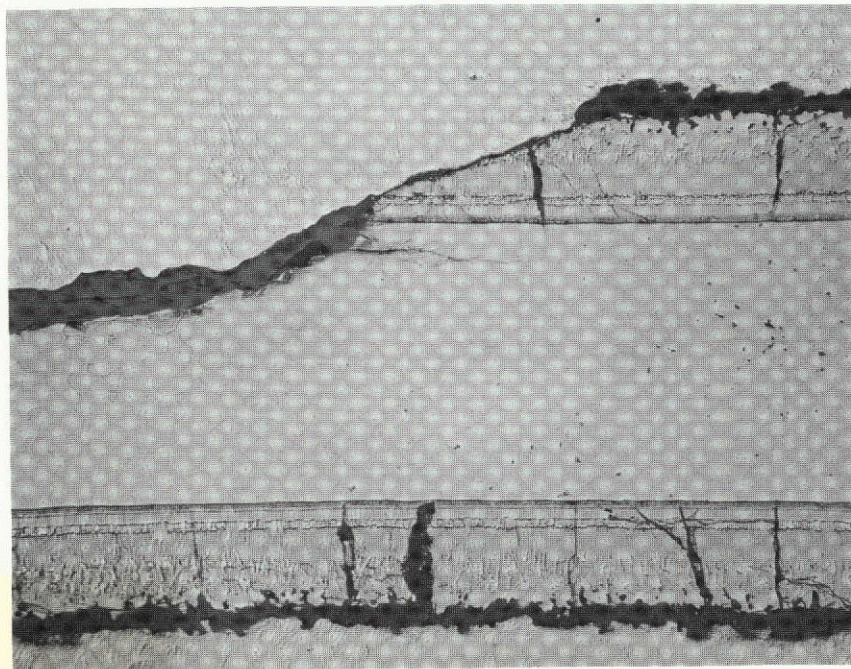
NICKEL BACKUP —
R-512E COATING —
B-1 CLADDING —
FS-85 CORE —



180X

NOMINAL 50 μ m B-1 CLAD

200X



— NICKEL BACKUP
— R-512E COATING
— FS-85 SUBSTRATE

UNCLAD FS-85

457-3409

FIGURE 22 EFFECT OF THREE PROFILE EXPOSURE CYCLES
ON CLAD AND UNCLAD FS-85

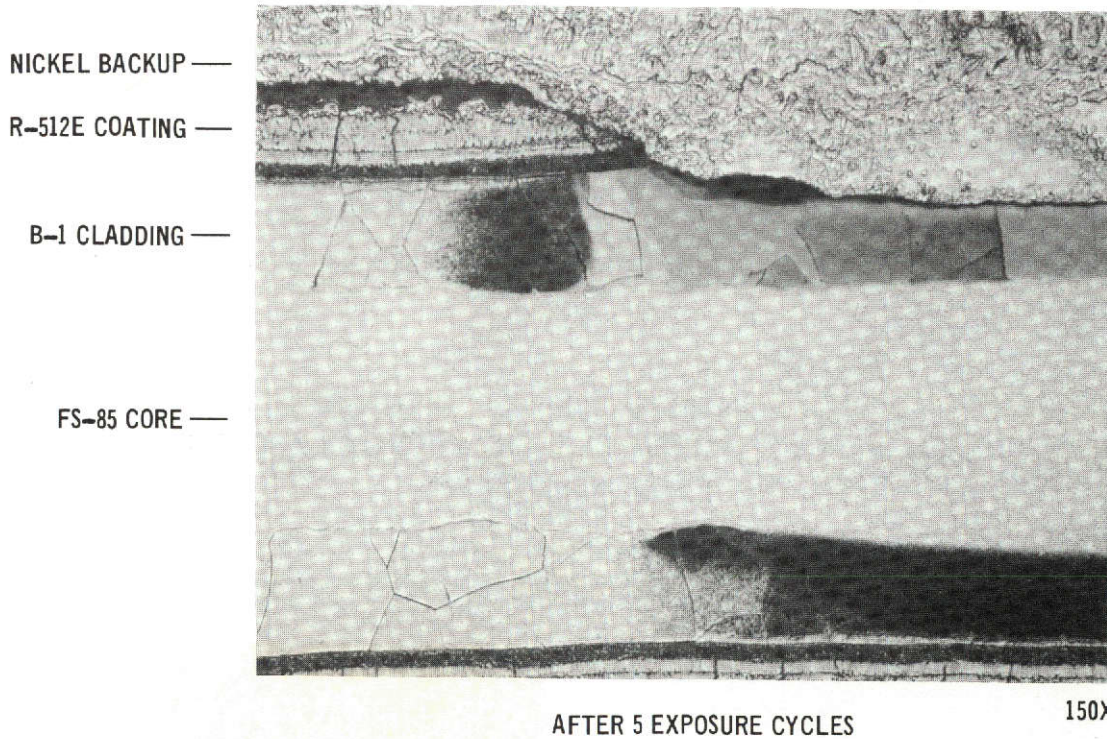
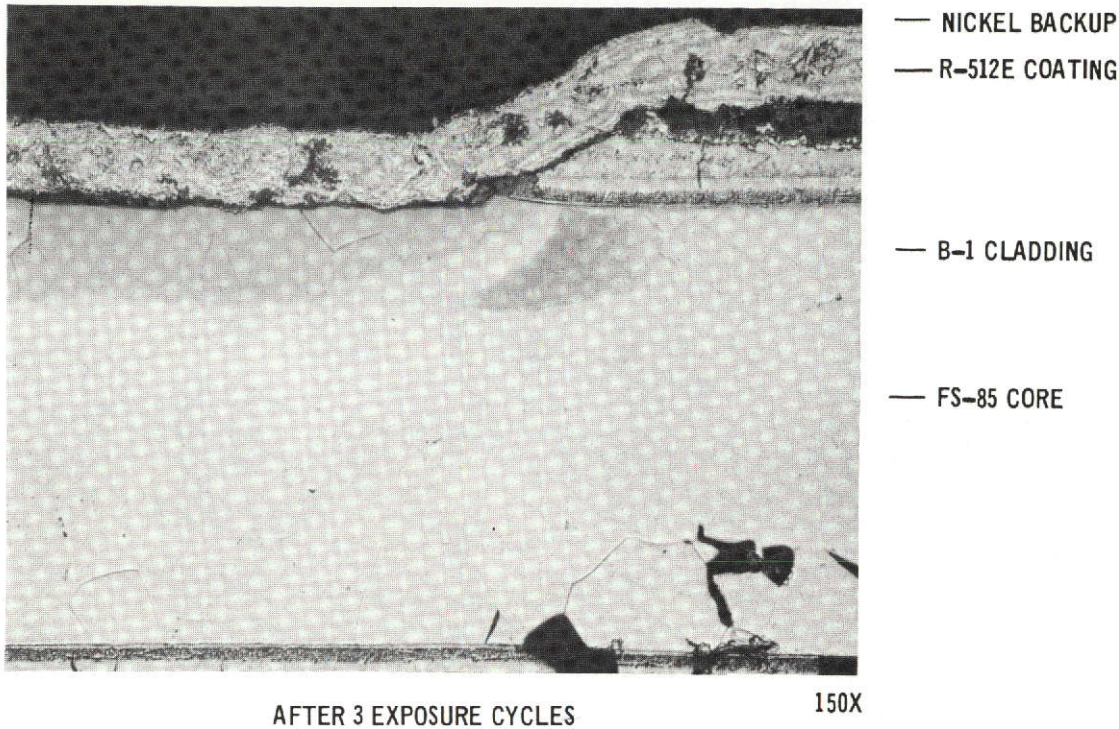


FIGURE 23 NOMINAL 100 MICROMETER THICK B-1 CLAD FS-85 AFTER
THREE AND FIVE EXPOSURE CYCLES

150X

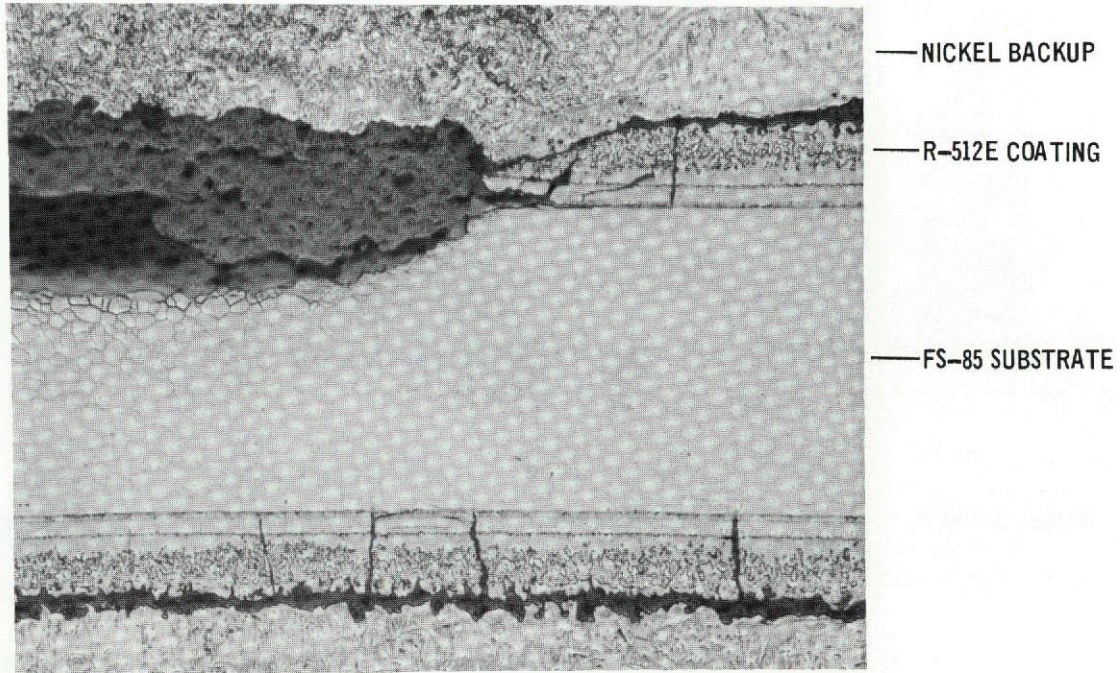
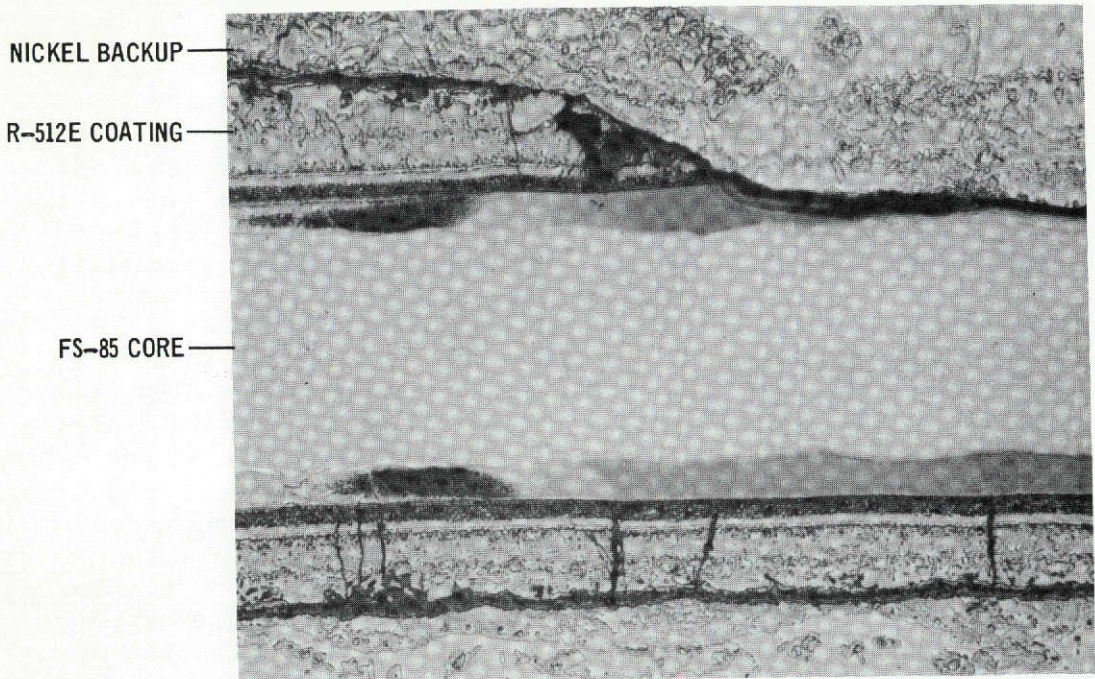
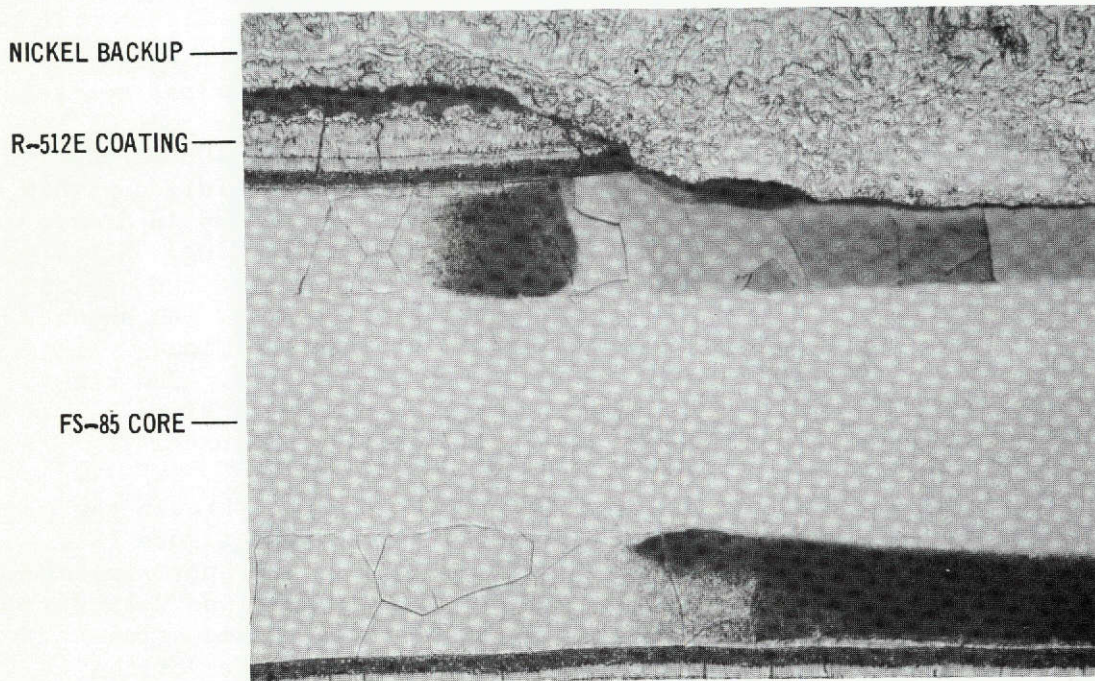


FIGURE 24 EFFECT OF FIVE REENTRY PROFILE EXPOSURE CYCLES ON UNCLAD FS-85

This page is reproduced at the back of the report by a different reproduction method to provide better detail.

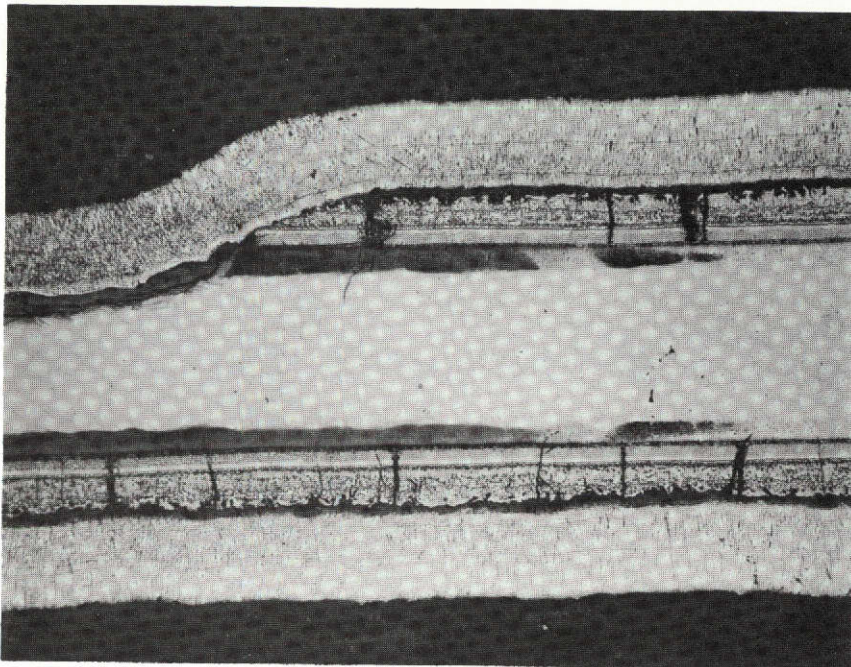
profile cycles. The B-1 clad specimens having a 50 micrometer thickness experienced continued cladding surface recession to the point of just reaching the FS-85 core, as shown in figure 25. The oxygen contaminated core area remained approximately the same as the area for the one and three cycle tests; it was slightly less than the contaminated area of the B-1 cladding and remaining essentially within the general area of the defect. After five cycles the nominal 100 micrometer B-1 clad showed a noticeable cladding surface recession, cladding contamination through the core to the opposite side, and a hardness increase within the defect area, (see figure 25). Thus, the 100 micrometer clad material at five cycles was behaviorally analogous to the 50 micrometer cladding at one cycle.

- (d) Results of Ten Profile Exposure Cycles - During the second group of five exposure cycles oxidation of the FS-85 continued for both the 50 micrometer clad and unclad systems, as shown in figure 26. The 50 micrometer clad experienced a significant change in the oxygen contamination area which increased to approximately 450 micrometers beyond the defect area after the loss of the cladding in the defect area at five cycles. The 100 micrometer clad specimens changed very little between the fifth and tenth cycle. The cladding surface continued to recede, as shown in figure 27, with the contaminated area remaining relatively unchanged.
- (e) Results of Fifteen Profile Exposure Cycles - Oxidation recession of the 100 micrometer cladding had almost reached the FS-85 load bearing core after 15 reentry cycles, as shown in figure 27. The zone of oxygen contamination remained the same at approximately 100 micrometers beyond the defect area. As the cladding became oxidized within the next few cycles, the oxidation contamination increased in area, but at a lower rate than the nominal 50 micrometer cladding. After 15 reentry profile cycles, the 50 micrometer B-1 clad and the unclad FS-85 were oxidized almost through the load bearing area. As shown in figure 29, there was approximately 115 micrometers of load bearing FS-85 remaining in the center of the defect area. The contamination zone of the unclad FS-85 remained about 2-1/2 times larger than the 50 micrometer B-1 clad material (see figure 19).
- (f) Results of Fifty Exposure Cycles - Holes were oxidized through the thickness of all four material systems (see table V and figure 18). The hole diameter for the unclad baseline materials was approximately 1 centimeter, and for the two clad systems the diameter was 0.15 centimeter. Photomicrographs of the edges of the oxidized holes are shown in figures 29 and 30. The beneficial properties of the cladding, particularly the 100 micrometer system, are illustrated by the small oxygen contaminated zone of figure 30. The continuation of the FS-85 core (determined by microhardness measurements) did not extend past the visually contaminated zone of the B-1 cladding, and was thus within 500 micrometers of the defect edge.

NOMINAL 50 μm B-1 CLADDINGNOMINAL 100 μm B-1 CLADDINGFIGURE 25 B-1 CLAD FS-85 AFTER FIVE REENTRY
PROFILE EXPOSURE CYCLES

This page is reproduced at the back of the report by a different reproduction method to provide better detail.

100X



200X

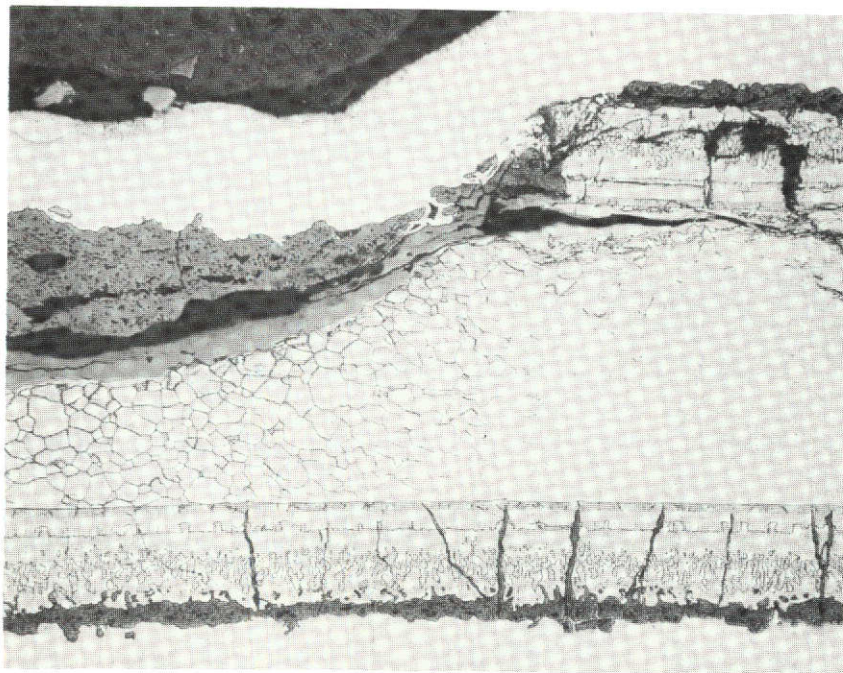


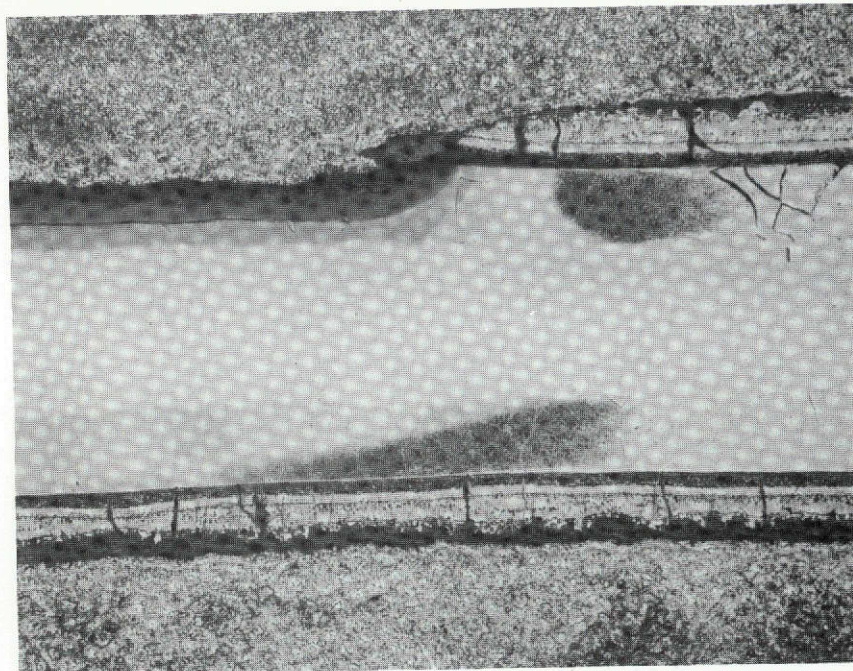
FIGURE 26 EFFECT OF TEN PROFILE EXPOSURE CYCLES
ON CLAD AND UNCLAD FS-85

457-3410

This page is reproduced at the back of the report by a different reproduction method to provide better detail.

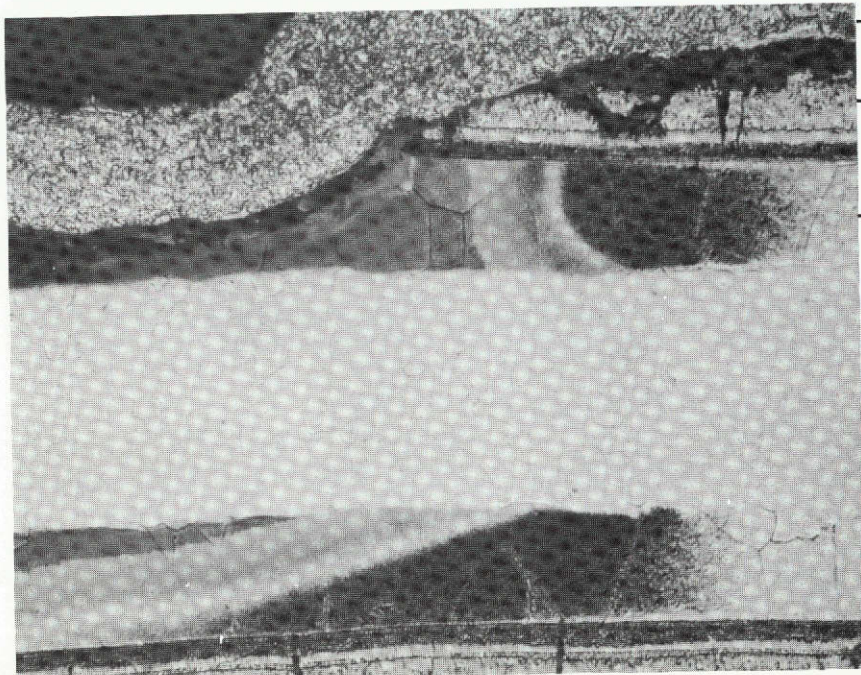
OUTER PROTECTIVE SKIN

100X



AFTER 10 CYCLES

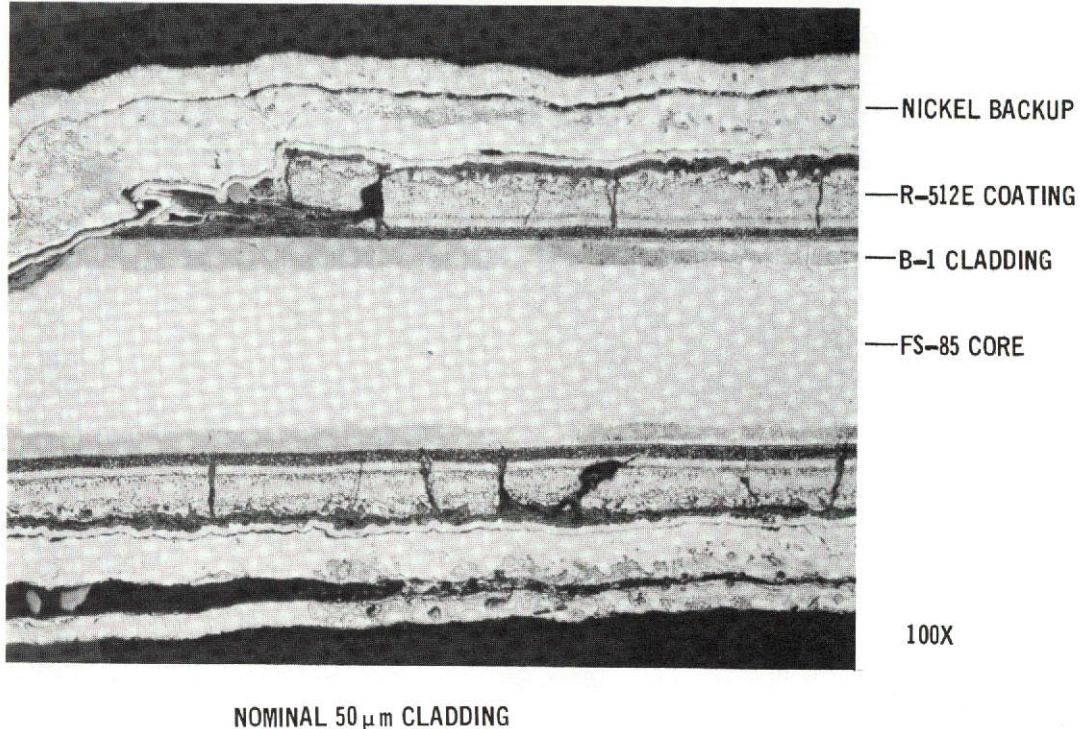
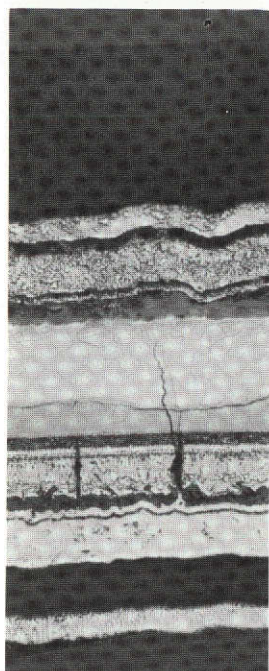
150X



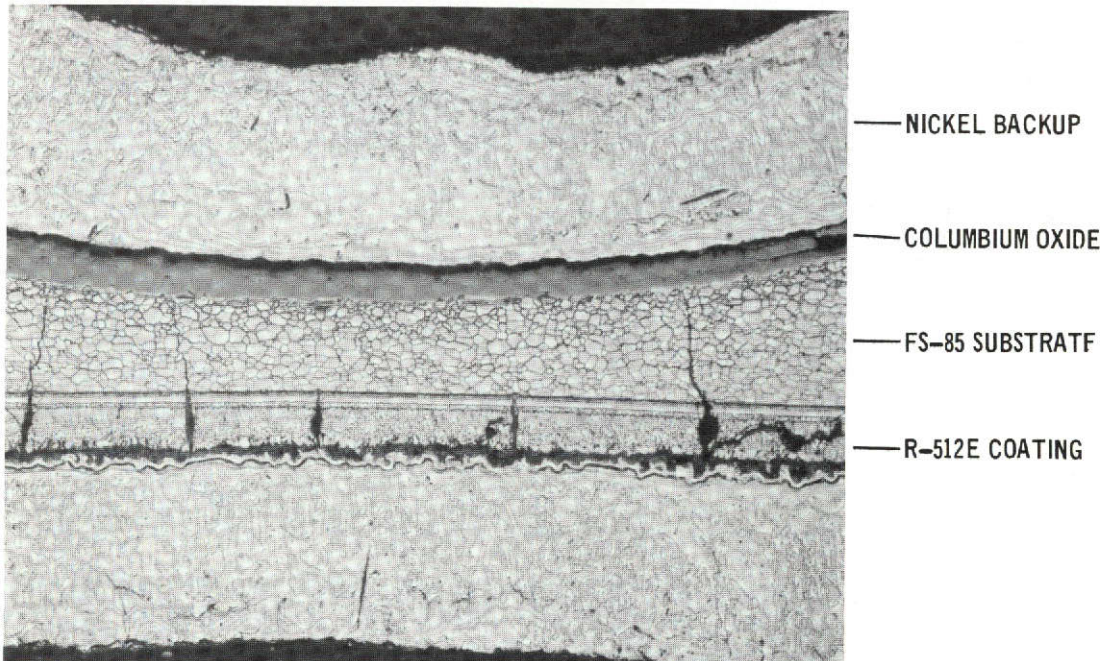
AFTER 15 CYCLES

FIGURE 27 NOMINAL 100 MICROMETER CLADDING ON FS-85
AFTER 10 AND 15 REENTRY PROFILE CYCLES

This page is reproduced at the back of the report by a different reproduction method to provide better detail.



100X



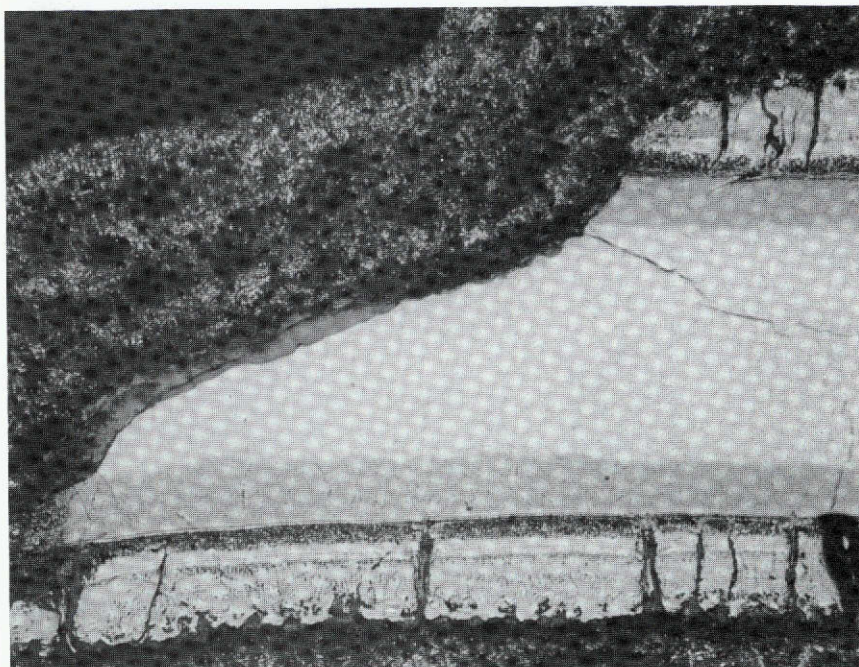
UNCLAD FS-85

FIGURE 28 EFFECT OF 15 REENTRY EXPOSURE CYCLES ON B-1 CLAD
AND UNCLAD FS-85

This page is reproduced at the back of the report by a different reproduction method to provide better detail.

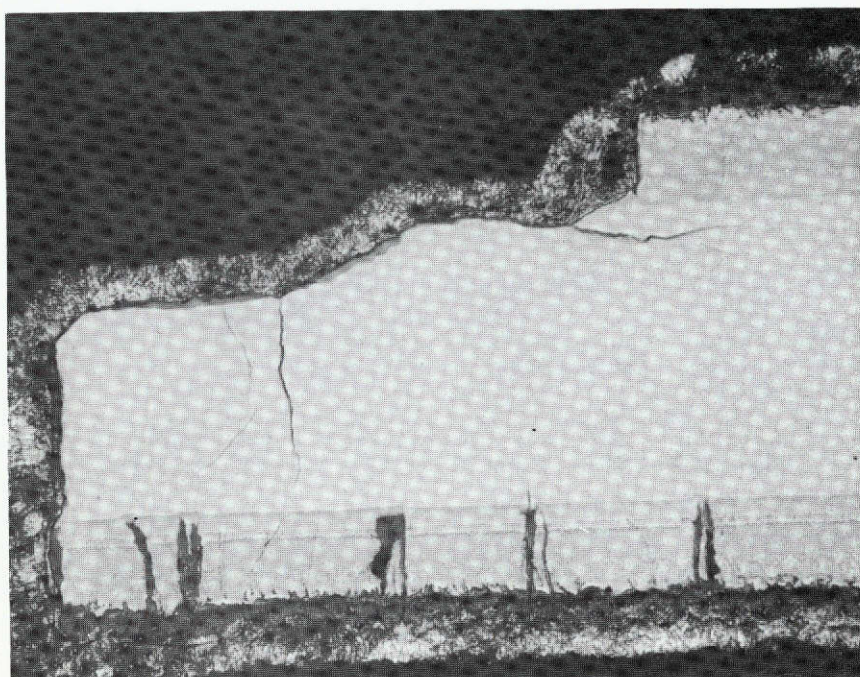
OUTER PROTECTIVE SKIN

150X



NOMINAL 50 μm B-1 CLAD

150X



UNCLAD FS-85

FIGURE 29 EFFECT OF 50 REENTRY PROFILE CYCLES
ON CLAD AND UNCLAD FS-85

This page is reproduced at the back of the report by a different reproduction method to provide better detail.

100X

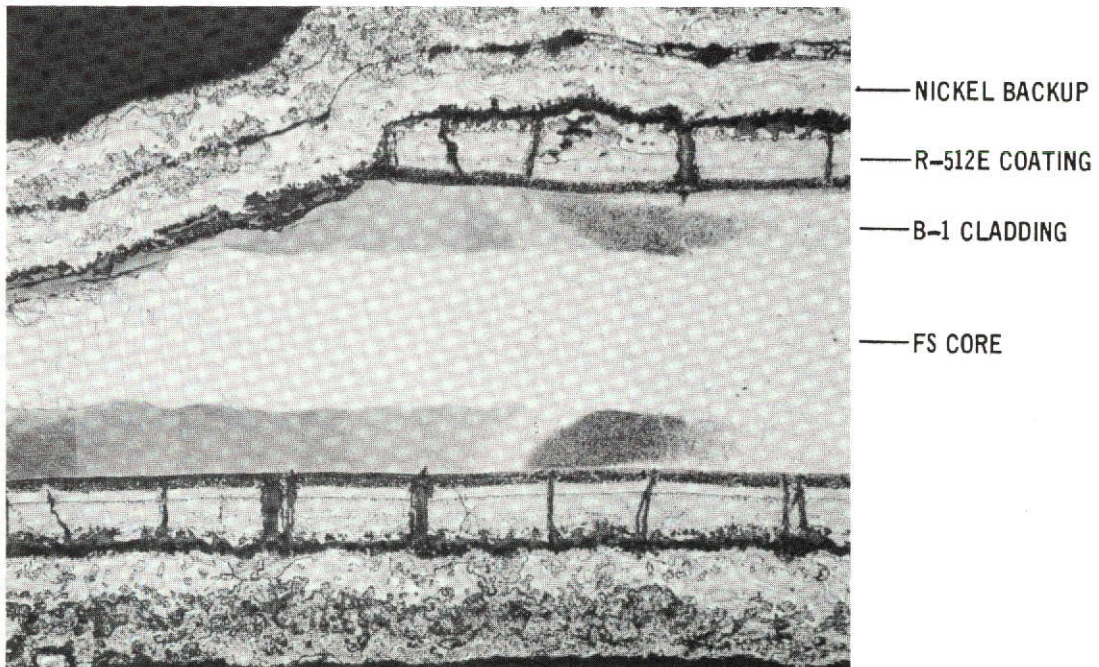


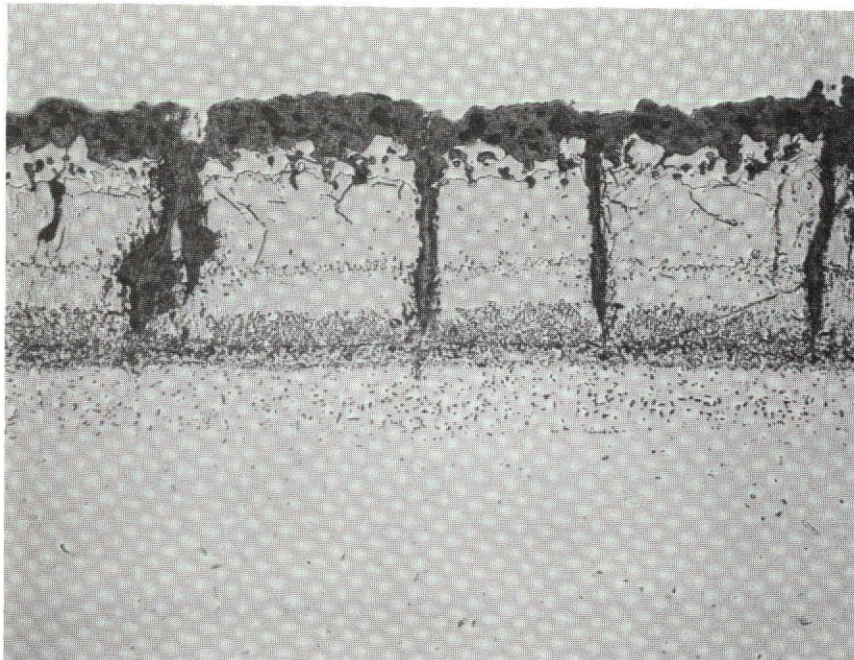
FIGURE 30 EFFECT OF 50 REENTRY PROFILE EXPOSURE CYCLES ON
NOMINAL 100 MICROMETER B-1 CLADDING

This page is reproduced at the back of the report by a different reproduction method to provide better detail.

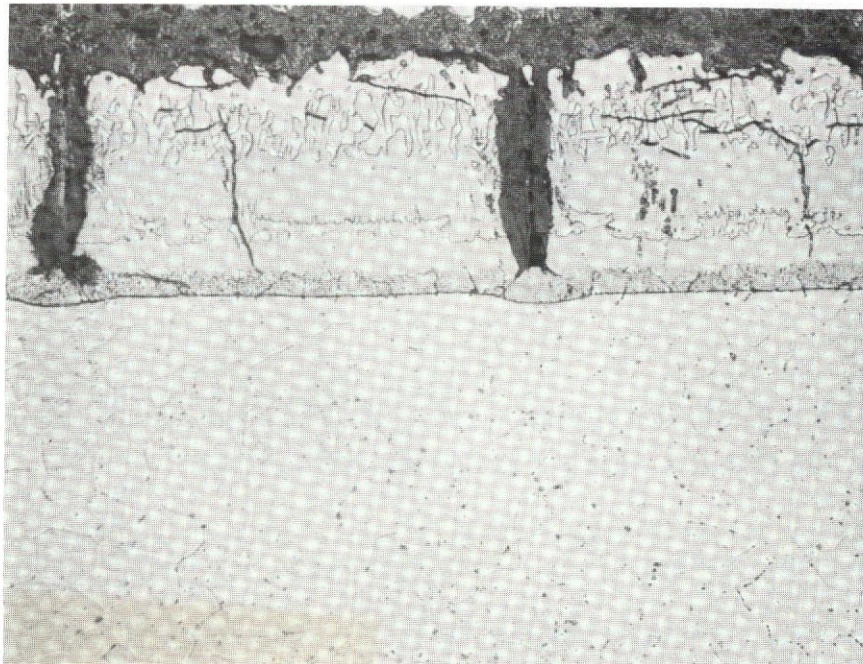
(g) Results of One Hundred Exposure Cycles - Exposures of 100 cycles were performed during each experimental effort on specimens without defects. Typical photomicrographs are presented in figures 31 and 32. The R-512E coating on both the B-1 clad and the unclad FS-85 substrate appeared normal for 100 reentry cycles. The FS-85 specimens without a cladding showed more interstitials precipitation than the FS-85 core of the clad specimens. The B-1 cladding showed relatively heavy precipitation, indicating that the cladding kept the FS-85 structure freer of interstitials than the unclad condition. This is an additional benefit of the clad system.

Direct comparison of the B-1 clad and unclad FS-85 illustrates the beneficial properties. Initially, the cladding prevents any effect upon the core in a defect area for up to five cycles, depending on the cladding thickness. The cladding then functions to retard the rate of loss of load bearing cross section by oxidation to prevent or minimize hole formation. Finally, the cladding mitigates oxygen contamination of the load bearing core. The value of these attributes is discussed in section 3, but in each case the benefit of the clad system over the unclad system was significant.

400X

NOMINAL 50 μm B-1 CLAD

400X



UNCLAD FS-85

FIGURE 31 MICROSTRUCTURE OF CLAD AND UNCLAD FS-85 COUPONS AFTER
100 REENTRY PROFILE CYCLES

457-3412

This page is reproduced at the back of the report by a different reproduction method to provide better detail.

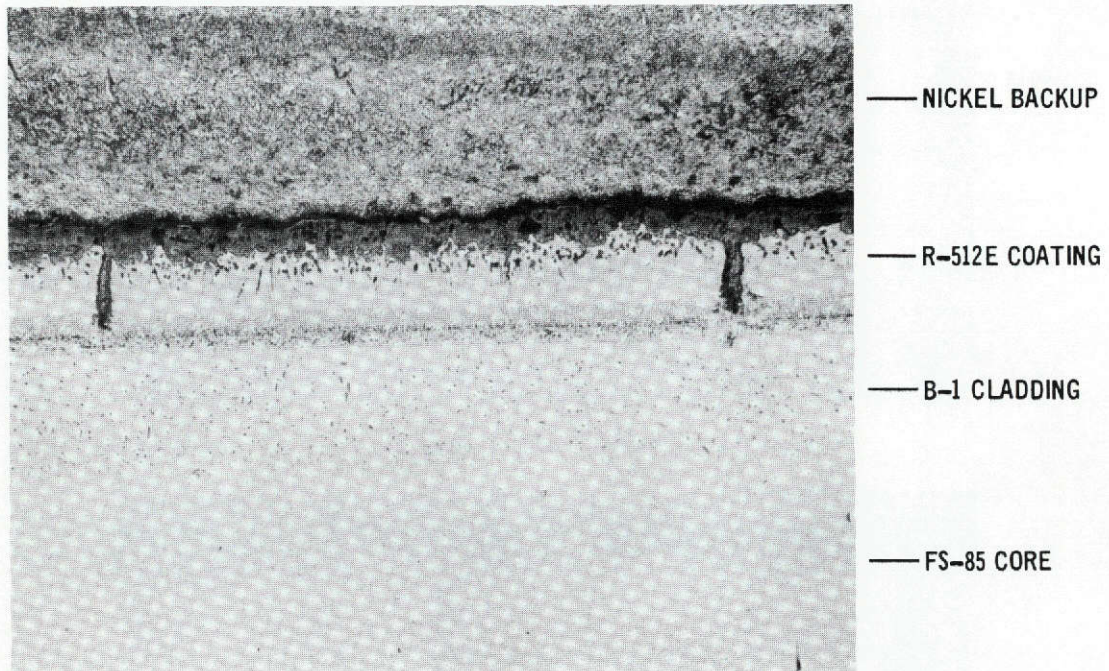


FIGURE 32 MICROSTRUCTURE OF NOMINAL 100 MICROMETER B-1 CLAD FS-85
AFTER 100 PROFILE REENTRY CYCLES

This page is reproduced at the
back of the report by a different
reproduction method to provide
better detail.

2.4 MECHANICAL PROPERTY DETERMINATION

While the primary purpose of the clad system was to provide increased reliability through improved oxidation resistance; nevertheless, it was essential to understand the strength properties of the clad system to assess its utility to a reentry vehicle. The initial assumption was that the cladding would neither contribute to nor detract from the strength of the FS-85 alloy load bearing core, and the mechanical property testing was designed to test this assumption. Since the tensile properties of the FS-85 alloy are known for various thermal exposure service cycles, the effects of the cladding can be identified. A baseline strength test was performed as a control for each experimental cladding strength test to ascertain the quality of the test and to provide a comparison of a clad and an unclad system. Strength tests were performed in each of the three tasks, and the testing was increasingly more comprehensive. This section will present the strength information gained, independent of the task in which it was learned; the detailed strength data for each task is presented in appendix A.

Strength data can be calculated and presented in several ways; the individual preference is dependent upon the manner in which the data is to be used. The design approach employed at MDAC-E is to account for the processes and service conditions which consume the load bearing cross section of the substrate and test to assure that the remaining columbium alloy substrate properties are unaffected and meet or exceed design criteria. This approach was consistent with the experimental requirements of this program, since the actual strength performance of the FS-85 load bearing core was the experimental question of interest and the most direct method of data comparison. Tensile strength data tables have up to four columns of experimental values. Column 1 presents the strength data based upon an area measured directly from the individual specimens prior to coating application. This provides for data based upon direct measurements but does not represent the true value of the FS-85 substrate because a portion (15 to 50 percent) was not considered load bearing, was consumed in forming the coating, or was consumed by reaction with the coating during thermal cycling. Thus, column 2 presents the strength data based upon the remaining metal after coating, column 3 presents the strength data based upon the remaining metal after 100 profile exposure cycles, and column 4 presents the strength data based upon the FS-85 core area for the clad specimens. In most cases, analogous FS-85 data derived from contract NAS 3-14307, "Fused Slurry Silicide Coatings for Columbium Alloy Reentry Heat Shields" (reference 7), is presented in column 5 for comparison with the results of this program.

2.4.1 Tensile Property Determination

Tensile testing was conducted in each of the experimental tasks and was the major strength test employed. Triplicate tensile specimens, 2.5 by 10 centimeters, with a 0.635-centimeter gauge width, were tested at room temperature, 760°C and 1320°C. The elevated temperature tensile tests were conducted in a helium atmosphere furnace with the specimen strain measured by cross head travel. Two conditions were tested, after coating application (before service) and after 100 profile exposure cycles. Profile exposure test conditions were

OUTER PROTECTIVE SKIN

the same as those previously described in section 2.3.1. Reentry temperature and air pressure conditions were simulated, but no stress was applied. Detailed strength results for each of the three experimental tasks are presented in appendix A. The strength data based on the load bearing FS-85 is summarized in table VI. Within the context of the limited amount of testing, the values represent the best estimate of the tensile properties of B-1 clad FS-85. The data was generated to make a qualitative assessment of the potential of the clad material for reentry vehicle applications and was not intended as design allowables. Since the tensile properties were found to be dependent upon the cladding thickness, the two ranges of cladding investigated will be treated separately.

2.4.1.1 Tensile Properties of Nominal 50 Micrometer Thick B-1 Clad Material

Claddings having a nominal thickness of 50 micrometers (35 to 65 micrometers) were investigated during all three experimental tasks. The tensile results were generally consistent for the individual experiments and tended to substantiate the idealized assumption that the core carried the loads and the cladding neither contributed nor detracted from the core strength. The clad material tends to have a slightly higher yield strength and a lower elongation. For purposes of assessment of the clad material's reentry application potential, it was concluded that the cladding could be considered as part of the oxidation protection system and had no influence on the strength of the FS-85 core.

2.4.1.2 Tensile Properties of Nominal 100 Micrometer Thick B-1 Clad Material

A nominal B-1 cladding thickness of 100 micrometers after coating was investigated during the final task. The tensile properties proved to be substantially different than the thinner clad material and the FS-85 substrate. The clad system was composed of approximately equal volumes of the FS-85 core and the B-1 cladding. The room temperature tensile properties prior to exposure cycling showed results which were approximately halfway between the properties of the FS-85 core and the B-1 cladding. Beyond this initial data point, B-1 tensile properties were not available for comparison. The following general strength characteristics were noted from table A3 (based upon the core area strength): (1) at room temperature and 760°C, the cladding contributes positively to the tensile yield and ultimate, but substantially reduces the elongation, and (2) at 1320°C, the positive strength contribution appeared to be lost. However, the test may be suspect based upon baseline results (see appendix A).

The data on the thicker cladding was less extensive than the data on the thinner clad system. However, it was significantly different in nature and shows that the strength of a clad system with equal volumes of cladding and core cannot be treated by the idealistic assumption that the cladding is part of the protection system and does not contribute to the core strength. The strength picture was more complicated and not sufficiently resolved.

TABLE VI
SUMMARY OF CLAD AND UNCLAD FS-85 TENSILE PROPERTIES

MATERIAL	TEST TEMP	EXPOSURE CONDITION	DATA SOURCE	AVERAGE FS-85 TENSILE PROPERTIES				REF. 7 FS-85 TENSILE PROPERTIES				
				YIELD		ULTIMATE		PERCENT ELONGATION	YIELD		ULTIMATE	
				MN/m ²	LB/IN ² x 10 ³	MN/m ²	LB/IN ² x 10 ³		MN/m ²	LB/IN ² x 10 ³	MN/m ²	LB/IN ² x 10 ³
FS-85 CORE/ B-1 CLADDING 35 TO 65 MICROMETERS	ROOM TEMP.	AS COATED	TABLES A1, A2 & A3 COLUMNS 4 & 5	509	73.9	620	89.8	10	476	69.1	639	92.7
		AFTER 100 CYCLES	TABLES A1 & A2 COLUMNS 4 & 5	501	72.6	618	89.6	8	475	68.9	633	91.9
	760°C	AS COATED	TABLES A2 & A3 COLUMNS 4 & 5	268	38.8	344	50.6	4	263	38.1	458	66.5
		AFTER 100 CYCLES	TABLE A2 COLUMNS 4 & 5	330	47.8	357	51.8	2	238	34.5	386	56.0
	1320°C	AS COATED	TABLES A2 & A3 COLUMNS 4 & 5	170	24.6	204	29.6	9	203	29.5	219	31.8
		AFTER 100 CYCLES	TABLE A2 & A3 COLUMNS 4 & 5	170	24.6	189	27.4	2	186	27.0	198	28.7
FS-85 SUBSTRATE/ R-512E COATING (BASELINE)	ROOM TEMP	AS COATED	TABLE A3 COLUMNS 2 & 5	476	69.0	604	87.6	17	476	69.1	639	92.7
		AFTER 100 CYCLES	TABLE A3 COLUMNS 3 & 5	440	63.8	613	88.9	15	475	68.9	633	91.8
	760°C	AS COATED	TABLES A2 & A3 COLUMNS 2 & 5	214	31.3	374	54.1	7	263	38.1	458	66.5
		AFTER 100 CYCLES	TABLES A2 & A3 COLUMNS 3 & 5	230	33.2	364	52.8	6	238	34.5	386	56.0
	1320°C	AS COATED	TABLES A2 & A3 COLUMNS 2 & 5	136	19.7	179	25.2	28	203	29.5	219	31.8
		AFTER 100 CYCLES	TABLES A2 & A3 COLUMNS 3 & 5	149	21.6	168	24.4	24	186	27.0	198	28.7
FS-85 CORE/ B-1 CLADDING 100 MICROMETERS/ R-512E COATING	ROOM TEMP	AS COATED	TABLE A3 COLUMNS 4 & 5	738	107	766	111	2	476	69.1	639	92.7
		AFTER 100 CYCLES		524	76.0	549	79.6	2	475	68.9	633	91.8
	760°C	AS COATED		405	58.8	516	74.8	4	263	38.1	458	66.5
		AFTER 100 CYCLES		299	43.4	334	48.4	3	238	34.5	386	56.0
	1320°C	AS COATED		128	18.5	174	25.3	-	203	29.5	219	31.8
		AFTER 100 CYCLES		168	24.4	173	25.1	-	186	27.0	198	28.7

2.4.2 Reentry Profile Cycling Under Load

A series of tests was performed in which B-1 clad and unclad tensile specimens were reentry profile tested under load to determine the performance under the combined effects of several reentry parameters. These tests have been very effective in finding weaknesses in oxidation protection material systems. The tests also have the advantage that the pragmatic end use criteria of carrying anticipated loads under service conditions substantiates many other less sophisticated tests and leads to confidence in the material system. This type of test is very effective for identifying material systems which have creep susceptibility problems. With the high titanium content of the B-1 cladding alloy, it was important to qualitatively evaluate the creep behavior of the clad system.

Tensile specimens with a nominal 50 micrometer and 100 micrometer B-1 cladding and an unclad FS-85 baseline were R-512E coated. Duplicate specimens were tested without defects and were gritblasted to form a 0.15 centimeter diameter coating defect in the center of the guage section. The specimens were exposed to the time, temperature, air pressure and stress reentry profile conditions of figure 17. The stress was based on the load-bearing FS-85 core of the clad specimens and the postcoat remaining substrate area of the baseline specimens. The specimens were examined for coating oxidation failure after each series of twenty to twenty-two cycles. The equipment was automatically controlled and would shut off if structural failure occurred. Scribe marks were put in the coated gauge section for creep deflection measurements before and after 100 cycles. For those specimens in which failure did not occur during stress profile cycling, tensile tests at room temperature were made to determine the remaining strength after 100 load cycles.

Results of the stress profile testing are presented in table VII, and the specimens after profile exposure cycling are shown in figures 33 and 34. The specimens for both clad systems and the FS-85 baseline went through 100 cycles without coating oxidation or structural failures. Creep deflections were essentially the same, 0.86 percent, for both the 50 micrometer clad system and the baseline unclad FS-85. The creep deflection in the 100 micrometer clad system was 0.65 percent, indicating a similar behavior to the tensile properties, in that the cladding was carrying some of the load. The tensile testing after profile cycling showed good strength retention for each of the material systems. As was expected, the defected tensile specimens did not make 100 profile cycles. The clad materials lasted approximately twice as many stress profile cycles (42 and 56 compared to 25) as the unclad baseline. This illustrates the capabilities of the cladding to retard oxidation of the load-bearing FS-85 core, in terms of service cycles. The stress profile proved to be a significant test, and the results were highly consistent. The load bearing capabilities of the system were established, and it was shown that the cladding does not adversely affect the good creep properties of the FS-85 alloy.

2.4.3 Exposure Cycling of Defected Tensile Specimens

The ability of the B-1 cladding to retard oxidation of the FS-85 core was demonstrated during the initial experimental task. A series of experiments was

TABLE VII
RESULTS OF REENTRY PROFILE CYCLING UNDER STRESS FOR CLAD AND UNCLAD
FS-85 COLUMBIUM ALLOY

SPEC. NO.	MATERIAL	DEFECT CONDITION	FAILURE CYCLE	PERCENT CREEP ELONGATION IN 100 CYCLES	RT CORE TENSILE STRENGTH AFTER 100 STRESS PROFILE CYCLES			
					YIELD		ULTIMATE	
					MN/m ²	LB/IN ² x 10 ³	MN/m ²	LB/IN ² x 10 ³
T-8	100 μm B-1 CLADDING	NO INTENTIONAL COATING DEFECTS	NO COATING OR STRUCTURAL FAILURES THROUGH 100 CYCLES	0.73	550	79.7	574	83.3
T-11	R-512E COATING			0.57	549	79.6	630	91.4
AV				0.65	550	79.6	604	87.4
M-26	50 μm B-1 CLADDING			0.83	467	67.7	548	79.5
M-27	R-512E COATING			0.92	445	64.6	498	72.3
AV				0.88	456	66.1	523	75.9
S-30	BASELINE - NO CLADDING			0.89	459	66.5	619	89.9
S-34	R-512E COATING			0.84	435	63.1	592	85.9
AV				0.86	447	64.8	606	87.9
T-7	100 μm B-1 CLADDING	0.15 CENTIMETER COATING DEFECT IN CENTER OF GAUGE AREA	58	SPECIMENS FRACTURED PRIOR TO 100 CYCLES				
T-10	R-512E COATING		54					
AV			56					
M-28	50 μm B-1 CLADDING		41					
M-29	R-512E COATING		44					
AV			42					
S-35	BASELINE - NO CLADDING		26					
S-36	R-512E COATING		25					
AV			25					

NOTE: STRENGTH BASED UPON CORE AREA FOR CLAD SPECIMENS AND FS-85 AFTER COATING AREA FOR BASELINE.

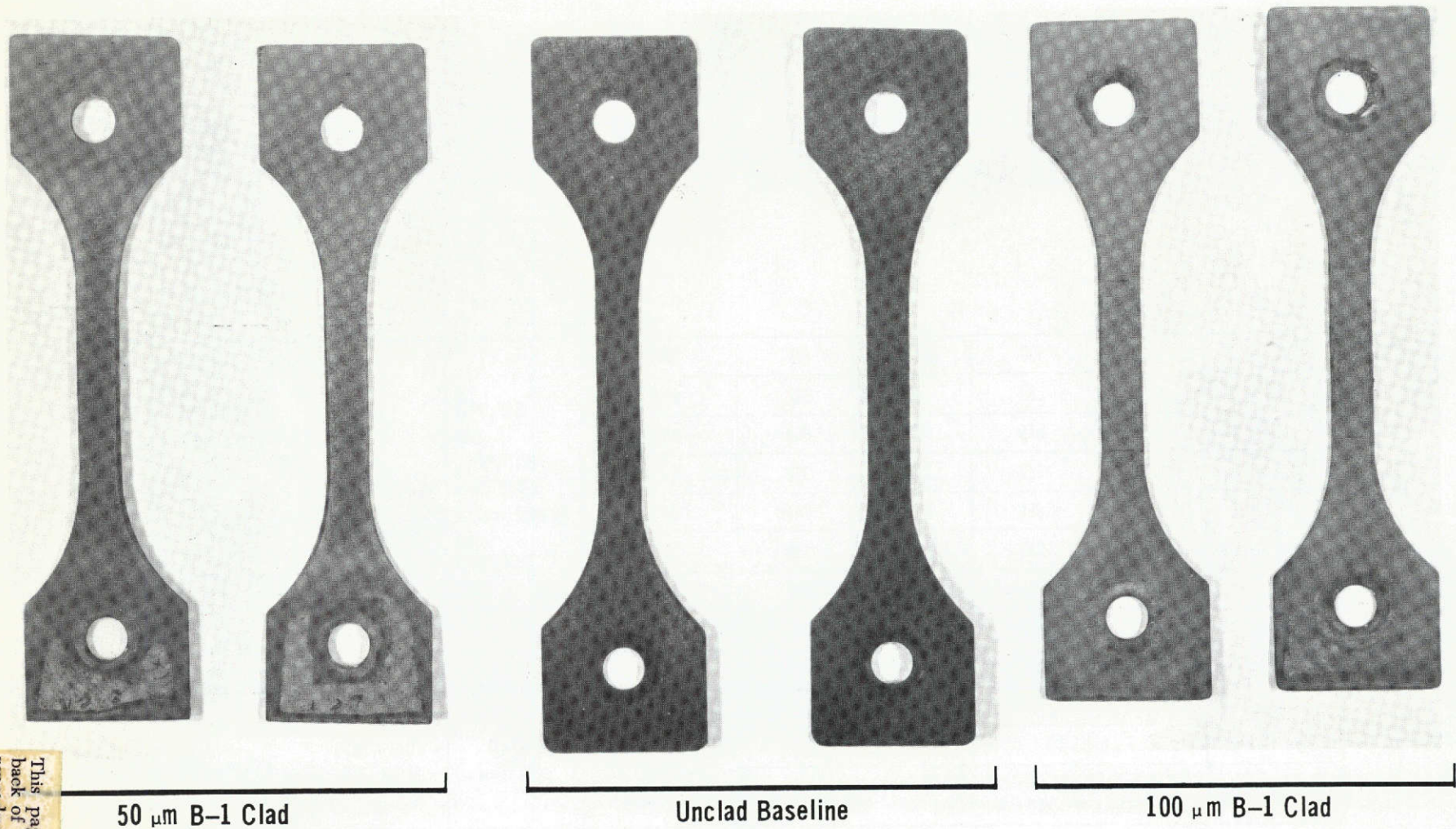


FIGURE 33 R-512E COATED CLAD AND UNCLAD FS-85 TENSILE SPECIMENS
AFTER 100 STRESS PROFILE CYCLES

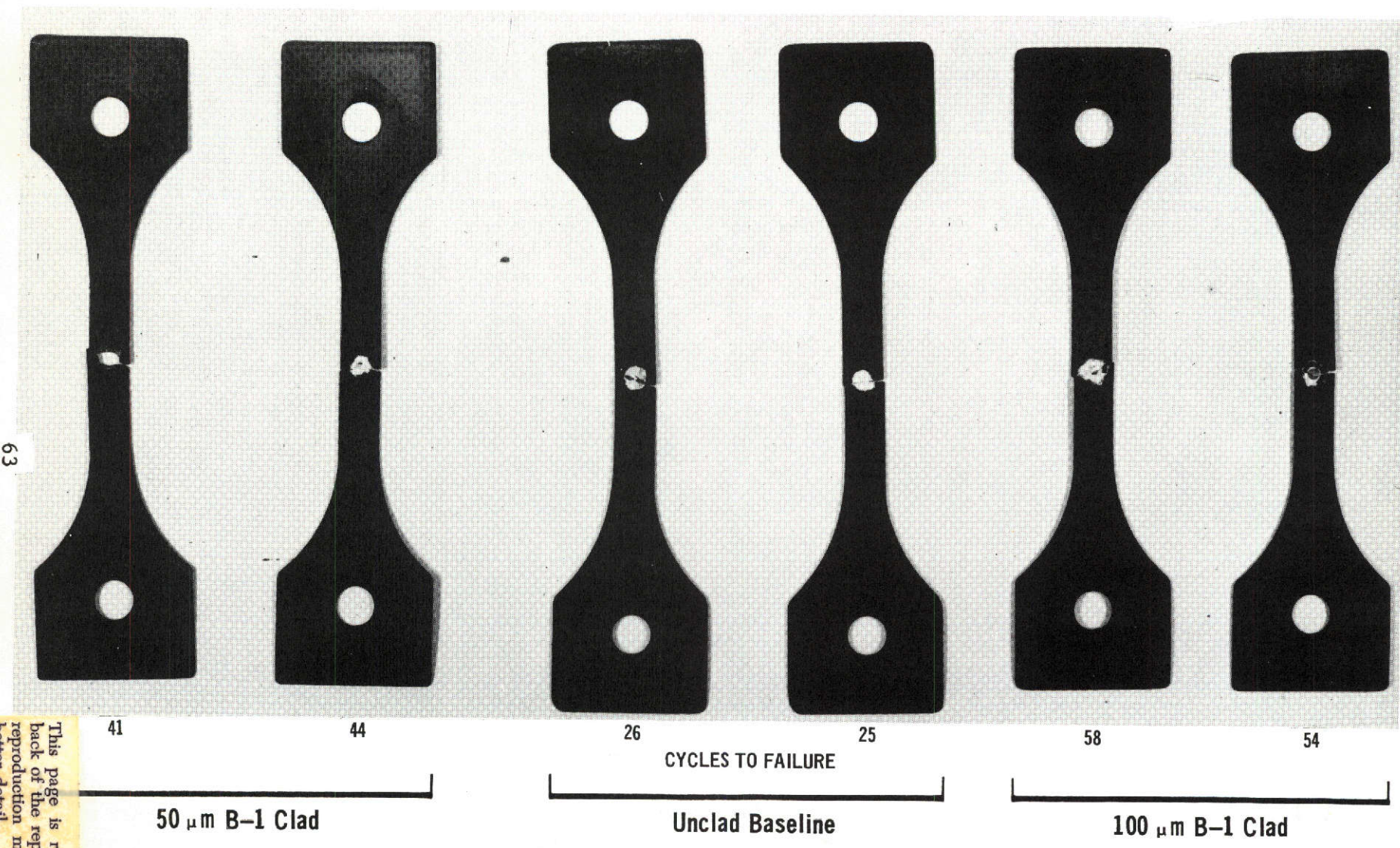


FIGURE 34 DEFECTED R-512E COATING ON CLAD AND UNCLAD FS-85 TENSILE SPECIMENS AFTER FAILURE DURING STRESS PROFILE CYCLING

OUTER PROTECTIVE SKIN

initiated to determine the ability of the cladding to maintain the mechanical properties of the load bearing core in the immediate area of a coating defect. Experiments were conducted during the final two tasks in which clad and unclad tensile specimens were intentionally defected after coating, exposed to various numbers reentry profile cycles, and tensile tested at room temperature.

Tensile specimens of B-1 clad and unclad FS-85 with the R-512E coating were defected as described in paragraph 2.3.1. The defects were 0.15 centimeter in diameter and were located in the center of the 0.635 centimeter gauge length. The specimens were exposed to the reentry temperature and pressure conditions of figure 17, but without stress. The task 2 experiment employed duplicate tensile specimens of B-1 clad FS-85 (nominal 50 micrometer clad thickness) and unclad FS-85 baseline, and were exposed to 1, 3 and 10 reentry profile cycles, with one additional set of specimens as a control defected and not exposed. During the final task, two cladding thicknesses (nominal 50 and 100 micrometers) were tested with an FS-85 baseline, and profile exposures of 1, 3, 5, 10 and 15 cycles were included. After exposure cycling, the specimens were tensile tested at room temperature, and metallographic sections were made to determine the extent of oxygen diffusion into the cladding and the core.

The results of tensile testing of the defected and exposed specimens are summarized on the graph of figure 35, and are presented in detail in tables B-1 and B-2 of appendix B. The ultimate tensile strength of each clad specimen (figure 35) was based upon the area of the remaining metal after coating. The baseline was based upon the area of the remaining metal after coating. The nominal 100 micrometer cladding specimens showed the highest strength, since the cladding was making a positive strength contribution as previously described in paragraph 2.4.1. The significant conclusion drawn was that the ultimate core strength was maintained through five exposure cycles, and the total strength loss after 15 cycles was only 22 percent. The yield strength (see table B-2) was very close to the ultimate strength through five cycles and was undefined for 10 and 15 cycles. The elongation was only 1 to 2 percent without exposure and was (as expected) 1 percent or less after exposure cycling. The contrast with the unclad FS-85 was sharp. The unclad material lost strength significantly after the first exposure cycle (28 percent) and continued to decrease with increasing exposure cycles as the FS-85 oxidized.

The B-1 cladding of nominal 50 micrometer thickness was tested during two tasks and yielded somewhat different results. The results achieved in the second task were similar to the results described above with the nominal 100 micrometer cladding. That is, the cladding provided retention of the tensile properties (within approximately 8 percent) through three reentry profile cycles, with the ultimate tensile strength decreasing slightly and the yield strength increasing. In the experiment conducted in the final task using nominal 50 micrometer B-1 cladding, there was a 16 percent decrease in ultimate strength and a slight (7 percent) decrease in yield strength. While the clad material represented a significant improvement over the performance of the unclad FS-85, the improvement was in magnitude and not in character as had been observed previously. This qualitative difference in performance is shown in figure 35. The two upper curves represent the 100 micrometer B-1 cladding and the 50 micrometer cladding results of task 2. The cladding provides property

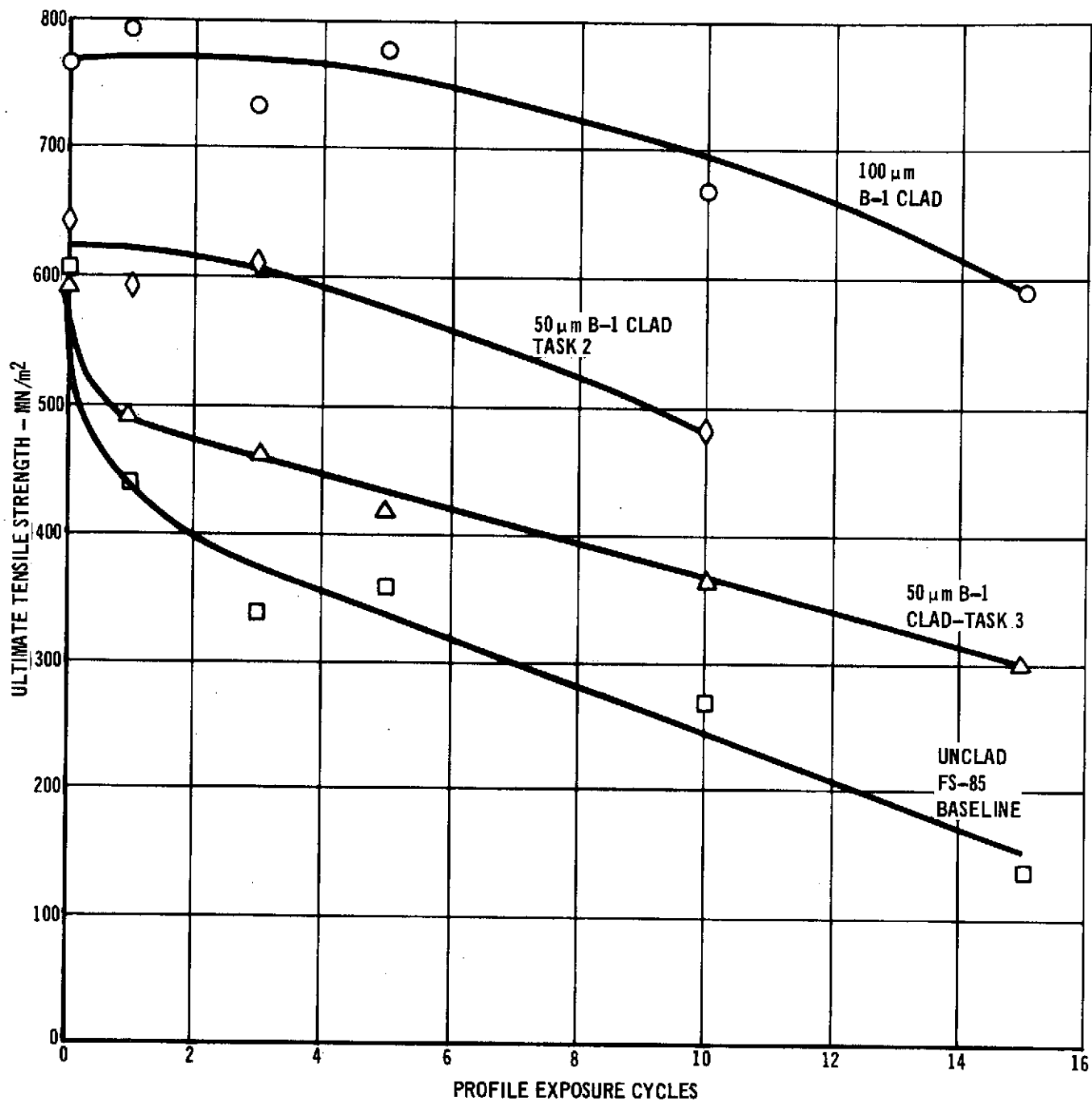


FIGURE 35. ROOM TEMPERATURE ULTIMATE TENSILE STRENGTH OF DEFECTED SPECIMENS AFTER VARIOUS REENTRY PROFILE EXPOSURES

OUTER PROTECTIVE SKIN

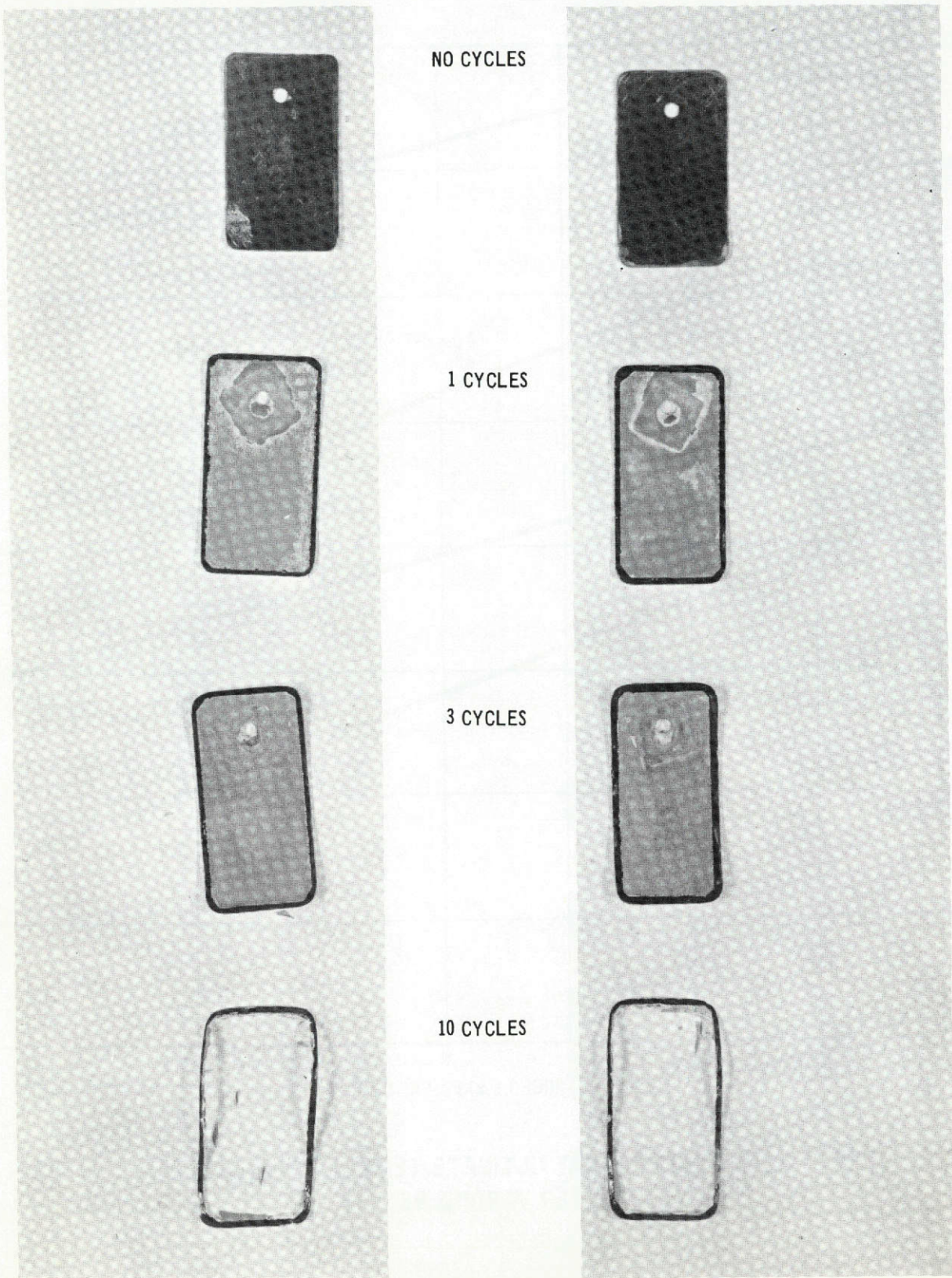


FIGURE 36 CLAD COUPONS WITHOUT R-512E COATED AFTER VARIOUS REENTRY PROFILE EXPOSURE CYCLES

457-3418

This page is reproduced at the back of the report by a different reproduction method to provide better detail.

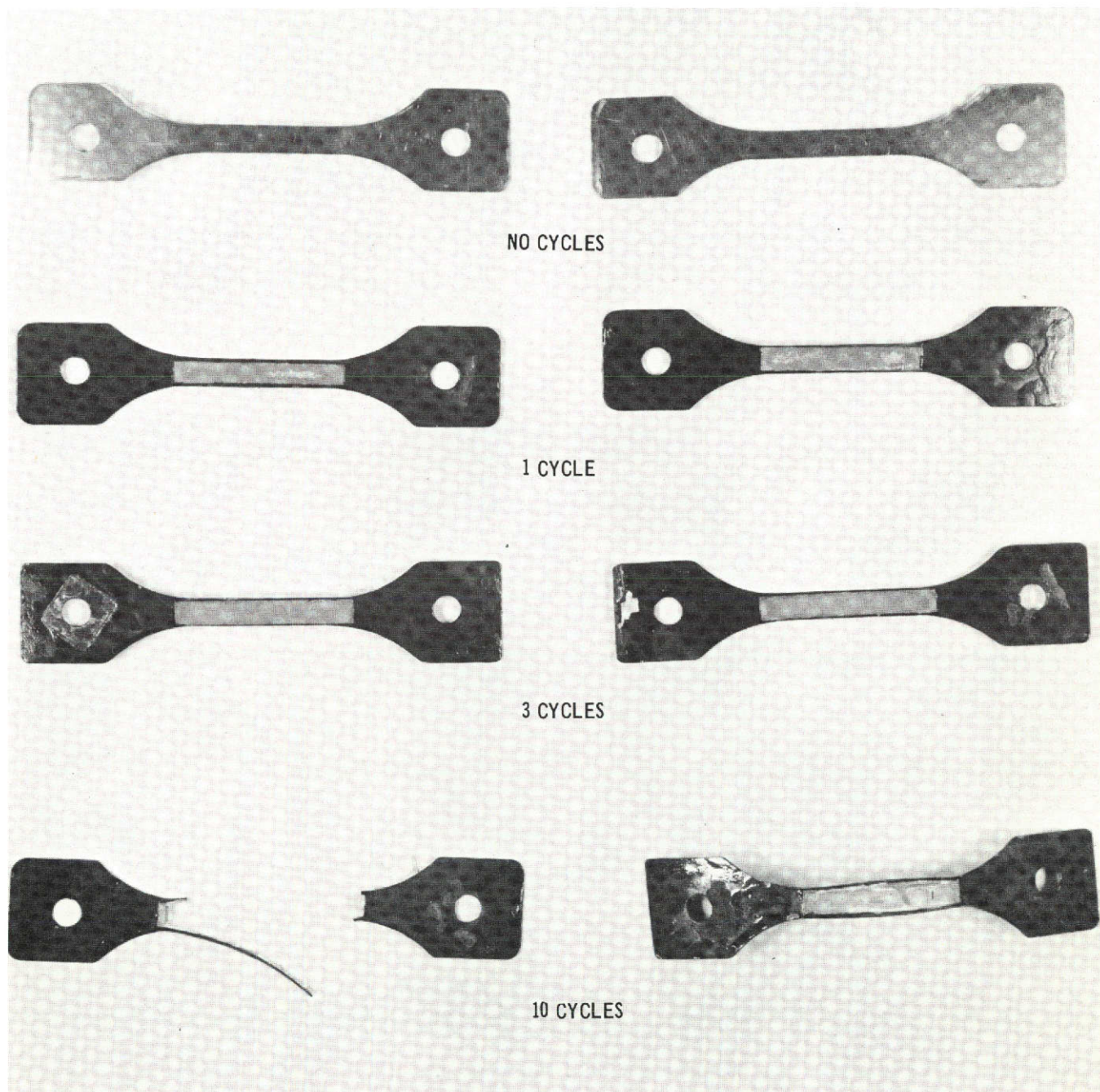


FIGURE 37 B-1 CLAD TENSILE SPECIMENS WITHOUT R-512E COATING AFTER
VARIOUS REENTRY PROFILE EXPOSURE CYCLES

457-3419

This page is reproduced at the back of the report by a different reproduction method to provide better detail.

TABLE VIII
TENSILE PROPERTIES OF UNCOATED CLAD SPECIMENS
AFTER VARIOUS PROFILE EXPOSURE CYCLES

SPEC. NO.	MATERIAL	PROFILE EXPOSURE CYCLES	TEST TEMP	STRENGTH				% ELONGATION
				YIELD MN/m ²	YIELD LB/in ² x 10 ³	ULTIMATE MN/m ²	ULTIMATE LB/in. ² x 10 ³	
E-4		0		717	104	765	111	12
E-7		0		717	104	772	112	11
AVG				717	104	769	111.5	11
E-9	FS-85	1		383	55.5	396	57.5	1
E-10	CORE	1		376	54.5	376	54.5	1
AVG				380	55.0	386	56.0	1
E-13	B-1			-	-	341	49.5	-
E-15	CLADDING	3		-	-	348	50.5	-
AVG				-	-	345	50.5	-
E-22		10						
E-31		10						
TOTALLY OXIDIZED								

457-3420

retention through three to five cycles, depending on cladding thickness. The lower two curves represent the unclad material and the second experiment with the nominal 50 micrometer cladding. The curves show qualitatively similar properties of immediate effect upon strength in the defect area. While the data does not support a clearly defined number of cycles of tensile property retention per unit thickness of cladding, the cladding proved beneficial in all cases.

2.4.4 Profile Exposure Evaluation of Clad Specimens Without Coating

The tensile testing of coated specimens with small defects exposed to various numbers of reentry profile cycles allowed evaluation of the ability of the cladding to protect the FS-85 core from oxidation at local coating defects. This experiment investigated the effects of local substrate property changes within an unaltered matrix. A second experiment was conducted with uncoated specimens exposed to various reentry profile cycles to determine the columbium property changes within the defect area. The size of the defect was much larger, and the effects of oxidation were experienced simultaneously from both sides of the specimen.

Clad tensile specimens and bend coupons of nominal 50 micrometer clad FS-85 sheet were tested without applying the R-512E fused slurry silicide coating. Since the FS-85 core was not protected by the B-1 cladding on the specimen edges, a glass matrix repair coating was applied to the edges. The grip ends of the tensile specimens were also glass repair coated to limit the area of oxidation to the test area and thus not starve the exposure furnace of available oxygen. Reentry profile exposure cycles (1, 3 and 10) were imposed on duplicate tensile and bend specimens. After exposure cycling, the specimens were tested at room temperature. Metallographic examination of each exposure condition was used to determine the metallurgical structure and microhardness of the clad material.

The bend and tensile specimens after exposure are shown in figures 36 and 37. Total consumption of the cladding and the FS-85 core occurred for the 10-cycle exposure specimens. The clad material passed the 2T bend test after one exposure cycle, but fractured after three exposure cycles. The tensile test results are presented in table VIII. The specimens which did not receive any exposure cycles were not annealed after sheet fabrication. The strength reduction after one exposure cycle resulted from a combination of thermal and oxidation effects of the reentry profile cycle. The tensile values after one cycle are identical to those of the three-cycle exposure specimens with 0.15 centimeter diameter coating defects (see table A-2, specimens E-30 and E-32). This was expected, since the specimens in this experiment had defects on both surfaces. The results confirm that the cladding does allow the FS-85 core to maintain good mechanical properties. As was the case for the local coating defect specimens, the yield strength was increased slightly with a small associated decrease in ultimate tensile strength and elongation (see table B-1, specimens E-26 and E-27 and table A-2, specimens E-1, E-2 and E-3). After three cycles, the uncoated clad specimens did not have a defined yield point or measurable elongation.

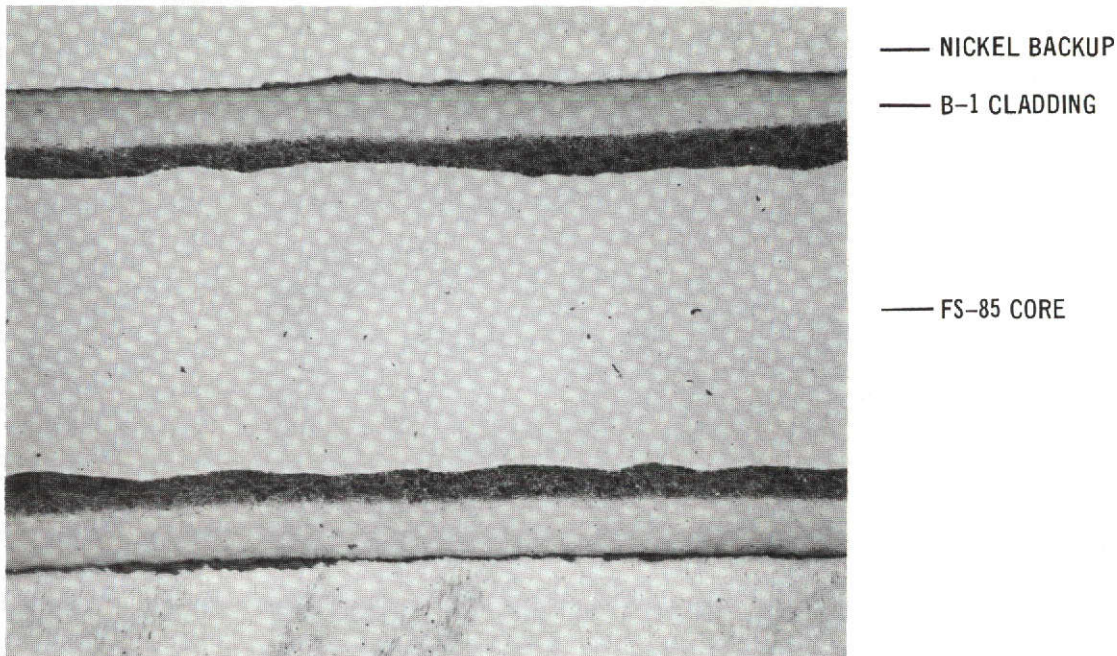
Typical photomicrographs of the B-1 clad specimens without R-512E coating after one and three reentry profile exposure cycles are shown in figure 38. Microhardness measurements after the 1-exposure cycle ranged from 185 to 195 (knoop), indicating no perceptible oxygen contamination of the FS-85 core. After three cycles, the core microhardness readings were up to 550 to 600. Figure 39 is a photomicrograph of the edge of a tensile specimen after three exposure cycles. The glass repair coating on the edge protected the cladding and provided an opportunity to observe the changes in metallographic appearance of the cladding produced by a gradient in stages of oxidation and oxygen content.

2.4.5 Tensile Properties of B-1 Alloy

A small amount of B-1 alloy was rolled into 0.05-centimeter thick sheet. Four tensile specimens were prepared, of which two were R-512E coated, and two were annealed for 1 hour at 1430°C to simulate the thermal cycle for coating application. The specimens were tensile tested at room temperature.

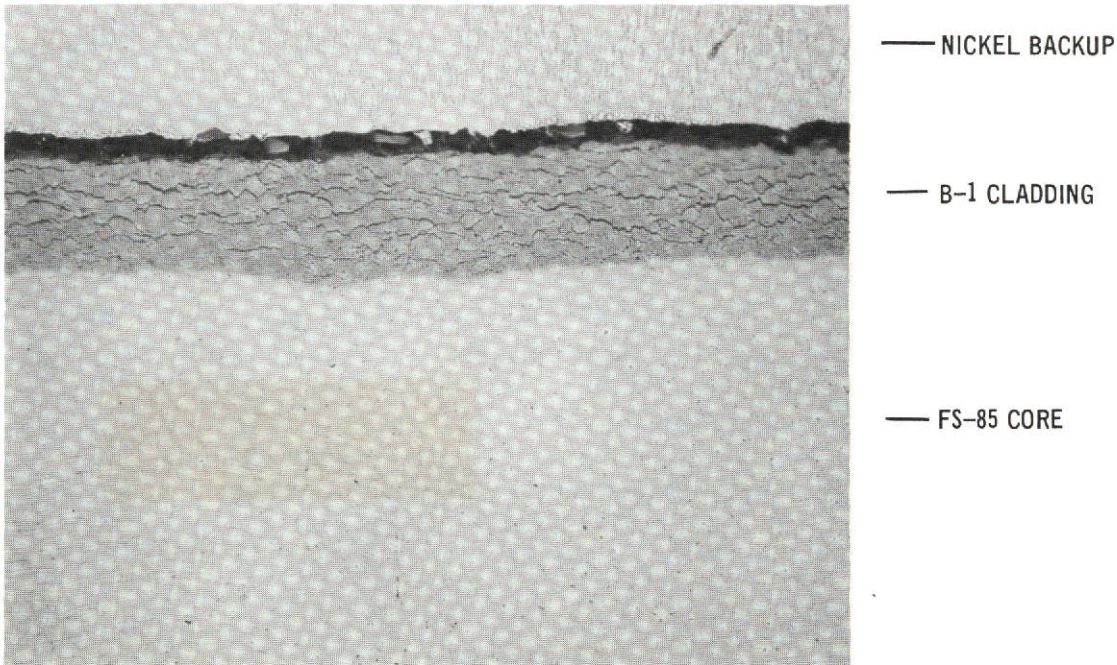
Tensile testing results are presented in table IX. The uncoated B-1 alloy was relatively strong, with an ultimate tensile strength in excess of 800 meganewtons per square meter and an elongation of 6 to 15 percent. After coating, the ultimate strength was less than half the uncoated value, with no defined yield point or measurable elongation. The coated material proved to be quite notch sensitive. The microstructures of the coated and uncoated B-1 material are shown in figure 40.

200X



ONE CYCLE

400X



THREE CYCLES

FIGURE 38 MICROSTRUCTURE OF UNCOATED B-1 CLAD ON FS-85 AFTER REENTRY PROFILE EXPOSURE CYCLING

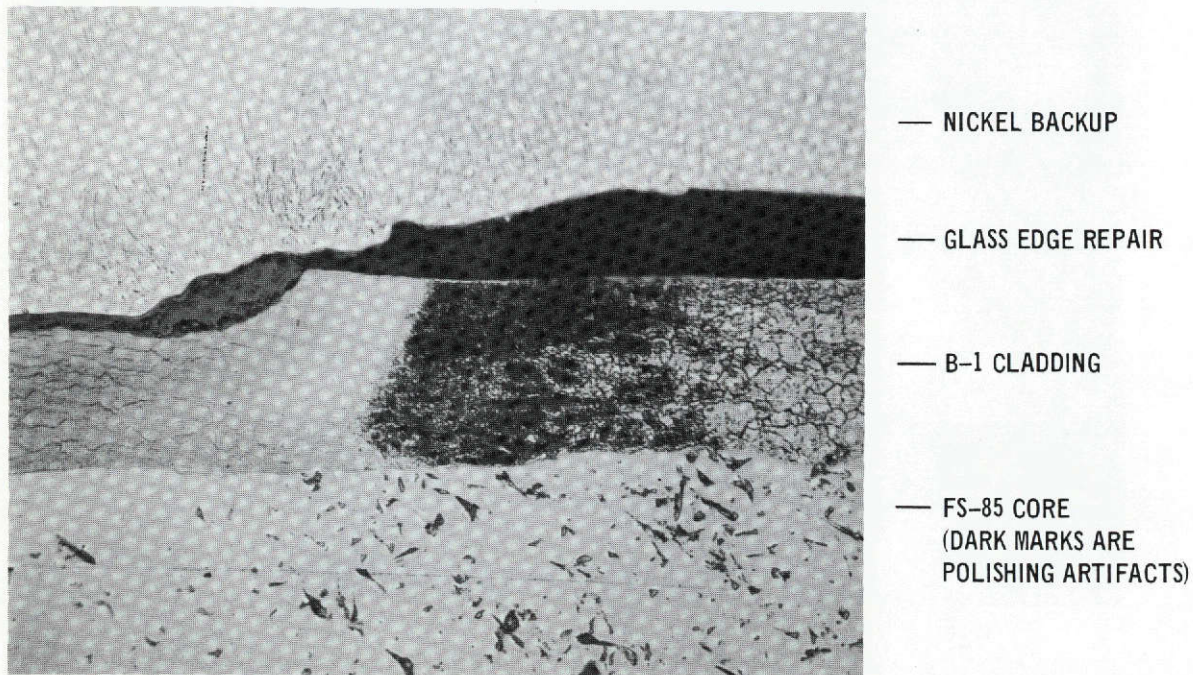


FIGURE 39 EDGE OF UNCOATED B-1 CLAD SPECIMEN AFTER 3 REENTRY PROFILE EXPOSURE CYCLES ILLUSTRATING OXYGEN CONTENT GRADIENT

457-3422

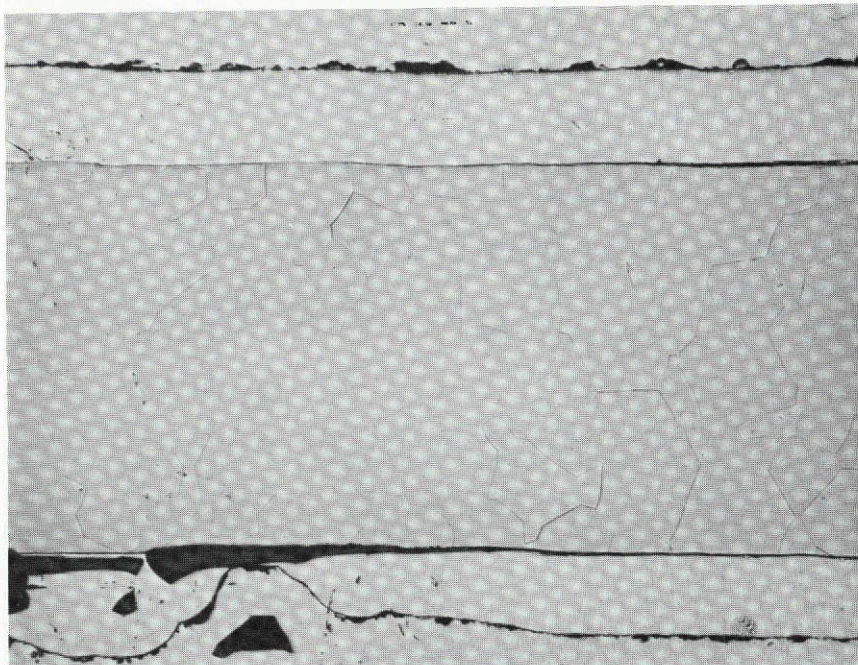
This page is reproduced at the back of the report by a different reproduction method to provide better detail.

TABLE IX
TENSILE PROPERTIES OF COATED AND UNCOATED B-1 ALLOY

SPEC NO.	MATERIAL	PROFILE EXPOSURE CYCLES	TEST TEMP	STRENGTH/PRECOAT AREA				% ELONGATION	STRENGTH/REMAINING METAL AREA			
				YIELD MN/m ²	YIELD LB/in. ² x10 ³	ULTIMATE MN/m ²	ULTIMATE LB/in. ² x10 ³		YIELD MN/m ²	YIELD LB/in. ² x10 ³	ULTIMATE MN/m ²	ULTIMATE LB/in. ² x10 ³
B1-1	B-1	NONE	-	-	-	396	57.4	0	-	-	423	61.4
B1-2	512-E	NONE	-	-	-	334	48.5	0	-	-	357	51.8
Avg	Coating	NONE	All at Room Temp	-	-	365	53.0	0	-	-	390	56.6
B1-3	B-1	NONE	786	114	820	119	15	-	-	-	-	-
B1-4	UNCOATED	NONE	772	112	807	117	6	-	-	-	-	-
Avg		NONE	779	113	814	118	-	-	-	-	-	-

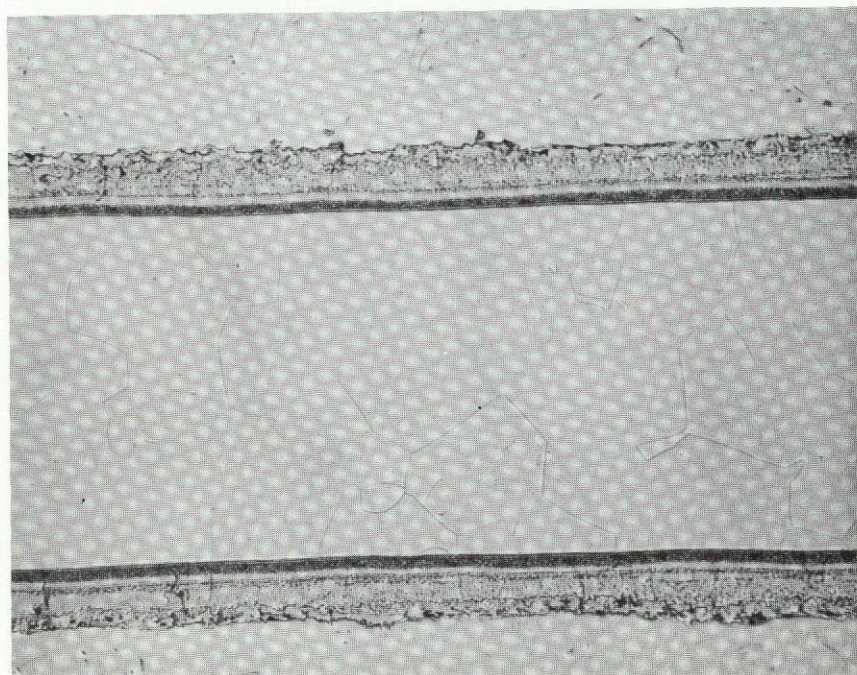
457-342:

100X



-B-1 ANNEALED
1 HOUR AT 1430°C

100X



-NICKEL
BACKUP
-R-512E
COATING

-B-1

FIGURE 40 MICROSTRUCTURE OF B-1 ALLOY SHEET

457-3424

This page is reproduced at the back of the report by a different reproduction method to provide better detail.

2.5 EMITTANCE MEASUREMENTS

Surface emittance of radiative cooled heatshield panels is very important because of its fourth power relation to surface temperature. Since the practicality of the outer skin protection system is dependent upon satisfactory emittance properties, suitable measurements were made as part of the evaluation process. Emittance specimens 2.5 by 2.5 centimeters were fabricated from both B-1 clad (nominal 50 micrometer thickness after coating) and unclad FS-85. Specimens were coated with the R-512E fused slurry silicide protective system per paragraph 2.2.4. Triplicate specimens were measured before profile exposure cycling and after 10, 50 and 100 profile exposure cycles as described in paragraph 2.3.1. Measurements were made at 870, 1090, and 1310°C for both ascending and descending temperatures.

Emittance measurements were made with a rotating sample emissometer consisting of four major components -- a high temperature furnace of modular design, a specially designed rotating sample holder, the optical transfer system, and a data acquisition system, as shown in figures 41 and 42.

The furnace consisted of a 36 centimeter cubical copper shell with heater element buss-bars located on the top of the furnace. The sample rotation mechanism and the entire optical system were built on a platform which attaches to the furnace top. The furnace itself was hung on the underside of the top flange of the vacuum chamber. Thus the furnace and the optical system could be lowered into the vacuum chamber (61 cm diameter and 122 cm deep) and the pressure reduced to as low as 1×10^{-6} torr. The furnace was heated by four elements located near inside corners. A specially designed graphite hair-pin type element was used in a nitrogen environment to the temperature limit of the insulation (1700°C). The insulation consisted of an inner 1.2 centimeter thickness of zirconia fiber board and an outer 3.8 centimeter layer of MDAC-E developed rigidized mullite fiber insulation (HCF). Furnace temperature was monitored using six thermocouples positioned at appropriate locations within the test chamber. Measurements were made when these thermocouples agreed within one percent.

The sample holder was fabricated from HCF, 15 centimeters in diameter and 2.5 centimeters thick, and held up to 8 emittance specimens, a reference blackbody groove (aspect ratio of 3 and wall emittance of 0.90), and a shield to establish a background signal level. A synchronous motor drove the specimens and the blackbody groove past the aperture in the end of the water-cooled sight tubes at 1.2 revolutions per second. Thus the time which the specimen was radiating to a cold surface was limited to approximately 60 microseconds per revolution.

The optical transfer system consisted of a sight tube, several apertures, the background shield, a mirror, and a 160 Hz chopper. The 7.6 cm diameter by 152 cm focal length paraboloidal mirror formed a reduced image of the end of the sight tube on the pyroelectric detector. An

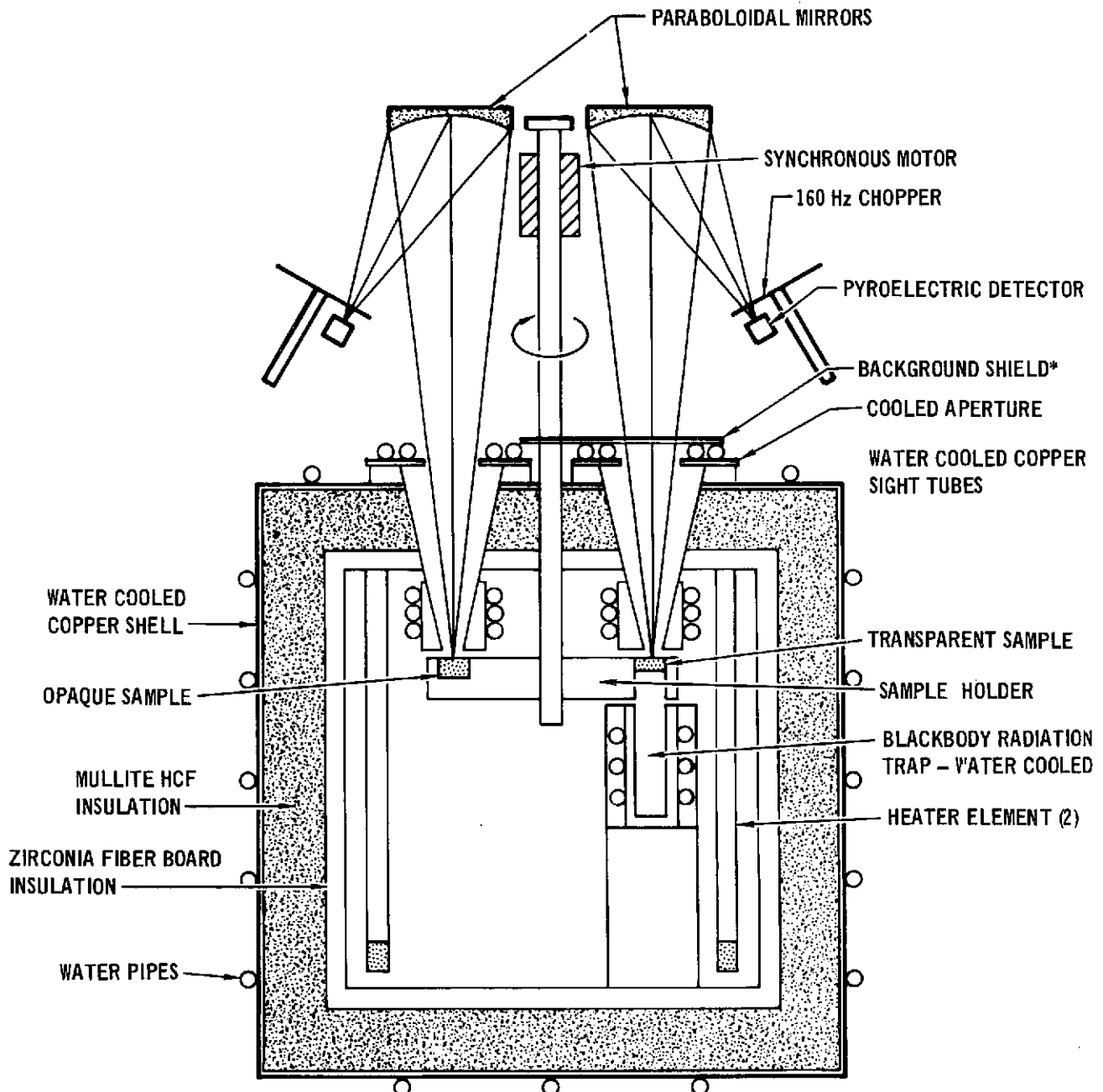


FIGURE 41 DIAGRAM OF ROTATING SAMPLE EMISSOMETER

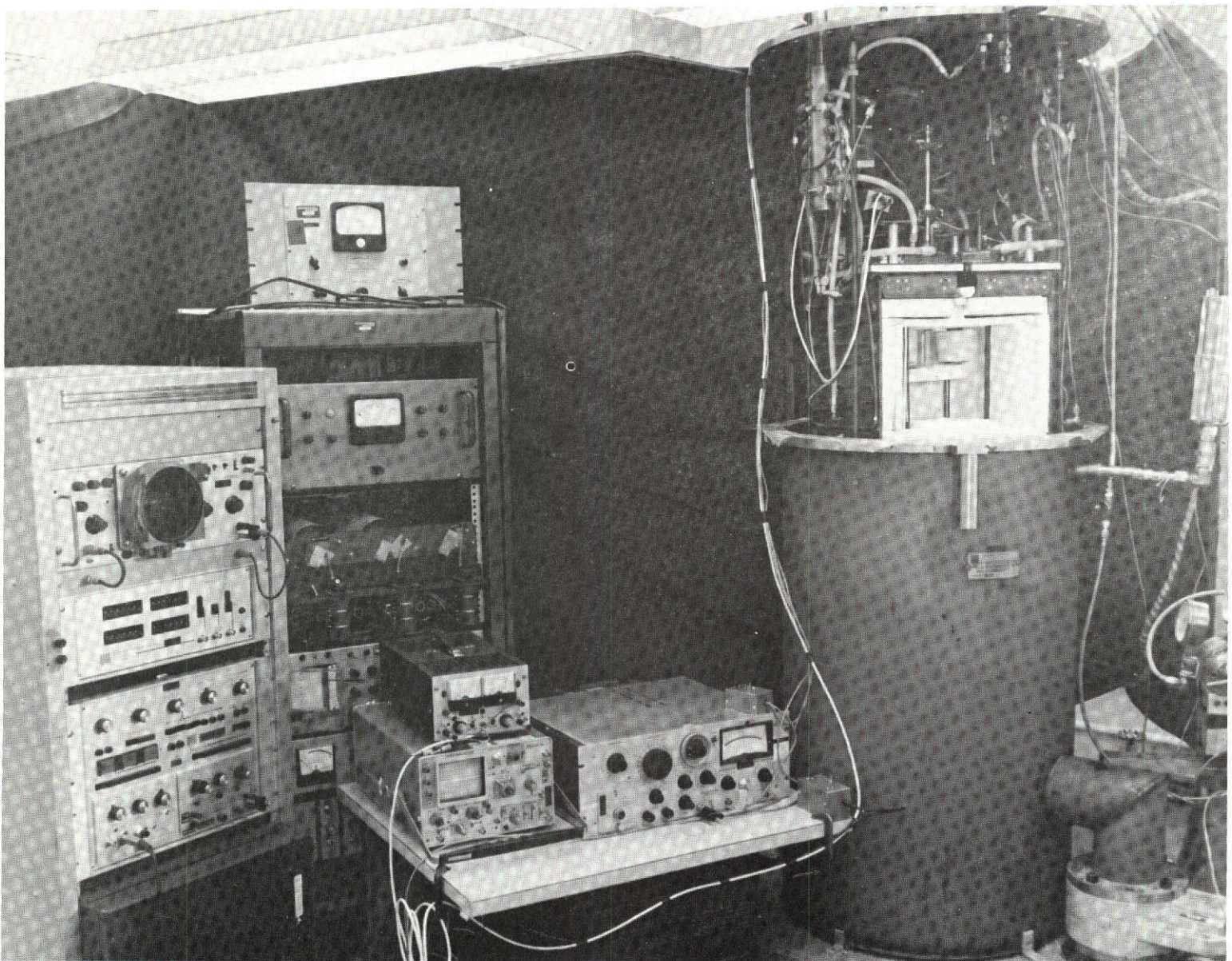


FIGURE 42 ROTATING SAMPLE EMISSOMETER

This page is reproduced at the back of the report by a different reproduction method to provide better detail.

aperture limited the field of view to minimize stray reflected radiation from the sight tube walls. The background shield was attached to the shaft of the sample holder and covered about 60 degrees out of the 360 degrees per revolution. Once each revolution it interrupted the flux from the sample and thus provided a suitable background reference signal level. A 160 Hz chopper modulated the flux in the optical system, and a reference signal was generated by a small lamp/photocell combination. If the sample was partially transparent, then flux emanating from the furnace walls, the sample holder, and the heater elements was transmitted through the sample into the optical transfer system along with the flux directly emitted by the sample. To separate these fluxes, a second sight tube was used together with a cold blackbody radiation trap located behind the sample to eliminate the transmitted flux, leaving only the direct emission from the sample.

The data acquisition system consisted of a detector, a lock-in amplifier, a signal averaging computer, and X-Y plotter, and a digital magnetic tape recorder. The detector was a Tem-Pres LCP-100S pyroelectric detector with a nominal 1-50 micrometer wavelength range. The detector crystal, mounted inside a TO-5 transistor can with a KRS-5 infrared window, was chosen because of its high sensitivity and small overall size. The detector was read by a PAR HR-8 lock-in amplifier tuned to the 160 Hz chopping frequency. This technique provided excellent noise rejection, which was extremely important, since the detector was a relatively high impedance device and was located about 5 centimeters from the heater element buss-bars. Output from the amplifier was connected to a Fabritek Model 1072 Signal Averager. The 1072 has a 1024 x 18-bit memory, a 12-bit a/d converter, and readout options. The signal-to-noise ratio of the data could be increased by a factor of 10 or more by averaging a number of scans, each scan corresponding to one complete revolution of the sample holder. The contents of the signal averager memory could be viewed on an oscilloscope, plotted on an X-Y recorder or read onto tape for further reduction on a CDC 6600 computer.

For opaque samples, the total normal emittance is

$$\epsilon_{TN} = \frac{V_S - V_{BG}}{V_{BB} - V_{BG}}$$

where V_S = detector signal due to the sample,

V_{BB} = detector signal due to the reference blackbody groove,

V_{BG} = detector signal due to the background shield.

The total hemispherical emittance of the fused slurry silicide coated columbium alloys is assumed to be equal to the total normal emittance. This assumption is based on the fact that the coated columbium and the coating oxide are perfect diffuse emitters. For this method, the presence of the blackbody groove and background shield on the sample holder itself means that the system was radiometrically recalibrated once per revolution,

that is every 800 milliseconds. This minimized system drift and permitted long periods of signal averaging, if necessary to improve the signal-to-noise ratio.

Emittance properties of fused slurry silicide coated FS-85 had recently been determined at MDAC-E under contract NAS3-14307 for Lewis Research Center. Considerable calibration and checkout had been accomplished under this contract to insure the accuracy of the emittance data. For this outer skin program, it was deemed appropriate to rerun a specimen previously exposed to 100 reentry profile cycles (number 13, reference 7) to establish that the data obtained with the rotating sample emissometer was consistent with the larger collection of emittance data previously obtained. Figure 43 presents this data as well as data established with platinum 13 percent rhodium. The data show very good agreement for both materials.

After exposing appropriate clad and unclad FS-85 specimens to the profile conditions of figure 17, emittance measurements were made at 870, 1090, and 1310°C using the rotating sample emissometer. In addition, one group of samples without prior exposure cycling was measured. The data generated is shown in figure 44 as a graph of the average values obtained and the in reading. The emittance profile cycling of the R-512E coating on the B-1 cladding alloy was consistently lower than the R-512E coating on the FS-85. However, the difference was small and both are considered typical for fused slurry silicide coated columbium. The emittance values of both coating/alloy combinations without profile exposure cycling were considerably lower because an oxide had not formed on the surface before exposure, and the 10-torr nitrogen atmosphere did not permit an oxide layer to be developed during the measurements. It was concluded that the emittance of the R-512E coating on the B-1 cladding is acceptable for use as an exterior thermal protection system material.

2.6 ELECTRON MICROPROBE ANALYSIS

Qualitative electron microprobe scans were made on typical 100 profile exposure cycle specimens for the first two program tasks. The results achieved are presented in figures 45 through 49. The most significant findings were the presence of a sharp interface between the B-1 cladding and the substrate and the absence of cladding alloy constituents migrating into the FS-85 core. This was a positive indication that titanium or aluminum was not diffusing into the FS-85 core to impair the mechanical properties (particularly creep strength) after long exposure times. The remaining scans indicated that the coatings were acting in a normal and predictable way, since the results obtained were similar to those found by HiTemCo, (reference 8).

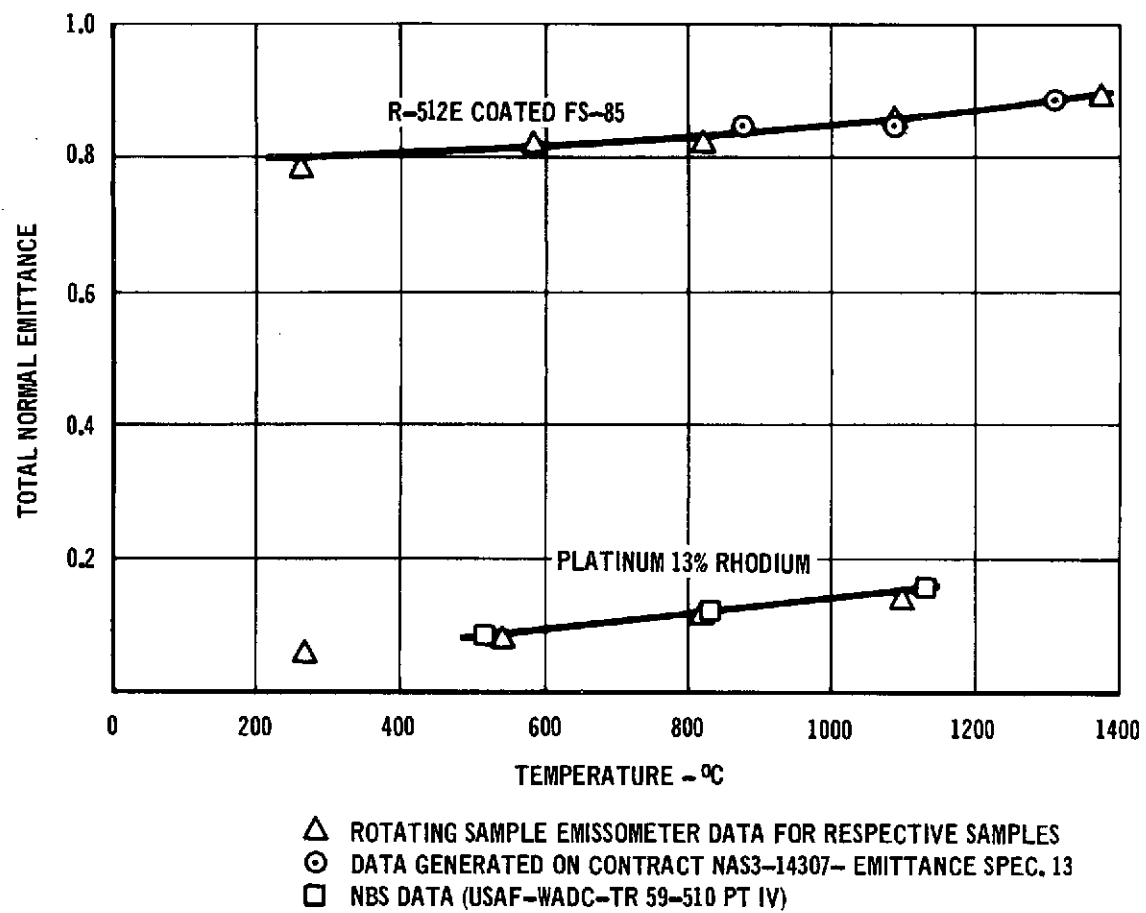


FIGURE 43 CHECK OUT RESULTS FOR ROTATING SAMPLE EMISSOMETER

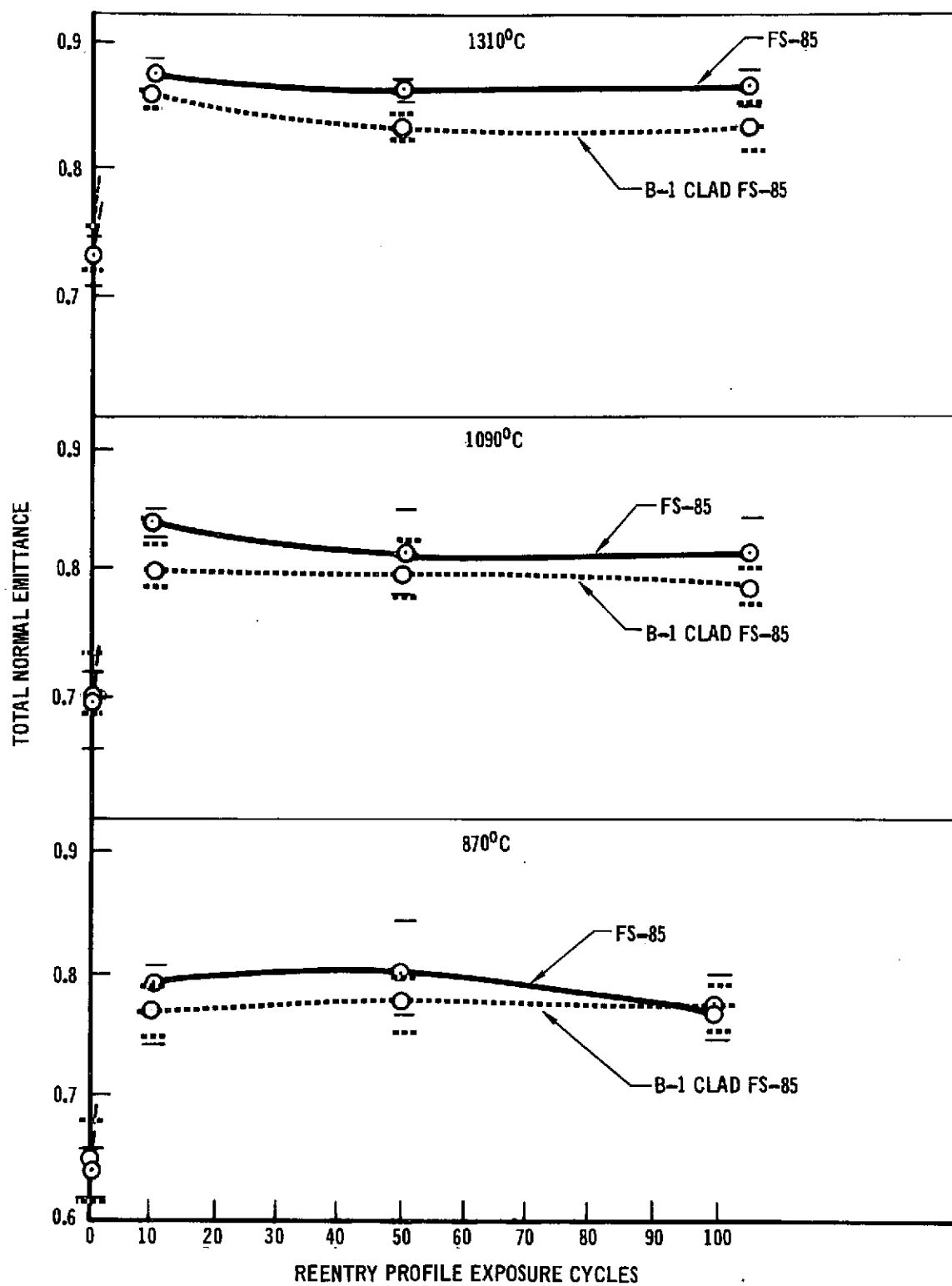


FIGURE 44 EMITTANCE OF R-512E COATED B-1 CLADDING AND FS-85

OUTER PROTECTIVE SKIN

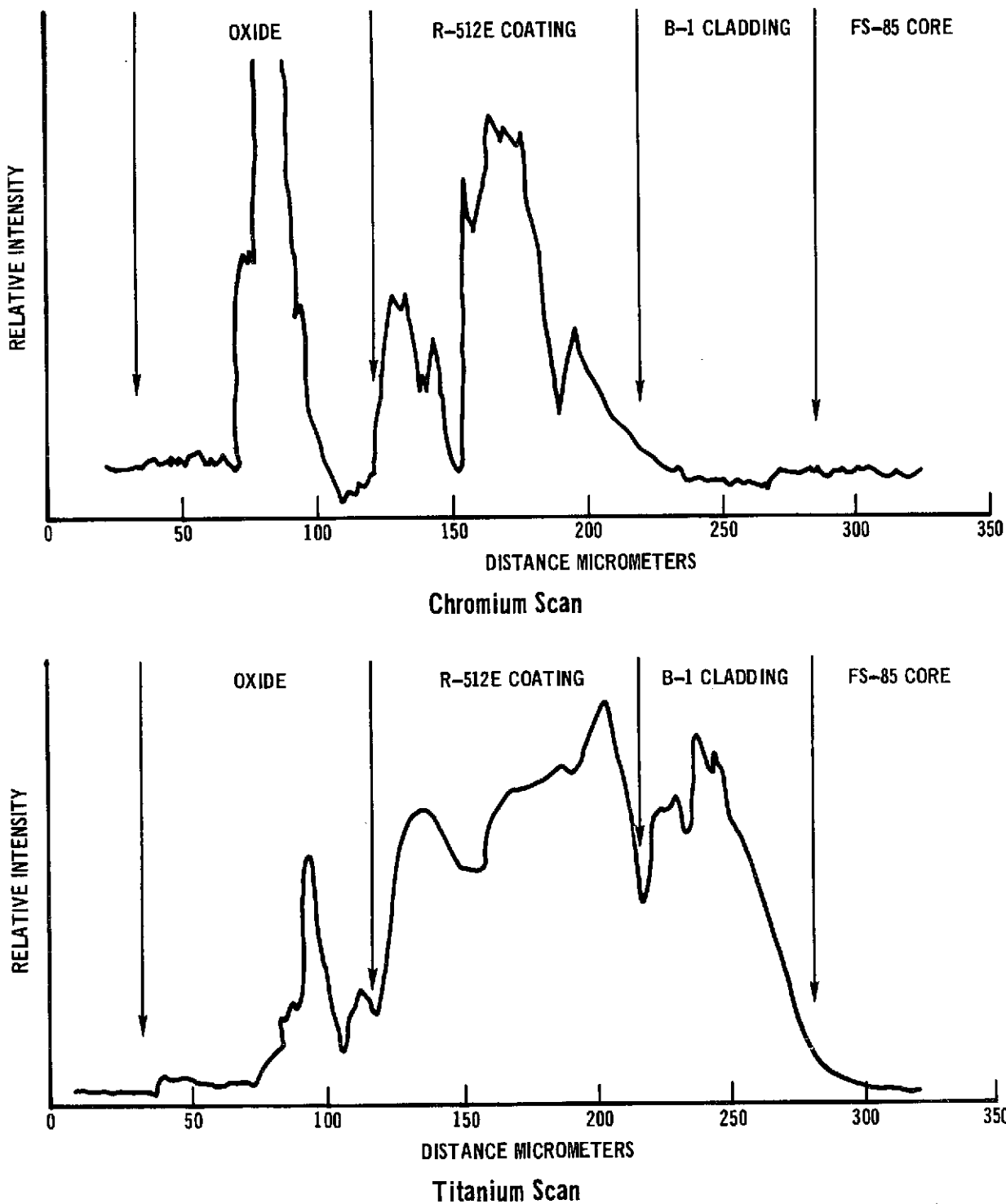


FIGURE 45 ELECTRON MICROPROBE SCANS OF B-1 CLAD FS-85 WITH THE R-512E COATING AFTER 100 REENTRY PROFILE CYCLES (TASK I EXPERIMENT)

OUTER PROTECTIVE SKIN

Report MDC E0913
September 1973

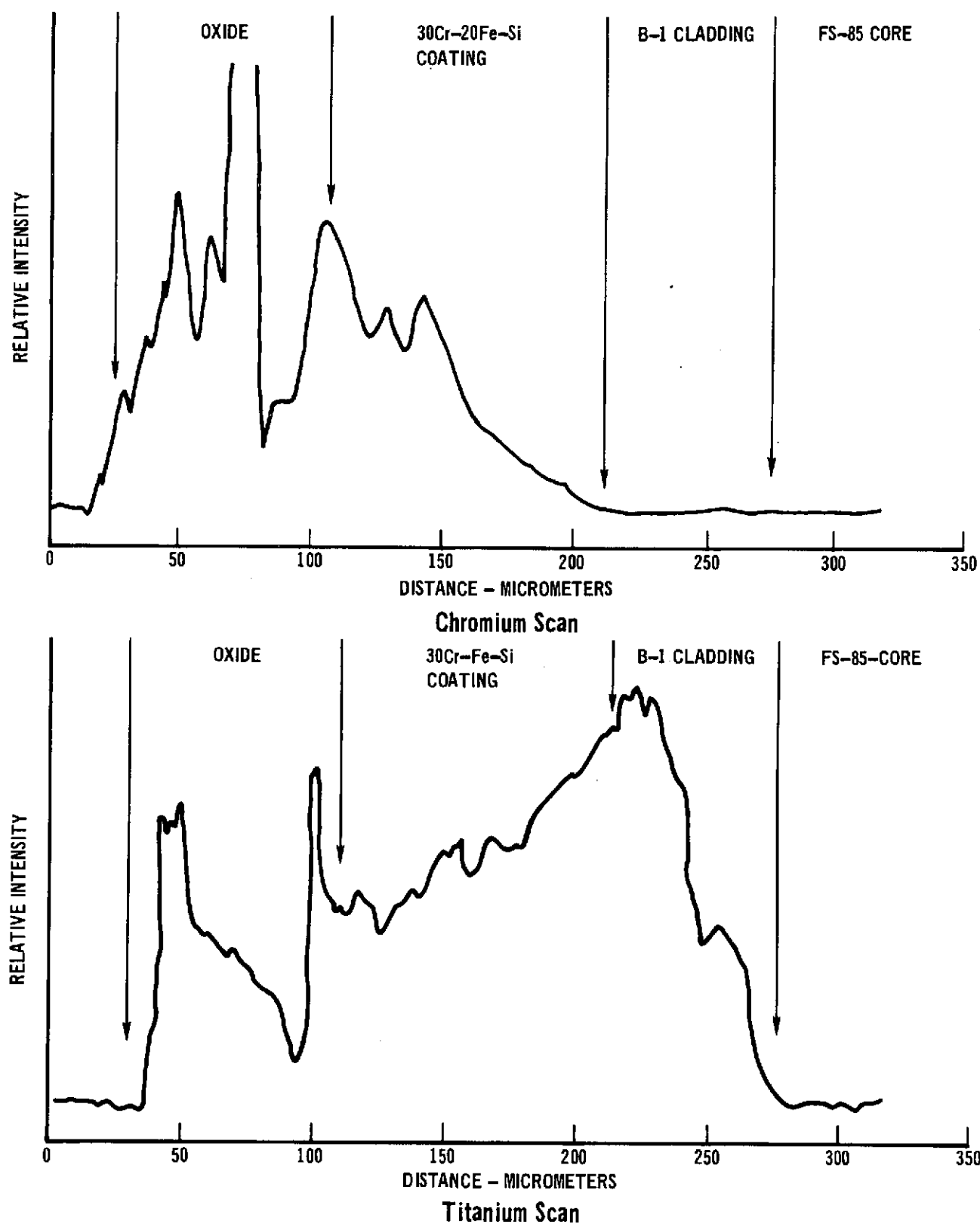
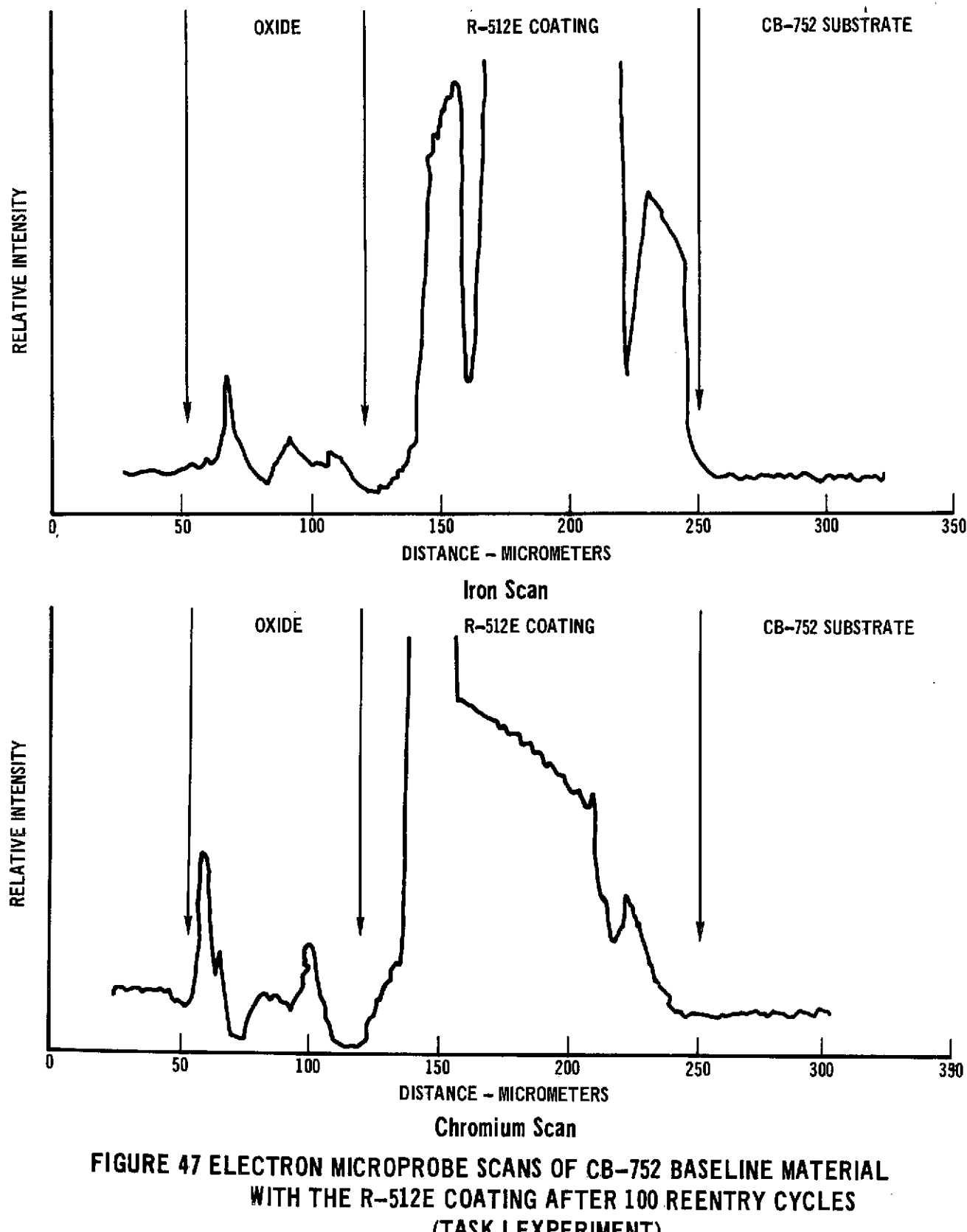


FIGURE 46 ELECTRON MICROPROBE SCANS OF B-1 CLAD FS-85 WITH 30Cr-20Fe-Si COATING AFTER 100 REENTRY PROFILE CYCLES (TASK I EXPERIMENT)

OUTER PROTECTIVE SKIN

Report MDC E0913
September 1973



**FIGURE 47 ELECTRON MICROPROBE SCANS OF CB-752 BASELINE MATERIAL
WITH THE R-512E COATING AFTER 100 REENTRY CYCLES
(TASK I EXPERIMENT)**

OUTER PROTECTIVE SKIN

Report MDC E0913
September 1973

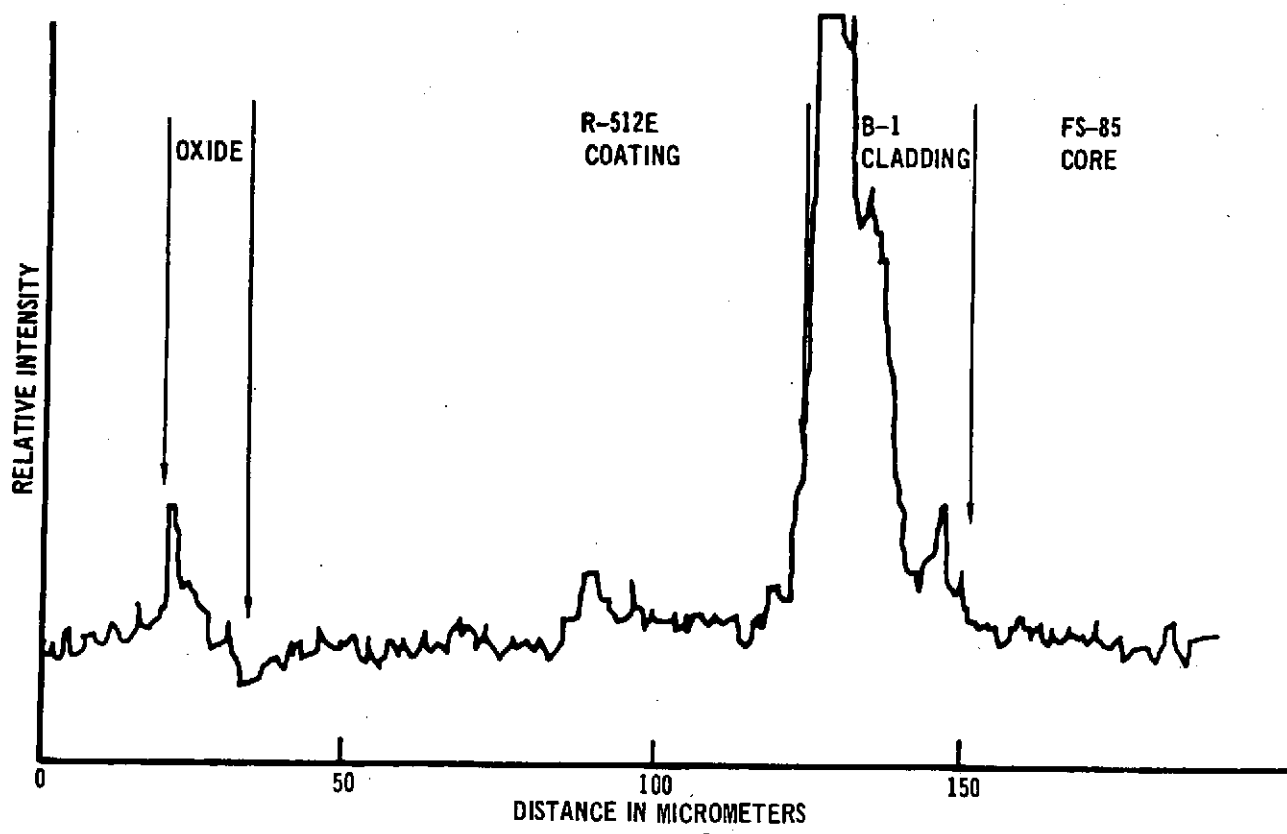
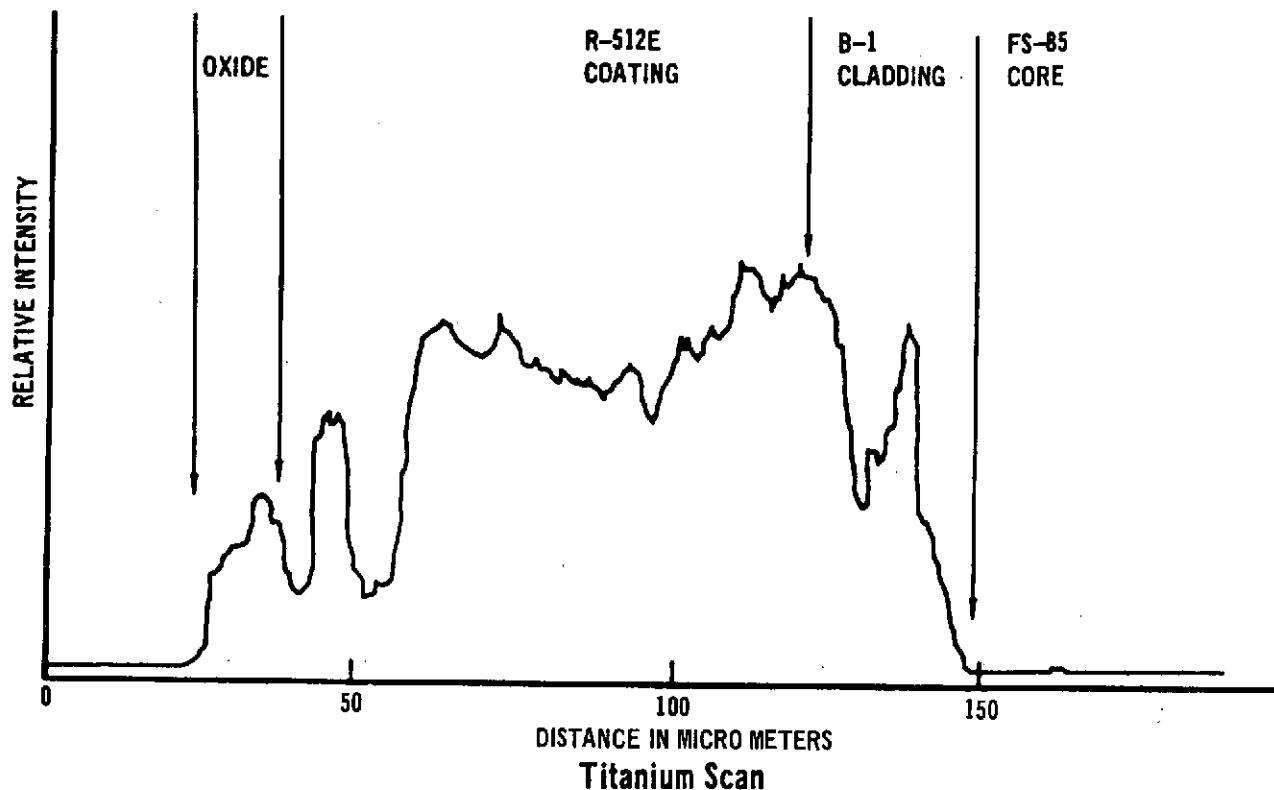


FIGURE 48 ELECTRON MICROPROBE SCANS OF B-1 CLAD FS-85 WITH THE R-512E COATING AFTER 100 REENTRY PROFILE CYCLES

OUTER PROTECTIVE SKIN

Report MDC E0913
September 1973

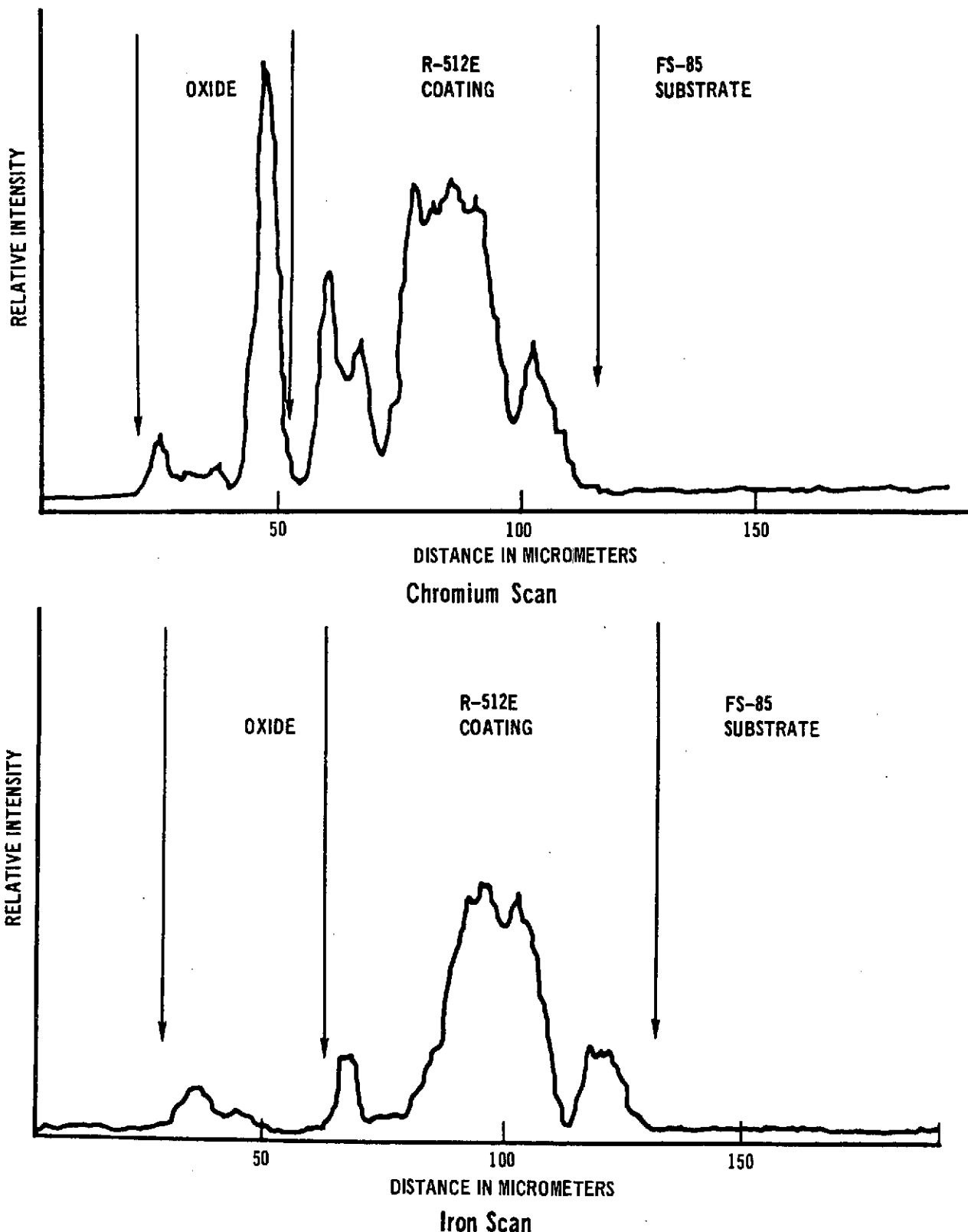


FIGURE 49 ELECTRON MICROPROBE SCANS OF R-512E COATED FS-85 WITHOUT CLADDING AFTER 100 REENTRY PROFILE CYCLES

3. DISCUSSION OF RESULTS

It is necessary to assess the results achieved on this program within the context of other cladding development efforts and the requirements of a hypersonic reentry vehicle system. This is the first experimental effort directed toward thermal protection systems for reentry vehicles, yet claddings for engine components offer some basis of comparison. The applicability of the clad system to an operational reentry system must consider such factors as increased reliability contrasted to increased weight and cost to determine the practicality of continued development of the outer skin protection concept.

3.1 COMPARISON WITH OTHER CLAD SYSTEMS

Other clad systems investigated for improved reliability of coated columbium have been for jet engine turbine components. In the case of turbine components, the hardware is not inspectable without disassembling the engine. Thus the maximum time of engine operation between maintenance overhauls is the minimum oxidation life of the protective system. While the average life of coated columbium is quite good, there is a small but statistically significant percentage of early or premature failures which severely limits the time between engine disassembly and inspection. Heat shield panels have a similar potential of early coating failures and increased potential danger of physical damage because of their exterior exposure. Heat shield panels have a decided advantage in that they are exposed for inspection between operational service cycles.

One of the initial investigations toward the development of the clad concept for a secondary zone of protection below a conventional coating was the development of the B-1 alloy by Westinghouse (reference 1). The object of the program was to improve the oxidation resistance of columbium alloys while maintaining a functional level of ductility. (See paragraph 2.1.1.2 for additional information on the B-1 alloy.) This alloy development work was the foundation of the program reported herein.

Battelle (reference 13) approached the cladding of FS-85 for turbine blade applications with another alloy, 42Ti-4Cr-4Al, designated T-166. While this program was plagued with several experimental difficulties, it was concluded that the concept and the T-166 alloy held high potential for providing a fail-safe columbium turbine blade operation for at least 50 flight operation cycles. The T-166 alloy, because of its high titanium content, is believed to be more oxidation resistant than the B-1 alloy. It was not possible to directly compare results of defect oxidation testing as the reference 13 results had no usable data for defects greater than 100 micrometers (4 mils). There was also no strength data, coating performance for the T-166 was too poor for an assessment of coatability and emittance data was not gathered. The T-166 alloy cladding on FS-85 was evaluated in a plasma test for three cycles, as reported in reference 10. While a defect of 0.1 centimeters in diameter was tested with impressive results, the exposure was not long enough for a valid comparison. Since the T-166 appears to have significant potential for heatshield applications, a comprehensive evaluation remains to be performed.

OUTER PROTECTIVE SKIN

3.2 UTILIZATION OF THE OUTER SKIN CONCEPT IN A REENTRY SYSTEM

The objective of the program was to evaluate the outer protective skin material to determine the feasibility of increasing the reliability of a coated columbium thermal protection system in a hypersonic reentry application. Several factors must be considered within the context of the current status of coated columbium technology to assess the system benefits provided by the outer protective skin material concept. An analysis at this stage of the materials life cycle must be qualitative and preliminary. However, the potential of the material and the areas requiring further development can be accurately assessed.

3.2.1 Cladding Thickness and Reentry System Reliability

The reliability of coated columbium thermal protection system panels depends on a definition of terms and criteria. The technology of coated columbium has progressed to a point that a significant degree of reliability is attributed to the material. As has been previously discussed, columbium oxidation has two distinct effects, loss of cross sectional load bearing area and property degradation through oxygen contamination. Within the context of local coating failures, the area affected is small compared to the skin area, and structural failure due to local property degradation is inconsequential. References 7 and 9 report testing panels with intentional defects in which design loads were sustained long after sizeable holes were oxidized through the skin. While structural failure is not of immediate consequence, ingestion of hot boundary layer gas into the vehicle is very significant. Thus, the reliable performance of a coated columbium panel depends first upon the prevention of oxidation holes in the skin, and mechanical property degradation in adjacent areas is a secondary consideration.

A significant amount of work has been accomplished in which reuse capabilities of coated columbium have been studied. Battelle (reference 10) has recently completed a study in which the degradation and reuse properties of coated columbium (unclad) were considered and the following conclusion drawn,

"In general summary, the overwhelming conclusion is that the R512E/FS85 system is the superior system of those investigated by an appreciable margin in all respects except one -- it is somewhat heavier. Nevertheless, it is considered highly probable that a properly designed and maintained reradiative TPS system based on R512E/FS85 would provide highly reliable service for the space shuttle mission. Even in the likely, but infrequent, event of local failure of the protective coating, fully reliable service could be expected for at least ten orbiter reentry flights. With any reasonable inspection and maintenance schedule, local coating failures should be detected and repaired in far fewer than ten flights after their occurrence."

This is in general agreement with MDAC-E findings and those of the industry in general, and, therefore, seems appropriate as the criterion for reliability of a coated columbium panel of the R-512E coated FS-85 baseline material.

Employing a B-1 cladding layer between the protective coating and the load bearing core increases the reliability of coated columbium material; the improvement is proportional to the B-1 thickness. The baseline reliability of a minimum of 10 reentries for R-512E coated FS-85 would be increased to 15 reentries with a nominal 50 micrometer B-1 cladding, and to 25 reentries with a nominal 100 micrometer cladding. These projections are based upon 5 and 15 cycles required to oxidize through the cladding to the core for the nominal 50 and 100 micrometer B-1 cladding thicknesses, respectively. These are considered conservative projections as they do not account for the beneficial qualities of the B-1 in reducing the oxidation rate of the core after the cladding has been consumed at a local defect site. Table V presented the estimated cycles to form a hole through the FS-85 sheet to be 21 cycles and for the 50 and 100 micrometer clad sheet 32 and 44 cycles, respectively. Thus, the cladding substantially improves the reliability in the primary area of concern, aerodynamic hole formation. While the degradation of mechanical properties in the immediate area of an oxidation site is considered of secondary importance, it should be noted that the B-1 cladding reduces this contaminated zone by more than an order of magnitude for the 100 micrometer cladding and by a factor of 2 for the nominal 50 micrometer cladding.

The cladding could be beneficially used on the interior surface as well as the exterior surface discussed in the preceding paragraph. Some concern has been expressed for coating defects on an interior surface (reference 11). In such cases, the interior air pressures can be sufficiently low so that no gross oxidation would occur which could reduce the sheet thickness, although the diffusion of oxygen into the sheet occurs at the same rate as proliferates from exterior failure sites. General coating breakdown or numerous coating failures could conceivably lead to mechanical property degradation over a significant area. While it is true that proper quality control on the coating process and correct handling procedures would mitigate the internal defect problem, the use of internal surface cladding would provide a reservoir of a nonload bearing material to absorb incoming oxygen. Current data on property degradation in an internal pressure environment is incomplete. Estimates of minimum reentry flight reliability over approximately 20 cycles are currently being used. The use of internal cladding would significantly increase this number, probably to 30 or 40 cycles. The use of internal cladding may not be justifiable on all internal surfaces solely on the basis of increased reliability. There may be critical areas where high static or fatigue loads may be present, thereby making the increased reliability achieved from internal cladding a viable approach.

A third potential use of the outer skin concept would be for leading edge applications. In areas where stagnation point heating and pressure are encountered, local coating defects will probably be more significant. Local coating defects or oxide modules could disturb the compressed boundary layer and cause an increase in local temperature and substrate oxidation rate. Minimum estimated reentry cycle reliability under these more stringent conditions are three to seven cycles. The use of panel reliability increase factors of 1.5 to 2.5, depending on cladding thickness, would increase the lower three cycle value to 4.5 to 7.5 reentries. The major contribution of such an increased

reliability would be to provide a fail-safe backup protection system in a small area of critical importance to the success of the total flight system.

Summarizing the assessment of minimum B-1 cladding thickness for increased reliability, the following can be projected:

- (1) Coated columbium heatshield panels have a minimum baseline reliability of ten cycles.
- (2) Increases in reliability through the B-1 clad outer skin concept are proportional to cladding thickness. At a cladding thickness of 50 micrometers, the minimum reliability is 15 reentries, and for a cladding thickness of 100 micrometers, it is 25 reentries.
- (3) Increased reliability through cladding internal panel surfaces to mitigate property degradation through internal coating breakdown without associated visual warning is possible. Reentry cycle reliability is estimated to be improved from a minimum 20 reentry baseline to an improved level of 30 to 40 cycles, with critically stressed areas are the most likely to benefit from the cladding approach.
- (4) The desired level of increased reliability depends upon the specific application and design criteria being employed. The use of the outer skin cladding concept for local critical areas, such as leading edges, provides an effective way of achieving a fail safe system.

3.2.2 Evaluation of Material Property Allowables

After determining the appropriate cladding thickness to achieve the desired level of increased reliability, the material strength properties must be considered. The best understanding of the tensile properties is presented in table VI. The amount of test data does not permit design allowables to be established, and there are conflicts at some points which remain to be resolved. Therefore, the assessment of material property allowables will deal with engineering approaches to design allowables and to clad material behavior characteristics.

The B-1 clad FS-85 tensile properties changed in behavioral character with changes in cladding thickness. The FS-85 core material is a ductile, tough moderate strength alloy, while the B-1 cladding alloy is a higher strength (room temperature) notch sensitive material with a ductile to brittle transition temperature close to room temperature. When the cladding is sufficiently thin, the properties of the composite are virtually the same as those of the FS-85 core. One can assume that the cladding is part of the oxidation protection system and neither contributes nor detracts from the load bearing capabilities of the core. This behavior occurs at nominal cladding thicknesses up to 50 micrometers. At cladding thicknesses of 100 micrometers the composite strength characteristics were found to be different from the strength characteristics of the core material. The most noticeable was the decrease in ductility which presumably was due to the notch sensitivity of the B-1. The 100 micrometer

B-1 cladding composite room temperature and 760°C strengths were higher than the anticipated strength based upon the core area and properties. The 1320°C strength was lower than anticipated. Thermal cycling for up to 100 reentries did not degrade the strength of the core for the 50 micrometer cladding thickness and the data for the 100 cycle material was unreliable because of oxidation failures in the exposure cycling. The creep properties, based upon 100 cycle stress profile tests were not degraded and fatigue properties were not considered.

In summary, cladding thicknesses of 50 micrometers or less did not contribute or detract from the core properties. Thicker claddings will influence the strength characteristics, and, therefore, the material must be considered as a composite. As the cladding has been examined only within narrow limits, its notch sensitivity and relatively high ductile to brittle transition temperature must be carefully considered with respect to brittle fracture in fatigue or biaxial stress loadings, and to size effects. The cladding clearly does not deleteriously affect the strength of the FS-85 alloy, but the clad material is not as forgiving and tough as the unclad material.

3.2.3 Assessment of Cladding Weight Penalty

Weight is a very important factor for reentry structures because of the high cost of putting vehicles into orbit. The effect of weight was determined by comparing the masses of clad and unclad FS-85 alloy sheet, since the design study indicated that equal thicknesses of load bearing core were required and no additional cladding would have to be included for manufacturing requirements. The weight assessment approach paralleled the logical design approach of determining the load bearing gauge required and adding material to allow for metal consumption during the manufacture and life of the panel.

Several programs (references 7, 9 and 11) have identified 200 micrometers of FS-85 as an appropriate skin load bearing thickness for a number of different panel designs for a multiple reentry vehicle. When mill tolerances and metal consumption allowances are applied, the required sheet gauge increases to 316 micrometers, which is a practical minimum thickness considering standard manufacturing and handling procedures. It should be noted that thicker load bearing cross sections have a proportionally lower percentage weight penalty associated with adding an outer skin cladding. The following assumptions were made prior to comparing the B-1 clad and unclad FS-85 sheet:

- (1) Premium rolling tolerance on clad sheet, for the core and total thickness, would be plus or minus 10 percent of the load bearing thickness.
- (2) An allowance of 25 micrometers would be required for such manufacturing aspects as acid pickling, local rework, blending surface defects, etc.
- (3) An allowance of 25.4 micrometers of metal surface recession would be required for a 76.2 micrometer fused slurry silicide coating, per coated surface.

- (4) An allowance of 10 micrometers per coated surface would be necessary for additional metal recession occurring in 100 reentry cycles.
- (5) The density of FS-85 is $10,600 \text{ kg/m}^3$ and B-1 alloy is $8,400 \text{ kg/m}^3$.

Various combinations of B-1 cladding thickness on one or both surfaces were used as a basis of comparing the masses of clad and unclad sheet material.

The results of comparing the mass of various cladding combinations are presented in table X. The first cladding thickness remaining after coating and 100 reentry cycles presented is 12.8 micrometers. This is not a practical thickness to consider for oxidation protection, but it does illustrate the thickness of cladding that can be achieved without any weight penalty. This "free" cladding is realized by replacing the heavier FS-85 with the lighter B-1 for that volume of metal consumed during coating and in service. The second cladding thickness presented is 25 micrometers, a minimum practical thickness necessary for the desired increase in reliability of an external surface. Given the parabolic relationship between cladding thickness and oxidation behavior, only 1 to 2 cycles of increased life at a defect site could be projected. This amount, while small, would enhance the fail-safe character of the system with a mass increase of only 3 percent.

An interesting concept would be to combine an appropriate amount of cladding on an exterior surface, for the desired increase in panel reliability life, with the weight free volume of B-1 on the internal surface. The benefits to internal reliability afforded by 12.8 micrometers of B-1 could be significant because of the low oxygen internal pressure. Furthermore, there would be no weight penalty and nominal additional cost (compared to cladding only one surface).

One of the most practical systems, considering all factors, is the 50 micrometer system applied to one surface. The increased reliability life based on the cycles necessary to consume the cladding in oxidation represented a total of five cycles. The mass of such a material was 3.66 kg/m^2 , or an increase of 9.25 percent compared with unclad FS-85. This weight penalty appears to be minimal in light of the increased reliability. Yet, the actual benefits of the increased reliability have to be assessed for the particular system being designed. The 100 micrometer cladding increased the reliability life to 25 reentry cycles, and the associated increase in mass over the unclad material was 21.8 percent. The effect of B-1 cladding on one and both surfaces is graphically presented in figure 50.

3.2.4 Panel Design and Fabrication

Several studies conducted in the recent past have dealt with coated columbium panels and their reusability for a minimum of 100 reentry cycles (references 7, 9, 10, 11 and 12). There is general agreement that columbium panels can perform satisfactorily to design conditions, and while local physical damage may shorten the total life, no immediate or catastrophic degradation will occur. With these types of questions settled, attention has turned toward producing coated columbium panels at lower cost and improved quality. It is appropriate to assess the practicality of the design and the manufacture of panels employing the outer skin clad material concept within

TABLE X
MASS OF CLAD AND UNCLAD FS-85 SHEET REQUIRED FOR COATED
HEATSHIELD PANELS FOR 100 REENTRY CYCLES

FS-85 LOAD BEARING THICKNESS (MICROMETERS)	REMAINING B-1 CLAD THICKNESS AFTER COATING AND 100 REENTRIES (MICROMETERS)		TOTAL THICKNESS OF CLAD & CORE AFTER COATING (MICROMETERS)	SHEET THICKNESS TO PURCHASE (MICROMETERS)	TOTAL MASS MASS OF PURCHASED SHEET (kg/m ²)	PERCENT MASS INCREASE OVER UNCLAD FS-85
	FIRST SURFACE	SECOND SURFACE				
220	UNCLAD FS-85		220	316	3.35	0
	12.8	0 ⁽¹⁾	233	329	3.35	0
	12.8	12.8	246	342	3.35	0
	25	0	245	341	3.45	3.05
	25	12.8	258	354	3.45	3.05
	25	25	270	366	3.56	6.27
	50	0	270	366	3.66	9.25
	50	25	295	391	3.76	12.2
	50	50	320	416	3.98	18.8
	100	0	320	416	4.08	21.8
	100	50	370	466	4.40	31.3
	100	100	420	516	4.82	43.8

NOTE: ⁽¹⁾ - "0" INDICATES THE SURFACE IS UNCLAD.

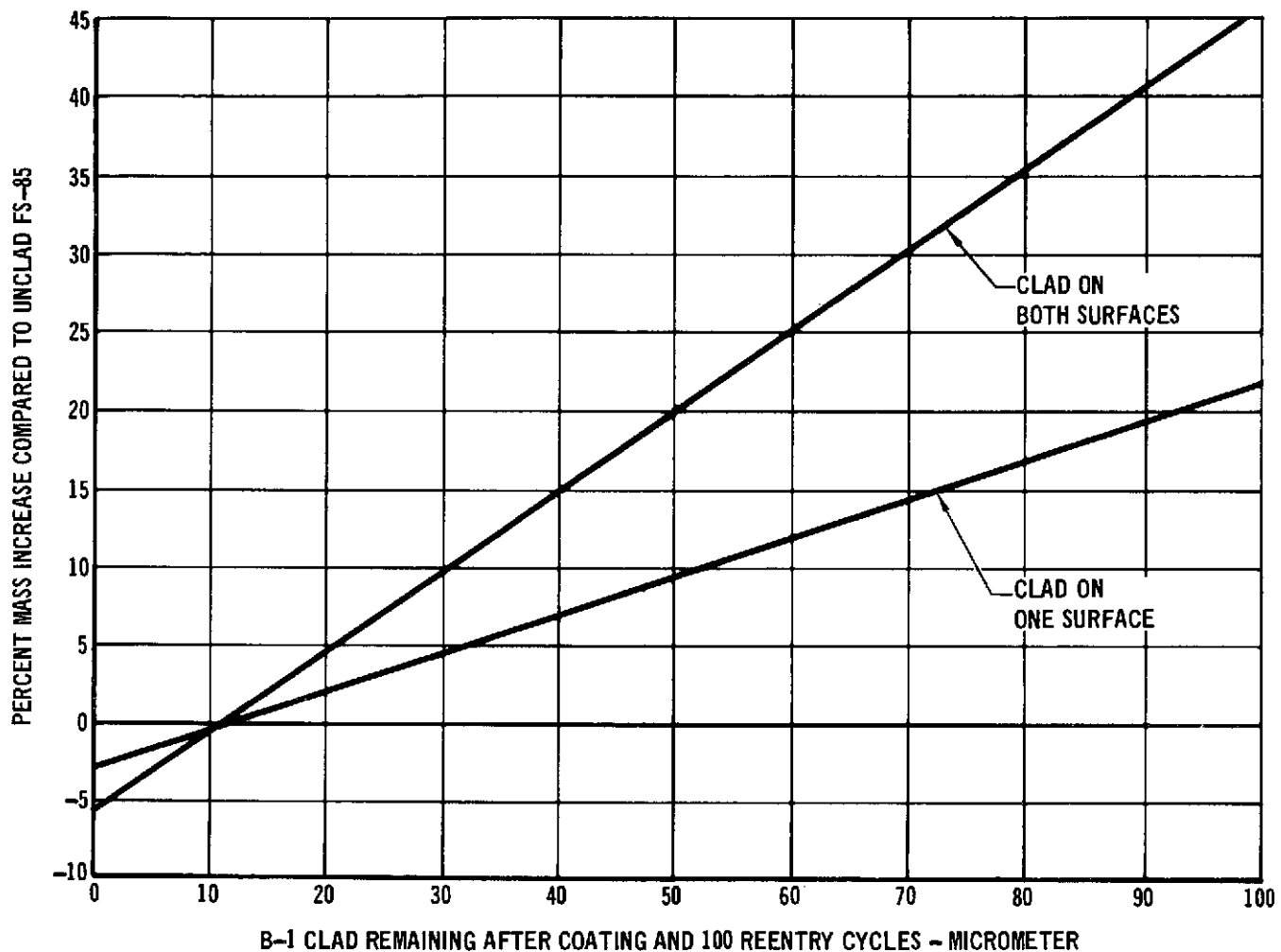


FIGURE 50 EFFECT OF B-1 CLADDING ON MASS OF FS-85 SHEET

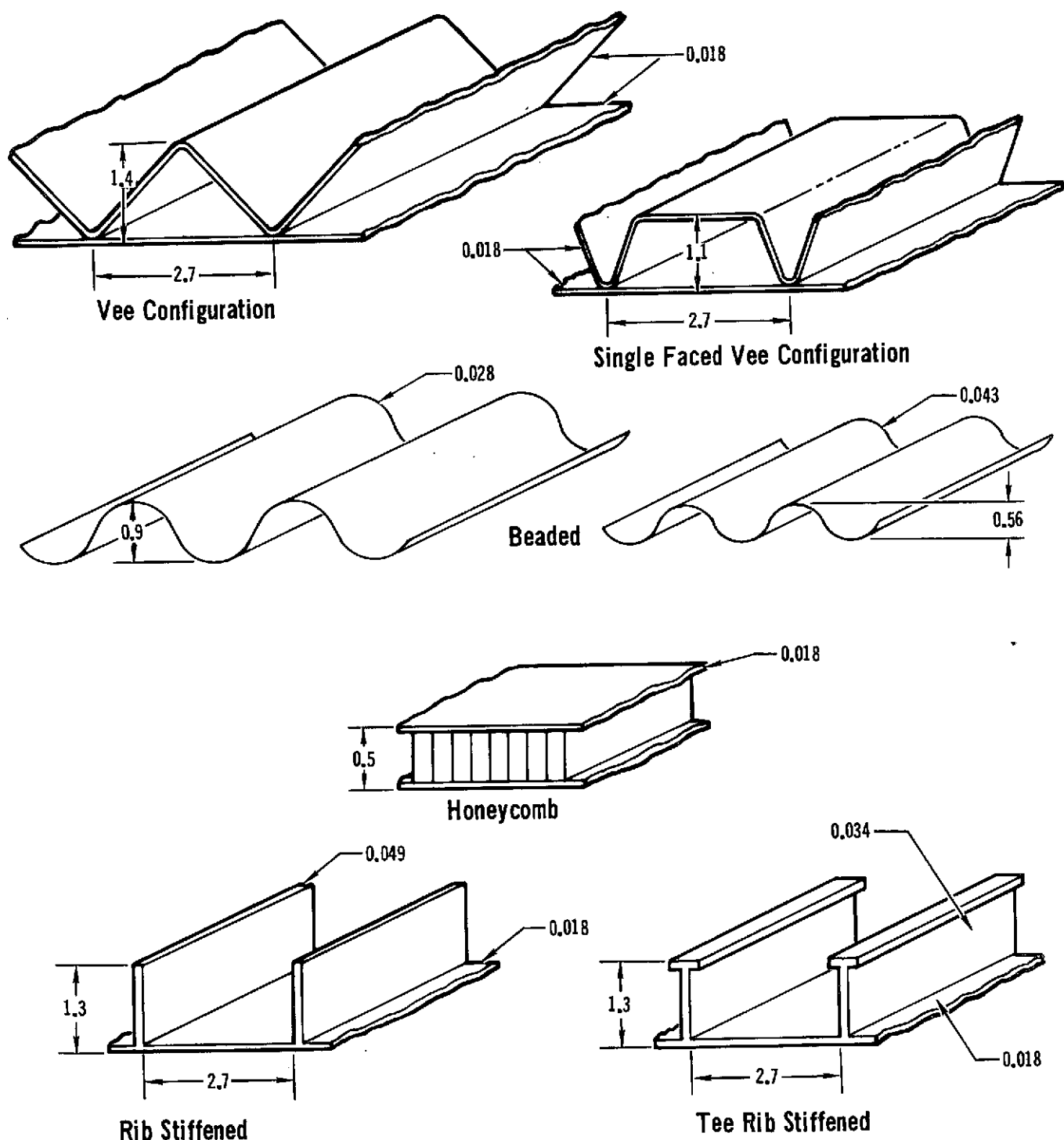
the context of present and future trends in the design and manufacture of columbium hardware.

Current columbium panel design approaches shown to be structurally efficient and capable of reliable coating protection are illustrated in figure 51. Each of the designs was assessed to determine the practicality of the clad material for that particular design. The beaded design is currently gaining more popularity because of its obvious simplicity and cost effectiveness. Convair is evaluating this design in a major structural panel assembly (reference 12). The outer skin clad material could be readily used with this design, and the cladding could be effectively employed on both interior and exterior surfaces. Likewise, the honeycomb design could be manufactured with the clad material included as face sheets and no problems related to the cladding would result. The probable use of the cladding would be on the exterior skin. The B-1 alloy could be readily diffusion bonded or brazed to the core, but little advantage could be realized since the honeycomb core and internal surfaces are not coated. Very little work has been accomplished on the defect sensitivity of the columbium honeycomb panel, but the extent of oxidation damage to the uncoated internal core after damage to the exterior skin has been questioned. The outer skin concept could be a significant contribution toward answering such questions and providing a fail-safe design.

The corrugated and rib stiffened designs are probably the most popular because of their structural efficiency. The rib stiffened design also has the advantage that all surfaces are readily accessible for coating application and inspection. These designs are commonly joined by fusion (electron beam) welding, which would be prohibitive for the clad material because the continuity of the clad layer would be destroyed at the weld. While fusion welds have been successfully used with these designs, the skin thicknesses at welding which produce the most weight efficient panels (250 to 350 micrometers) are difficult to weld without causing local skin distortion. To remove such distortion creep forming operations are required during postweld stress relieving. Processes are, therefore, being developed to fabricate the vee corrugated and rib stiffened designs which produce distortion free hardware at substantially lower costs. One of the most promising of these processes, Forged Upset Diffusion Joining (FUDJ), employs the principle of not fusing the metal to be joined and thus eliminates the distortion in thin gauge materials. This lack of fusion requirement is common with and complementary to the outer skin cladding requirement of not destroying the continuity of the cladding layer.

The FUDJ weld process involves fabricating and cleaning detail parts in the same manner as if electron beam welding was to be performed. Joining is accomplished by resistance roll seam welding in which the pressure is increased and the temperature is reduced to preclude fusion and the formulation of a cast weld nugget. The parts are superficially bonded at this point so they can be handled without damaging the joint, but the required joint strength has not been developed. The part is put through a vacuum heat treatment cycle, with minimal or no tooling required, which effects a diffusion bonding of the joint. Figure 52 shows typical vee corrugated and rib stiffened joints of unclad columbium alloys. Full size (50 by 50 centimeters) panels have been

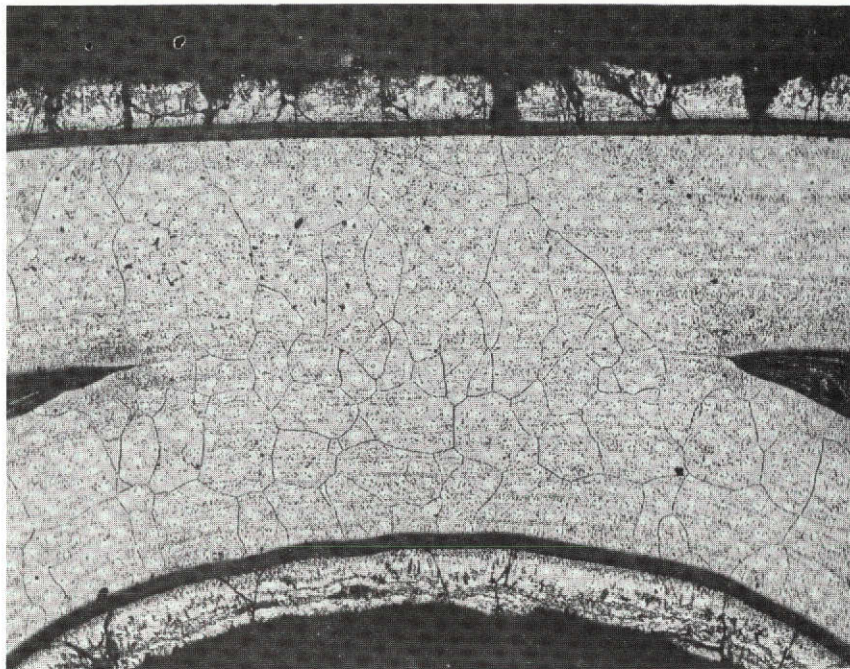
OUTER PROTECTIVE SKIN



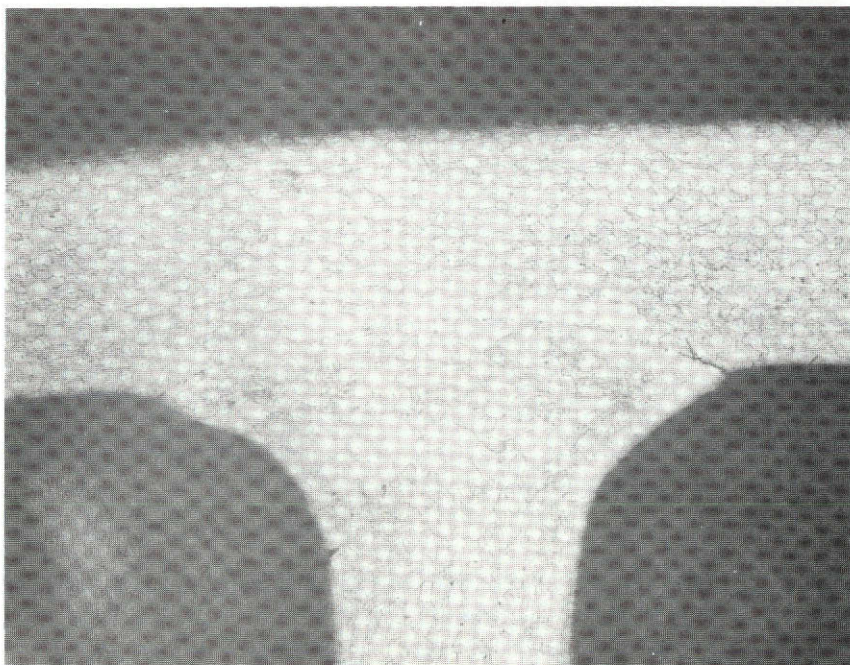
NOTES:

- (1) DIMENSIONS ARE IN CENTIMETERS
- (2) MATERIAL THICKNESSES REPRESENT LOAD BEARING CROSS SECTION.

FIGURE 51 CURRENT COLUMBIUM DESIGN APPROACHES



Vee Corrugated Joint



Rib Stiffened Joint

FIGURE 52 FUDJ WELDED COLUMBIUM JOINTS

This page is reproduced at the back of the report by a different reproduction method to provide better detail.

successfully manufactured in this manner. The quality of the hardware and the low fabrication cost make the process very attractive.

The outer skin cladding material integrates well with this new joining technology. The application of the cladding on the exterior surface could be easily accomplished by using the present processing since as the external skin wheel of the roll seam resistance welding is a flat rim wheel and does not damage the skin. The joining and subsequent diffusion bonding occur on the opposite surface of the sheet from the cladding. Should the cladding be desired on the internal surfaces, the clad material could be bonded to itself. Joining and diffusion bonding schedules would have to be developed and strength tests performed. However, the bonding of the B-1 to the FS-85 was accomplished so easily in the manufacture of the clad material that no bonding problem is anticipated. Figure 53 schematically shows FUDJ joins the B-1 cladding on the exterior and both surfaces. Thus for the current and future design approaches for coated columbium panels, the cladding concept for improved reliability appears to easily integrate itself into the mainstream of manufacturing technology.

3.2.5 Survey of Cost Factors

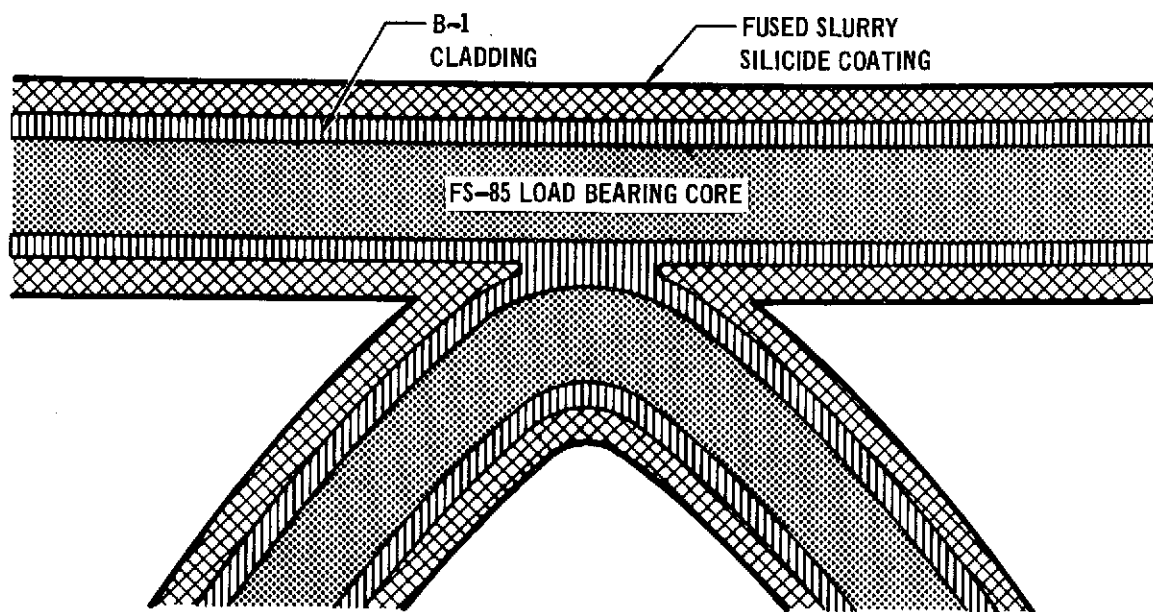
A goal in producing the B-1 clad FS-85 outer skin material for this program was that the processes used should be compatible with standard production techniques for refractory metal sheet. With the successful achievement of this goal, it can be stated that no major problem is anticipated for the production of large quantities of the clad sheet material at a nominal cost. Assuming the development of production processing schedules and production quantities, the only significant additional cost factors in producing the clad sheet are the roll bonding step and increased inspection operations. Projected costs for large production quantities of the clad sheet would be approximately 15 percent greater than for unclad sheet.

In preparation for production of clad sheet, several aspects would have to be scaled up. The first step would be the preparation of the clad sheet for bonding to the load bearing core. The B-1, or other alloys with similar moderate oxidation resistance, are difficult to melt because of the disparity in melting points between the constituents. A development of techniques for melting ingots of sufficient size for either 60 or 120 centimeter wide sheet would have to be carried out. Electrode preparation would be a major consideration, for which powder metallurgical techniques should be considered. The reduction of quality ingots to sheet for bonding is not expected to be a problem.

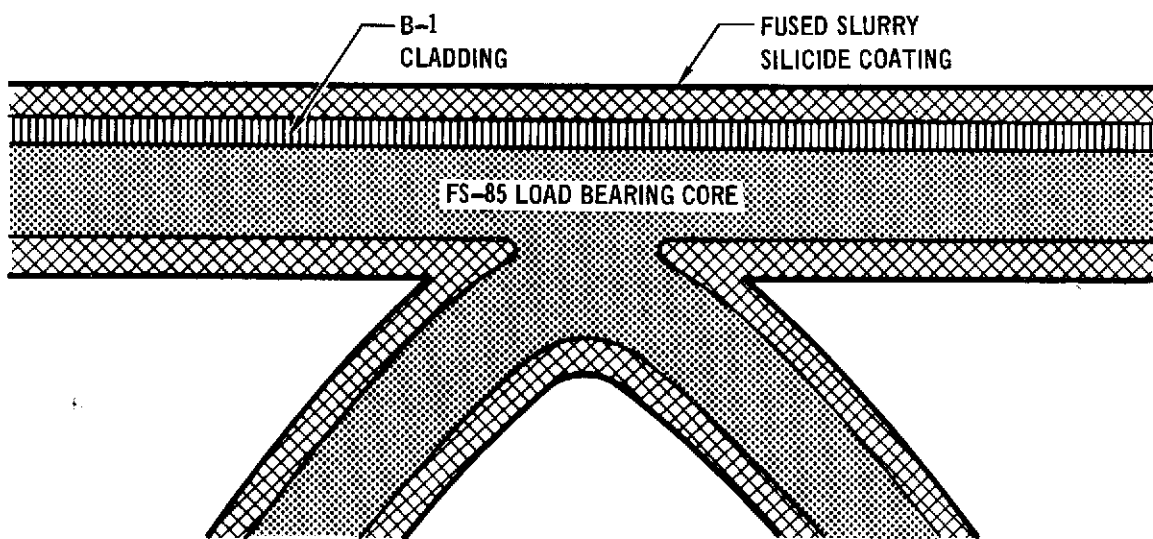
Bonding of the cladding to the load bearing core can be accomplished by hot roll bonding. This, of course, requires furnaces and facilities for hot rolling, but it is believed to be the best approach for production processing. A bonding approach for intermediate quantities of sheet for production size panels would be explosive bonding. There may be a problem of waviness at the interface associated with explosive bonding, but sheet reductions of 80 to 90 percent could be expected to diminish this effect to within acceptable limits.

OUTER PROTECTIVE SKIN

Report MDC E0913
September 1973



Outer Skin Cladding on Both Surfaces of FUDJ Joint



Outer Skin Cladding on Exterior of FUDJ Joint

FIGURE 53

Rolling of the bonded products requires a heavy stiff mill to maintain good quality sheet of acceptable flatness.

In summary, the manufacture of clad sheet would require some development and scale up effort, but no major technical problems are foreseen. Producing intermediate quantities of production size sheets poses some significant problems in availability of the heavy duty quality roll bond and reduction mill equipment used in production of other sheet products.

The manufacture and coating of heatshield panels are not expected to generate any increased costs over unclad columbium sheet. One aspect of panel manufacture that could increase cost would be the application of cladding to the edges of panels or detailed parts, should this be desirable. It has been assumed that the primary benefit of the cladding would be backup protection of exterior surfaces; while this is expected to be valid for most applications (because of the non-structural criticality of panel edges), some special cases may arise in which edge cladding would be desirable. In such cases, processes for applying the cladding after detail parts have to be cut to size would have to be developed. It has been suggested (reference 13) that physical vapor deposition would be an appropriate process for applying cladding to edges, with an associated increase in manufacturing costs.

Operational cost factors are difficult to assess. There are no projected increases in operational costs associated with the use of the outer skin claddings, and this program showed that panel life would be extended. A primary operational benefit of the clad outer skin would be that local coating damage could be detected and repaired before core material oxidation occurred, thereby prolonging the life and increasing the reliability. While the reduction of operational inspection and the repair and refurbishment associated with the clad material could result in significant reductions of total system cost, data upon which to base specific predictions are not available.

4. CONCLUSIONS AND RECOMMENDATIONS

The outer skin program investigated the feasibility of improving the reliability of coated columbium thermal protection systems by including a moderately oxidation resistant columbium alloy cladding between the load bearing substrate and a protective coating. In the event of local coating damage the oxidation resistant cladding would provide temporary protection for the load bearing core. The experimental system employed a FS-85 load bearing core, a B-1 alloy cladding and the R-512E fused slurry silicide coating. The following conclusions were drawn:

- (1) B-1 clad FS-85 can be produced in 10 centimeter wide sheet of good quality. During this program the bonding of the cladding to the core was excellent, the cladding interface progressed to a smooth uniform plane and the cladding thickness was uniform and consistent. No problems were encountered in the manufacture of the cladding which would preclude the manufacture of large quantities of the clad sheet at a nominal cost increase over unclad sheet. Only a moderate scale-up program would be necessary.
- (2) The R-512E fused slurry silicide coating performs well on the B-1 cladding; it has a life in excess of 100 reentry cycles. The R-512E coating on FS-85 was found to be slightly better than the R-512E coating on the B-1, based upon metallographic examination after 100 reentry cycles, and so subtle improvement of the B-1 coating could be predicted.
- (3) The B-1 cladding significantly retards oxidation of the load bearing columbium core. After 50 reentry cycles the presence of the B-1 cladding reduced the volume of columbium lost due to oxidation by a factor of approximately 20.
- (4) The B-1 cladding limits the area of oxygen contamination in the load bearing core adjacent to a defect site. In the case of an intentional coating defect 0.15 centimeters in diameter, the oxygen contamination zone was found to be essentially the same as the defect size until the cladding was consumed by oxidation. This occurred at 5 cycles for the 50 micrometer B-1 cladding and 15 cycles for the 100 micrometer cladding. After 50 reentry cycles, the oxygen contamination of the FS-85 beneath the 100 micrometer cladding had penetrated into the core to only one third the depth that it penetrated into the unclad FS-85.
- (5) Strength properties of an outer skin composite system are the same as those of the FS-85 core for B-1 cladding thicknesses up to 50 micrometers. For B-1 cladding thicknesses of 100 micrometers there is an influence on composite strength with increased tensile properties and reduced ductility. Both cladding thicknesses were

found to carry design tensile loads for 100 cycles successfully when tested under the combined reentry effects of time, temperature, pressure, and stress.

- (6) The B-1 cladding prevents deterioration of the FS-85 core mechanical properties in the area of coating defects. No tensile property deterioration was found for up to 5 cycles when the defect area was protected by 100 micrometers of B-1 cladding. During testing of defected tensile specimens under the combined reentry conditions of time, temperature, pressure, and stress, clad specimens carried design loads approximately twice as long as unclad specimens.
- (7) The emittance of the R-512E coated B-1 is slightly lower than the emittance of R-512E coated FS-85. Both, however, are acceptable for use on the exterior of a reentry vehicle.

The following recommendations are made for further development and characterization of the outer skin material system:

- (1) The T-166 (see paragraph 3.1) and B-1 alloys should be comprehensively evaluated simultaneously to determine the more appropriate cladding alloys for the outer skin protection of coated columbium thermal protection system panels.
- (2) Advanced joining techniques, like Forged Upset Diffusion Joining, should be investigated to demonstrate their applicability to clad sheet and to determine joint strength allowables.
- (3) Protective coating studies should be undertaken to investigate oxidation mechanisms of edge protection for fused slurry silicide coatings. Physical and chemical coating characteristics for optimum edge protection must be defined and balanced with surface requirements for maximum coating system effectiveness.
- (4) A scale-up program should be undertaken to provide the capability of producing B-1 clad sheet a minimum of 60 centimeters in width.

5. REFERENCES

1. Cornie, J. A. and Goodspeed, R. C., "Development of Ductile Oxidation Resistant Columbium Alloy," Technical Report AFML-TR-69-64, July 1969.
2. Torgerson, R. T., "Development and Evaluation of C-129Y Columbium Alloy," D2-20280-1, Boeing Aircraft Company, 1964.
3. Anon., "B-66 Columbium Base Alloy," STD-52-364 Corrective Sheet, Westinghouse Electric Corporation, Astronuclear Laboratory, 1962.
4. Schmitt, F. F. and Ogden, H. R., "The Engineering Properties of Columbium and Columbium Base Alloys," DMIC Report 188, September 1963.
5. Sessler, J. G., et al, "Aerospace Structural Metals Handbook," AFML-TR-68-115, Mechanical Properties Data Center, Belfour Stulen, Inc., 1968.
6. Tavasoli, A. A., "Development of Columbium Alloy WC-3015, NASA TND-6390, July 1971.
7. Fitzgerald, B. G., "Fused Slurry Silicide Coatings for Columbium Alloy Reentry Heat Shields," Final Technical Report NASA CR 121216 and NASA CR 134483, August 1973
8. Priceman, S. and Soma, L., "Development of Fused Slurry Silicide Coatings for Elevated Temperature Oxidation Protection of Columbium and Tantalum Alloys," AFML-TR-68-210, December 1968.
9. Culp, J. D., "Field Repair of Coated Columbium Thermal Protection Systems (TPS)," Final Technical Report MDC E0681, McDonnell Douglas Astronautics Company - East, 15 September 1972.
10. Bartlett, E. S., et al, "Degradation and Reuse of Radiative-Thermal-Protection-System Materials For The Space Shuttle," Battelle Final Technical Report Under Contract NAS8-26205, August 1972.
11. Anon., "Supplemental Structural Test Program - Final Report Large TPS Panels," Report No. MDC E0562, McDonnell Douglas Astronautics Company - East, 30 March 1972.
12. Black, W. E. and Rummler, D. R., "Evaluation of Columbium Alloy Thermal Protection Systems For Space Shuttle," AIAA Paper No. 73-378, March 1973.
13. Bartlett, E. S. and Browning, M. F., "Investigation of Corrosion-Resistant Coatings for Service at 2500°F," Battelle-Columbus For Contract N00019-71-C-0421, 5 July 1972.

APPENDIX A

DETAILED TENSILE TEST DATA

The tensile properties of B-1 clad FS-85 with the R-512E fused slurry silicide coating are summarized and discussed in section 2.4.1. This appendix presents the specific values obtained for each test sequence and points out possible anomalies. An assessment of the quality of the data is also provided.

1. TASK 1 TENSILE TEST RESULTS - The tensile testing accomplished during the initial experimental effort was limited to room temperature testing. The data obtained, presented in table A-1, was very consistent. The experimental data is presented in four columns, as discussed in Section 2.4. column 1 employs an area based upon the specimen dimensions before coating. column 2 employs an area based upon the effective metal remaining after fused slurry silicide coating. A ratio of 8.5 micrometers of substrate alloy consumed for each 25.4 micrometers of coating form was used. Column 3 areas are based upon an additional 10 micrometers per coated surface being consumed in 100 reentry profile exposure cycles. Column 4 strength values are based upon the actual thickness of the FS-85 core. With the exception of specimens B-8, 9 and 10 (table A-1) which sustained oxidation failures in the gauge section, the properties of the FS-85 core are the same as unclad FS-85 properties both before and after thermal cycling. The coated B-1 clad FS-85 offered superior characteristics strength to the coated Cb-752 baseline system, and it was concluded that coated FS-85 alloy sheet would provide a more meaningful baseline material.

2. TASK 2 TENSILE TEST RESULTS - Tensile testing for the second experimental effort was expanded to include elevated temperature tests at 760°C and 1320°C. The testing also included a substitution of R-512E coated FS-85 for the Cb-752 alloy baseline previously used. The results obtained are presented in table A-2. The room temperature strength was virtually the same as those determined in the initial task. It was further established that the properties at 760 and 1370°C compared very favorably with the unclad FS-85 properties previously established per reference 7. The strengths were essentially the same after 100 profile exposures, indicating that the cladding and core had distinctive identities and functions.

The unclad FS-85 properties of the baseline system were below typical tensile properties by 10 to 15 percent at each test temperature. The sheet used was known to be under nominal strength, but the change of the baseline material from Cb-752 to FS-85 between the first two tasks did not permit sufficient time to procure FS-85 sheet of typical properties. This did not prove to be a major shortcoming, since comparable R-512E coated FS-85 properties were available.

TABLE A1
TENSILE PROPERTIES OF B-1 CLAD FS-85 AND UNCLAD Cb-752 - TASK 1

SPEC NO.	MATERIAL SYSTEM	PROFILE EXPOSURE CYCLES	COLUMN 1 STRENGTH PRECOAT AREA				% ELONGATION	COLUMN 2 STRENGTH REMAINING METAL				COLUMN 3 STRENGTH 100 CYCLE REMAINING				COLUMN 4 STRENGTH CORE AREA				COLUMN 5 COMPARATIVE FS-85 STRENGTH REF.7				
			YIELD		ULTIMATE			YIELD		ULTIMATE		YIELD		ULTIMATE		YIELD		ULTIMATE		YIELD		ULTIMATE		
			MN/m ²	LB/in ² x 10 ³	MN/m ²	LB/in ² x 10 ³		MN/m ²	LB/in ² x 10 ³	MN/m ²	LB/in ² x 10 ³	MN/m ²	LB/in ² x 10 ³	MN/m ²	LB/in ² x 10 ³	MN/m ²	LB/in ² x 10 ³	MN/m ²	LB/in ² x 10 ³	MN/m ²	LB/in ² x 10 ³			
B-1	FS-85	NONE	292	42.3	371	53.8	8	346	50.2	439	63.7					493	71.5	626	90.8					
B-2	CORE/	NONE	301	43.7	365	52.9	9	359	52.1	435	63.1					516	74.9	625	90.7					
AV	B-1	NONE	276	43.8	364	53.4	8	332	51.8	437	63.8					508	73.2	625	90.3	476	63.1	532	92.7	
B-3	CLADDING	100	299	43.4	353	51.1	5	354	51.3	418	60.1	381	55.3	450	65.3	515	74.5	608	88.1					
B-4	R-512E	100	293	42.5	354	51.4	8	346	50.1	418	60.5	372	54.0	450	65.3	507	73.6	613	89.0					
B-5	COATING	100	297	43.0	358	51.9	7	351	50.9	424	61.4	377	54.7	455	66.0	504	73.1	608	88.2					
AV			276	43.0	358	51.5	7	350	50.8	420	60.7	377	54.3	457	66.5	509	73.7	610	88.4	473	63.5	533	91.4	
B-6	FS-85	NONE	293	42.5	362	52.6	7	343	49.7	474	61.5					506	73.4	626	90.8					
B-7	CORE/	NONE	301	43.6	367	53.3	7	355	51.5	435	63.1					515	74.7	631	91.5					
AV	B-1	NONE	297	43.1	363	52.9	7	349	51.1	434	62.3					513	74.1	629	91.7	476	63.1	539	92.7	
B-8(1)	CLADDING	100	276	40.1	277	40.1	7	327	47.4	327	47.5	352	51.1	353	51.2	471	68.4	472	68.5					
B-9(1)	30Cr-20Fe-Si	100	263	38.1	265	38.4	2	311	45.2	314	45.5	333	48.3	336	48.7	445	64.6	449	65.1					
B-10(1)	COATING	100	263	38.2	268	38.9	-	311	45.2	317	45.9	335	48.7	341	49.5	453	65.7	461	66.8					
AV			263	38.2	270	39.1	1	319	45.9	319	46.3	340	49.4	343	49.8	456	65.2	451	66.4	475	68.9	633	91.8	
X-1	Cb-752/	NONE	355	51.5	476	69.1	16	426	61.8	571	82.9													
X-2	NONE	360	52.2	488	70.7	18	433	62.8	586	85.0														
AV	R-512E	NONE	358	51.8	482	69.8	12	430	62.2	579	84.0													
X-3	COATING	100	344	50.0	451	65.4	-	413	60.0	541	78.5	449	65.1	588	85.2									
X-4		100	347	50.3	450	65.2	11	416	60.4	540	78.3	452	65.6	586	85.0									
X-5		100	346	50.2	449	65.7	15	414	60.1	538	78.1	449	65.2	586	84.7									
AV			346	50.1	450	65.3	13	414	60.2	540	78.3	450	65.3	586	85.0									

NOTE: 1. COATING OXIDATION FAILURES OCCURRED IN THE REDUCED GAUGE TEST SECTION OF SPECIMENS B-8, B-9 AND B-10 DURING THE PROFILE EXPOSURE CYCLING.

TABLE A2

TENSILE PROPERTIES OF B-1 CLAD FS-85 AND UNCLAD FS-85 BASELINE - TASK 2

SPEC. NO.	MATERIAL	PROFILE EXPOSURE CYCLES	TEST TEMP °C	COLUMN 1				% ELONGATION 2.9 cm	COLUMN 2				COLUMN 3				COLUMN 4				COLUMN 5				
				STRENGTH/PRECOAT AREA					STRENGTH REMAINING METAL				STRENGTH/100 CYCLE REMAINING METAL				STRENGTH CORE AREA				COMPARATIVE FS-85 STRENGTH (REF 7)				
				YIELD MN/m ²	YIELD LB/in ² x 10 ³	ULTIMATE MN/m ²	ULTIMATE LB/in ² x 10 ³		YIELD MN/m ²	YIELD LB/in ² x 10 ³	ULTIMATE MN/m ²	ULTIMATE LB/in ² x 10 ³	YIELD MN/m ²	YIELD LB/in ² x 10 ³	ULTIMATE MN/m ²	ULTIMATE LB/in ² x 10 ³	YIELD MN/m ²	ULTIMATE MN/m ²	YIELD LB/in ² x 10 ³	ULTIMATE LB/in ² x 10 ³	YIELD MN/m ²	ULTIMATE MN/m ²	YIELD LB/in ² x 10 ³	ULTIMATE LB/in ² x 10 ³	
E-1		NONE	RT	293	42.5	361	52.4	14	347	50.3	427	62.0					518	75.2	639	92.6					
E-2		NONE	RT	288	41.7	361	52.4	12	341	49.4	427	62.0					508	73.7	638	92.5					
E-3		NONE	RT	292	42.3	363	52.7	12	345	50.1	430	67.4					515	74.1	641	93.0					
E-4		NONE	RT	281	42.8	362	52.5	12	344	51.3	428	63.0					511	73.3	639	92.0	67%	145.1	629	92.7	
E-5		NONE	760	156	22.6	202	78.3	4	184	26.7	240	31.8					275	39.9	358	51.9					
E-6		NONE	760	169	24.5	218	31.7	5	200	29.0	258	32.4					298	43.7	385	55.8					
E-7		NONE	760	180	26.1	227	32.9	3	212	30.7	257	36.7					325	47.2	409	58.3					
E-8		NONE	760	183	26.8	238	33.1	4	195	26.1	251	30.0					292	42.4	388	55.7	36%	143.1	628	92.6	
E-11		FS-85	NONE	1320	108	15.6	132	19.2	4	132	19.2	164	23.8					196	23.5	243	35.2				
E-12		CORE	NONE	1320	113	16.4	134	19.4	3	134	19.4	158	21.0					199	28.9	236	34.3				
B-1		NONE	1320	116	15.8	132	19.2	3	139	20.2	158	22.9					201	29.2	239	33.2					
Avg		CLADDING	NONE	1320	112	16.3	138	18.3	2	125	18.1	168	21.2					525	28.9	236	34.3	30%	143.3	628	92.8
E-16 (1)		R-SIZE	100	RT	234	33.9	234	33.5	—	277	40.2	277	40.2	299	43.4	299	43.4	404	58.6	404	58.6				
E-17		COATING	100	RT	283	41.1	354	51.4	10	336	48.8	420	60.9	363	52.7	454	65.6	494	71.6	616	89.3				
E-18		COATING	100	RT	283	41.1	355	51.5	10	336	48.7	421	61.1	363	52.7	455	66.0	492	71.4	618	89.6				
E-19 (1)			100	RT	283	41.7	354	51.4	9	125	18.2	160	21.3	293	32.2	293	32.2	493	71.3	617	93.4	47%	142.2	625	92.3
E-19 (1)			100	760	161	23.3	161	23.3	1	129	22.4	189	24.4	203	29.4	203	29.4	294	42.2	294	42.7				
E-20			100	760	175	25.4	182	26.4	1	206	29.9	214	31.1	221	32.1	230	33.4	321	45.6	334	48.4				
F-25			100	760	181	27.7	215	31.2	3	227	32.9	255	37.0	246	35.7	277	40.2	338	49.0	380	55.2				
E-23			100	760	183	26.8	238	32.2	2	235	33.8	235	34.0	231	32.8	238	32.8	350	47.3	357	56.8	35%	142.0	625	92.7
E-24			100	1320	110	16.0	113	16.4	2	136	19.8	140	20.3	138	20.1	142	20.6	215	31.2	221	32.1				
E-21 (1)			100	1320	96	13.9	105	15.3	—	130	18.8	133	19.3	121	17.5	132	19.2	203	29.5	211	30.6				
E-21 (1)			100	1320	117	17.0	120	17.4	22	114	16.6	125	18.2	148	21.4	151	21.9	178	25.9	195	28.5				
K-1			NONE	1320	103	14.9	109	16.1	—	133	18.5	136	19.8	133	19.8	137	19.9	205	34.7	215	34.8	31%	142.8	627	92.7
K-2			NONE	RT	305	44.2	421	61.1	16	379	55.0	524	76.0												
K-3			RT	323	46.8	429	62.2	16	400	56.0	534	77.5													
K-4			NONE	RT	323	46.8	433	62.8	18	389	51.9	537	77.6												
K-5			NONE	760	167	45.9	428	62.0	17	323	51.8	523	73.2												
K-6			NONE	760	173	25.1	292	42.4	—	216	31.3	365	52.3												
K-7			NONE	760	167	24.2	285	41.5	7	207	30.0	357	51.8												
K-8			NONE	760	171	24.8	294	42.7	7	214	31.0	367	53.3												
K-9			NONE	1320	117	17.0	144	20.9	—	146	21.2	180	26.1												
K-10			NONE	1320	134	19.4	162	23.5	11	167	24.2	202	29.3												
K-11			NONE	1320	117	17.0	150	21.7	28	145	21.1	185	26.9												
K-12			NONE	1320	125	17.5	133	19.3	19	151	21.9	158	23.0	407	59.0	560	81.2								
K-13			RT	295	42.8	405	58.3	—	367	51.3	505	73.3	410	59.4	563	81.7									
K-14			RT	297	43.1	410	59.4	12	370	53.6	510	73.9	410	59.4	563	81.6									
K-15			RT	296	43.0	408	59.2	12	369	53.5	509	73.8	409	59.3	563	81.5									
K-16			RT	298	43.0	408	59.1	12	369	53.5	509	73.8	409	59.3	563	81.5									
K-17			RT	760	172	24.9	264	38.3	5	213	30.9	328	47.6	236	34.3	364	52.8								
K-18			RT	760	183	26.5	272	39.4	6	228	33.0	339	49.2	254	36.8	377	54.7								
K-19			RT	760	181	26.3	270	39.2	5	225	32.7	336	48.8	250	36.3	372	54.0								
K-20			RT	760	178	25.3	267	38.9	8	227	32.7	339	48.5	251	36.2	371	53.8								
K-21			RT	1320	121	17.5	133	19.3	19	151	21.9	158	23.0	168	24.4	165	26.8								
K-22			RT	1320	114	16.5	126	18.3	9	143	20.8	173	25.1	156	22.6	172	25.0								
K-23			RT	1320	125	18.2	138	20.0	18	166	22.8	166	24.1	175	25.4	152	27.9								
Avg			100	1320	120	17.3	131	19.3	19	153	21.5	158	23.0	164	24.3	163	26.7								

(!) - OXIDATION FAILURE OCCURRED IN GAUGE LENGTH - VALUES NOT INCLUDED IN AVERAGES.

3. TASK 3 TENSILE TEST RESULTS - The tensile testing of the final task repeated the property determination of the second task and included a thicker B-1 cladding of 100 micrometers. Two anomalies occurred in this sequence of testing which reduced the utility of the tensile data generated. First, the clad specimens exposed for 100 profile exposure cycles experienced numerous coating oxidation failures in the gauge section. The occurrence was quite unusual and is described in section 2.2.4. The second irregularity occurred in the elevated temperature testing. The data obtained was approximately 10 percent lower than would be expected from the known properties of the FS-85 baseline material and the data previously obtained during the second task. The fact that the room temperature properties for the baseline material and the 50 micrometer B-1 clad material were normal and as expected would cause suspicion of the testing instead of the material. No specific differences between the temperature measurement or other aspects of the test procedure could be identified.

The data obtained are presented in table A-3. It was clear that the two B-1 alloy cladding thicknesses (50 and 100 micrometers) exhibit different strength characteristics. The thinner cladding specimens, within the context of the anomalies previously discussed, performed similarly to the cladding evaluated in previous experiments. That is, the cladding appeared to be functioning as part of the protection system and had little influence upon the strength characteristics of the FS-85 load bearing core. The B-1 cladding at a thickness of 100 micrometers had a pronounced effect upon the FS-85 core strength. Notably, the room temperature and 760°C strength was increased and the ductility was markedly reduced at all temperatures.

OUTER PROTECTIVE SKIN

TABLE A3
TENSILE PROPERTIES OF B-1 CLAD FS-85 AND UNCLAD FS-85 BASELINE – TASK 3

NOTE: 1 SPECIMENS DAMAGE WHILE INSTALLING IN TEST MACHINE AND VALUES, WHEN OBTAINED, NOT INCLUDED IN AVERAGE.

FOLDOUT FRAME

B

OUTER PROTECTIVE SKIN

Report MDC E0913
September 1973

TABLE A3
TENSILE PROPERTIES OF B-1 CLAD FS-85 AND UNCLAD FS-85 BASELINE - TASK 3

SPEC NO.	MATERIAL SYSTEM	PROFILE EXPOSURE CYCLES	TEST TEMPERA-TURE	COLUMN 1 STRENGTH - PRECOAT AREA				% ELONGATION 2.5 cm	COLUMN 2 STRENGTH-REMAINING METAL				COLUMN 3 STRENGTH - 100 CYCLE REMAINING METAL				COLUMN 4 STRENGTH - CORE AREA				COLUMN 5 STRENGTH - COMPARATIVE FS-85 (REFERENCE 7)						
				YIELD		ULTIMATE			YIELD		ULTIMATE		YIELD		ULTIMATE		YIELD		ULTIMATE		YIELD		ULTIMATE				
				MN/m ²	LB/IN ² x10 ³	MN/m ²	LB/IN ² x10 ³		MN/m ²	LB/IN ² x10 ³	MN/m ²	LB/IN ² x10 ³	MN/m ²	LB/IN ² x10 ³	MN/m ²	LB/IN ² x10 ³	MN/m ²	LB/IN ² x10 ³	MN/m ²	LB/IN ² x10 ³	MN/m ²	LB/IN ² x10 ³	MN/m ²	LB/IN ² x10 ³			
T-1	FS-85	NONE	ROOM	316	45.8	337	48.9	2	354	51.3	378	54.8					712	103.3	760	110.2							
T-6	CORE		TEMP	321	46.6	329	47.7	2	360	52.1	367	53.3					735	106.5	752	109.0							
T-18				331	48.0	340	49.2	1	370	53.7	380	55.1					765	111.2	785	113.8							
AV	NOMINAL	NONE		323	46.8	335	48.6	2	361	52.4	375	54.4					738	107.0	766	111.0	476	69.1	639	92.7			
T-5	100 μm	100		217	31.5	221	31.9	2	243	35.3	246	35.7	256	37.1	259	37.6	491	71.2	498	72.2							
T-12	B-1	100		235	34.2	241	35.0	2	263	38.1	269	39.0	276	40.0	282	41.0	552	80.0	565	81.9							
T-14		CLADDING	100	234	34.0	259	37.5	2	262	38.0	290	42.0	276	40.0	305	44.2	529	76.7	584	84.8							
AV			TEMP	229	33.2	240	34.8	2	256	37.1	268	38.9	269	39.0	282	40.9	524	76.0	549	79.6	475	68.9	633	91.8			
T-20 (1)	R-512E	NONE	760°C	94	13.7	136	19.7	1	106	15.3	152	22.1					207	30.0	297	43.1							
T-23				165	23.9	221	32.1	4	184	26.7	247	35.8					381	55.3	511	74.1							
T-24				195	28.3	237	34.4	5	219	31.8	267	38.7					429	62.2	520	75.5							
AV				180	26.1	229	33.2	3	202	29.3	257	37.2					405	58.8	516	74.8	263	38.1	458	66.5			
T-15		100		135	19.5	139	20.2	3	150	21.8	155	22.5	158	22.9	163	23.7	310	45.0	321	46.5							
T-16		100		128	18.5	138	20.0	3	143	20.7	155	22.5	150	21.8	163	23.7	288	41.8	313	45.4							
T-17		100		-	-	158	22.9	-	-	176	25.6	-	-	160	23.0	-	-	369	53.5								
AV			760°C	131	19.0	145	21.0	2	146	21.2	162	23.5	154	22.4	162	23.5	299	43.4	334	48.4	238	34.5	386	56.0			
T-2		NONE	1320°C	58	8.3	75	10.9	-	64	9.3	84	12.2					130	18.8	170	24.6							
T-3		NONE		54	7.8	81	11.7	-	60	8.7	88	12.8					122	17.6	178	25.9							
T-4				58	8.5	72	10.5	65	65	9.5	87	12.6					131	19.0	174	25.3							
AV		NONE		57	8.2	76	11.0	-	63	9.2	86	12.5					128	18.5	174	25.3	203	29.5	219	31.8			
T-25		100		75	10.8	144	20.9	-	84	12.1	84	12.2	88	12.8	89	12.9	171	24.8	172	25.0							
T-26				78	11.3	119	17.2	-	87	12.6	90	13.1	91	13.2	95	13.7	177	25.7	184	26.7							
T-27				70	10.1	147	21.4	-	78	11.3	81	11.8	92	11.9	85	12.4	157	22.8	164	23.7							
AV		100	1320°C	74	10.7	137	19.8	-	83	12.0	85	12.4	87	12.6	90	13.0	168	24.4	173	25.1	186	27.0	198	28.7			

NOTE: 1 SPECIMENS DAMAGE WHILE INSTALLING IN TEST MACHINE AND VALUES, WHEN OBTAINED, NOT INCLUDED IN AVERAGE.

A
B

FIGURE FRAME

APPENDIX B**DEFECT TENSILE TEST DATA**

Tensile specimens were tested with coating defects in the center of the gauge section, after various exposure profile cycles. The data is discussed in section 2.4.3 and the average results are presented in figure 35. This appendix presents the specific data obtained in tables B-1 and B-2.

457-3416

TABLE B1
EFFECT OF COATING DEFECTS ON TENSILE PROPERTIES OF CLAD AND UNCLAD FS-85 ALLOY COLUMBIUM - TASK 2

SPEC NO.	MATERIAL SYSTEM	PROFILE EXPOSURE CYCLE	TEST TEMP.	STRENGTH/PRECOAT AREA				ELONGATION % IN 1 INCH	STRENGTH/REMAINING METAL AREA				STRENGTH/CORE AREA			
				YIELD MN/m ²	ULTIMATE MN/m ²	YIELD LB/in ² x 10 ³	ULTIMATE LB/in ² x 10 ³		YIELD LB/in ² x 10 ³	ULTIMATE LB/in ² x 10 ³	YIELD MN/m ²	ULTIMATE MN/m ²	YIELD LB/in ² x 10 ³	ULTIMATE LB/in ² x 10 ³	YIELD LB/in ² x 10 ³	ULTIMATE LB/in ² x 10 ³
E-26	FS-85	0	ROOM TEMP	302	362	43.8	52.5	11	51.7	62.0	356	427	537	645	77.9	93.5
E-27	CORE / 50 μm BY	0		292	361	42.3	52.4	12	50.0	61.8	345	426	519	642	75.3	93.2
AVG				297	362	43.0	52.4	11	50.8	61.9	350	426	528	644	76.6	93.4
E-28	CLADDING	1		306	323	44.4	46.9	3	52.4	55.4	361	382	544	575	78.9	83.4
E-29	R-512E	1		310	345	45.0	50.1	5	53.2	59.3	367	409	543	605	78.7	87.7
AVG	COATING			308	334	44.7	48.5	4	52.8	57.4	364	396	544	590	78.8	85.6
E-30		3		316	318	45.8	46.2	1	54	54.5	372	376	566	572	82.1	82.9
E-32		3		328	353	47.6	51.2	- (1)	56	60.3	386	416	591	636	85.7	92.2
AVG				322	336	46.7	48.7	1	55	57.4	379	396	578	604	83.9	87.6
E-33		10		-	278	-	40.4	-	-	47.7	-	329	-	494	-	71.6
E-35		10		-	255	-	37.0	-	-	43.6	-	301	-	460	-	66.7
AVG				-	266	-	38.7	-	-	45.6	-	315	-	477	-	69.2
K-22	FS-85	0		339	449	49.2	65.1	16	61.7	81.7	425	563				
K-23	SUBSTRATE / R-512E	0		322	427	46.7	61.9	12	58.6	77.6	404	535				
AVG	COATING			330	438	48.0	63.0	14	60.2	79.6	415	549				
K-24		1		-	268	-	38.9	-	-	48.5	-	334				
K-25		1		-	323	-	46.9	-	-	58.8	-	405				
AVG				-	296	-	42.9	-	-	53.6	-	370				
K-26		3		-	287	-	41.7	-	-	52.3	-	360				
K-28		3		-	268	-	38.8	-	-	48.4	-	334				
AVG				-	278	-	40.2	-	-	50.4	-	347				
K-29		10		-	247	-	35.8	-	-	44.8	-	309				
K-30		10		-	223	-	32.3	-	-	41.8	-	288				
AVG				-	235	-	34.0	-	-	43.3	-	299				

NOTES: (1) SPECIMEN BROKE OUTSIDE GAUGE AREA.

OUTER PROTECTIVE SKIN

TABLE B2
ROOM TEMPERATURE TENSILE PROPERTIES OF CLAD AND UNCLAD DEFECTED SPECIMENS
AFTER VARIOUS REENTRY PROFILE EXPOSURES - TASK 3

SPEC NO.	MATERIAL SYSTEM	PROFILE EXPOSURE CYCLES	COLUMN 1 STRENGTH - PRECOAT AREA				% ELONGA-TION	COLUMN 2 STRENGTH - REMAINING METAL				COLUMN 4 STRENGTH - CORE AREA				
			YIELD		ULTIMATE			YIELD		ULTIMATE		YIELD		ULTIMATE		
			MN/m ²	LB/in ² × 10 ³	MN/m ²	LB/in ² × 10 ³		MN/m ²	LB/in ² × 10 ³	MN/m ²	LB/in ² × 10 ³	MN/m ²	LB/in ² × 10 ³	MN/m ²	LB/in ² × 10 ³	
M-36		NONE	300	43.6	345	50.1	10	353	51.2	406	58.8	528	76.7	606	87.9	
M-39		NONE	277	40.1	333	48.3	10	324	46.9	389	56.4	497	72.1	598	86.7	
M-41		NONE	255	37.0	301	43.7	9	296	42.9	349	50.6	491	71.2	579	83.9	
AV		NONE	277	40.2	326	47.3	10	324	47.0	381	53.2	585	73.3	594	86.2	
M-9	FS-85 CORE	1	274	39.7	278	40.4	1	329	47.7	329	47.7	465	67.4	472	68.4	
M-10		1	277	40.1	296	42.9	1	326	47.3	349	50.6	476	69.0	509	73.9	
AV		1	276	39.9	284	41.6	1	329	47.5	333	49.2	470	68.2	490	71.6	
M-11	NOMINAL 50 μm	3	233	33.8	260	37.8	-	275	39.9	307	44.5	401	58.2	448	65.0	
M-12		3	242	35.2	273	39.7	-	286	41.5	323	46.7	418	60.6	471	68.3	
AV		3	239	34.5	266	38.8	-	280	41.2	315	45.6	410	59.4	460	66.6	
MK-13	CLADDING	5	222	32.1	258	37.4	-	262	38.1	304	44.2	383	55.5	444	64.4	
MK-14		5	219	31.8	222	32.2	-	257	37.2	259	37.6	396	57.4	400	58.0	
AV		5	220	32.2	240	35.8	-	260	37.6	282	40.9	390	56.5	422	61.2	
M-15	R-512E COATING	10	184	26.7	217	31.4	-	211	30.6	249	36.1	326	47.2	384	55.6	
M-16		10	189	27.4	193	28.0	-	221	32.1	227	32.9	336	48.7	344	49.9	
AV		10	186	27.0	205	29.7	-	216	31.4	238	34.5	331	49.0	364	52.8	
M-17		15	159	23.0	167	24.2	-	187	27.1	197	28.6	273	39.6	288	41.7	
M-18		15	175	25.3	179	26.0	-	205	29.7	210	30.5	310	44.9	318	46.1	
AV		15	167	24.2	173	28.1	-	196	28.4	204	29.6	222	42.8	303	43.9	
T-1		NONE	316	45.8	337	48.9	2	354	51.3	378	54.8	712	103.3	760	110.2	
T-6		NONE	321	46.6	329	47.7	2	360	52.1	367	53.3	735	106.5	752	109.0	
T-18		NONE	331	48.0	340	49.2	1	370	53.7	380	55.1	765	111.2	785	113.8	
AV		NONE	323	46.2	335	48.6	2	361	52.4	375	54.4	738	107.0	766	111.0	
T-28	FS-85 CORE	1	352	51.1	365	52.9	-	395	57.3	408	59.3	784	113.8	812	117.8	
T-29		1	317	45.9	333	48.3	-	353	51.2	372	53.9	732	106.2	770	111.7	
AV		1	334	46.5	349	50.4	-	374	54.3	390	56.6	758	110.4	791	114.8	
T-30	NOMINAL 100 μm	3	294	42.6	305	44.3	-	327	47.4	349	49.3	696	101.0	724	105.0	
T-31		3	317	46.0	329	47.7	-	355	51.5	368	53.4	715	103.7	740	107.4	
AV		3	306	44.3	317	45.0	-	341	49.4	354	51.4	706	102.4	732	105.2	
T-33	CLADDING	5	323	46.8	326	47.3	-	360	52.2	364	52.7	753	109.2	761	110.4	
T-35		5	338	48.2	333	48.3	-	370	53.7	371	53.8	789	114.4	790	114.6	
AV		5	328	47.5	336	47.8	-	365	53.0	368	53.2	771	111.3	776	112.5	
T-36	R-512E COATING	10	-	-	279	43.1	-	-	-	331	48.0	-	-	705	102.2	
T-37		10	-	-	288	41.8	-	-	-	323	46.9	-	-	639	92.7	
AV		10	-	-	292	42.4	-	-	-	327	47.6	-	-	672	97.4	
T-38		15	-	-	294	42.6	-	-	-	329	47.1	-	-	661	95.9	
T-39		15	-	-	235	34.1	-	-	-	263	38.1	-	-	529	76.7	
AV		15	-	-	264	38.1	-	-	-	296	42.6	-	-	595	85.3	
S-2		NONE	415	60.1	537	77.9	17	481	69.7	623	90.3					
S-3		NONE	407	59.1	511	74.2	12	472	68.4	592	85.9					
S-4		NONE	411	59.6	516	74.9	18	475	68.9	596	86.5					
AV		NONE	411	59.5	521	75.6	16	476	69.0	604	87.6					
S-44	FS-85 BASELINE	1	-	-	377	54.7	-	-	-	437	63.4					
S-31		1	-	-	380	55.1	-	-	-	440	63.9					
AV		1	-	-	398	54.5	-	-	-	459	63.6					
S-32	R-512E COATING	3	266	38.5	301	43.7	-	300	43.5	340	49.3					
S-33		3	266	38.6	295	42.8	-	309	44.8	342	49.6					
AV		3	266	38.6	298	43.2	-	304	42.7	341	49.4					
S-40		5	-	-	308	44.6	-	-	-	355	51.5					
S-45		5	-	-	320	46.4	-	-	-	371	53.7					
AV		5	-	-	314	45.6	-	-	-	363	52.6					
S-47		10	-	-	219	31.8	-	-	-	253	36.7					
S-48		10	-	-	251	36.4	-	-	-	291	42.2					
AV		10	-	-	235	34.1	-	-	-	272	39.4					
S-51		15	-	-	103	15.0	-	-	-	120	17.3					
S-53		15	-	-	131	18.9	-	-	-	151	21.9					
AV		15	-	-	117	17.0	-	-	-	136	19.6					

NOTES: 1. VALUES FOR SPECIMENS WITH NO EXPOSURE CYCLES OBTAINED FROM TABLE A-3.

2. DASH INDICATES NO DEFINED YIELD POINT OR AN ELONGATION LESS THAN ONE PERCENT.

APPENDIX C

CONVERSION FACTORS TO INTERNATIONAL SYSTEM OF UNITS (SI)

<u>English Unit</u>	<u>x</u>	<u>Factor</u>	<u>=</u>	<u>SI Unit</u>
inch (in)		2.54		centimeter (cm)
Fahrenheit ($^{\circ}$ F)		5/9 (F-32)		Centigrade (Celsius) ($^{\circ}$ C)
mil		25.4		micrometer (μ m)
thousand pounds/inch ² (KSI)		6.89		meganewton/meter ² NM/m ²
pound/foot ³ (lb/ft ³)		16.02		kilogram/meter ³ (kg/m ³)
pound/foot ² (lb/ft ²)		4.88		kilogram/meter ² (kg/m ²)
pound (lb)		0.454		kilogram (kg)

THE FOLLOWING PAGES ARE DUPLICATES OF
ILLUSTRATIONS APPEARING ELSEWHERE IN THIS
REPORT. THEY HAVE BEEN REPRODUCED HERE BY
A DIFFERENT METHOD TO PROVIDE BETTER DETAIL